



# Instrumentation biomédicale et étude des applications sur des effets de champs magnétiques

Huetzin, Aaron Pérez Olivas

## ► To cite this version:

Huetzin, Aaron Pérez Olivas. Instrumentation biomédicale et étude des applications sur des effets de champs magnétiques. Automatique / Robotique. Université Paris Saclay (COMUE), 2015. Français. NNT : 2015SACLV031 . tel-01357937

**HAL Id: tel-01357937**

**<https://theses.hal.science/tel-01357937>**

Submitted on 30 Aug 2016

**HAL** is a multi-disciplinary open access archive for the deposit and dissemination of scientific research documents, whether they are published or not. The documents may come from teaching and research institutions in France or abroad, or from public or private research centers.

L'archive ouverte pluridisciplinaire **HAL**, est destinée au dépôt et à la diffusion de documents scientifiques de niveau recherche, publiés ou non, émanant des établissements d'enseignement et de recherche français ou étrangers, des laboratoires publics ou privés.

NNT : 2015SACLV031



THESE DE DOCTORAT  
DE L'UNIVERSITE PARIS-SACLAY,  
préparée à l'Université de Versailles Saint-Quentin

ÉCOLE DOCTORALE N° 580  
Sciences et technologies de l'information et de la communication

Spécialité de doctorat Automatique

Par

Huetzin Aaron Pérez Olivas

Instrumentation biomédicale et étude des applications  
sur des effets de champs magnétiques

**Thèse présentée et soutenue à l'Université de Versailles, le 14 décembre 2015 :**

**Composition du Jury :**

Mr, Juncar, Patrick	Professeur Cnam	Président
Mr, Meyrueis, Patrick	Professeur Université de Strasbourg	Rapporteur
Mr, Yskandar, Hamam	Professeur Tshwane U. of Technology	Rapporteur
Mr, Alayli, Yasser	Professeur Université de Versailles	Directeur de thèse
Mr, Guan, Hongyu	Ingénieur Université de Versailles	Co-directeur de thèse
Mr, Linares, Jorge	Professeur Université de Versailles	Invité
Mr, Topsu, Suat	Professeur Université de Versailles	Invité
Mr. Garcia, Jorge	Ingénieur de Recherche Oledcomm	Invité

**Titre :** Instrumentation biomédicale et étude des applications sur des effets de champs magnétiques

**Mots clés:** Instrumentation magnétique, biomédecine, stimulation magnétique.

**Résumé:** La dynamique de culture de cellules peut être modifiée lors de l'application de champs magnétiques fluctuants afin d'stimuler la prolifération et longévité de cellules mais sans affecter leur viabilité. Cela se fait avec les conditions expérimentales et paramètres optimaux. Dans cette thèse je montre l'étude à différents types de cellules tels que l'Entamoeba histolytica et invadens, les lymphocytes humains et l'HEK-293E pour obtenir quelques paramètres importants qui puissent nous permettre à mieux comprendre les effets subis par elles quand un champ magnétique est appliqué. L'objectif de mon travail est d'étudier la culture de cellules et sa dynamique quand elle ressent un champ magnétique d'une certaine intensité, à une certaine fréquence, le nombre de fois d'application et les effets que le

champ peut l'induire. Je considère aussi la concentration de fluides paramagnétiques dans le milieu de culture chargé d'amplifier l'effet de stimulation. Finalement, je parlerais de la conception d'une instrumentation capable de pourvoir aux cellules les meilleures conditions de reproduction telle que la température, espace, distribution efficace du champ magnétique et sa forme de radiation. La conception d'une nouvelle instrumentation qui puisse tenir en compte des nouvelles variables est aussi traitée. Cette même instrumentation s'est révélée très robuste pour être aussi appliquée dans d'autres sujets d'étude biomédicale avec des faibles modifications. Son utilisation en diagnostique de dislocation de la hanche, la mesure de fréquences dans la région gastroesophagale pour étudier la dynamique du métabolisme.

**Title :** Biomedical Instrumentation and Study of Magnetic Field Effect Applications

**Keywords:** Magnetic instrumentation, biomedicine, magnetic stimulation.,

**Abstract:** This thesis has the objective to determine the effect produced by weak magnetic field stimulation on the following types of cell cultures: Entamoeba histolytica, Entamoeba invadens, human lymphocyte, and HEK-293T. Changes in cell's proliferation and longevity without affecting their viability are thus studied. We intend to understand the effect produced by the magnetic field and gadolinium in the different levels of cell organization (organelle, macro molecules, and chemical reactions). We are mainly interested in asserting the behavior of cells in a controlled manner, for example when applying oscillating magnetic

fields at different frequencies and time intervals as well as the addition of certain concentrations of super-paramagnetic fluid in the growing medium. Here I present effects on the cell motility of Entamoeba invadens cell cultures and the change in the natural cell behavior, such as controlled agglutination, cell movement velocity, membrane structural form. I also present the effects and dynamic responses on the growth of Entamoeba cells by applying an oscillating magnetic field in specific audio frequencies such as 100 Hz, 800 Hz, 1500 Hz, and 2500Hz, at six minutes time periodic intervals.

*To my Wife, who followed and supported me in this adventure. To my supervisors, who gave me all the tools, friendship, and knowledge to accomplish this lovely project. To my collaborators and friends who trust, work, and put all their heart into finding a way to overcome all the obstacles that we meet in the way. To my family, who has given all the support to make my dreams come true.*





## CONTENT TABLE

<b>1</b>	<b>INTRODUCTION.....</b>	<b>1</b>
1.1	THEORETICAL FRAMEWORK .....	2
1.2	MAGNETISM AND MAGNETIC FIELD (MF) .....	4
1.2.1	MAGNETIC FIELD .....	4
1.2.2	BIOT - SAVART .....	4
1.2.3	AMPERE'S LAW .....	6
1.2.4	APPLICATIONS OF THE BIOT - SAVART AND AMPERE .....	7
1.2.5	FARADAY LAW .....	9
1.2.6	INDUCTANCE .....	10
1.2.7	AC CIRCUITS.....	10
1.2.8	QUASI STATIONARY AC CIRCUITS.....	10
1.2.9	MAGNETIC FIELD IN A COPPER WINDING'S VORTEX-TYPE COIL .....	11
1.3	MAGNETIC FIELD AND CONTRAST AGENTS.....	12
1.4	CELL GROWN BEHAVIOR UNDERGOING RANDOM SEGMENTS OF OSCILLATING MAGNETIC FIELD .....	13
1.5	MAGNETIC EXPOSURE SYSTEM TO STIMULATE HUMAN LYMPHOCYTE PROLIFERATION .....	14
1.6	INCREASING SURVIVAL IN KIDNEY HEK-293T CELLS IN THE PRESENCE OF MAGNETIC FIELD VORTICES AND NANO-FLUID .....	15
1.7	JUSTIFICATION .....	15
1.8	GENERAL OBJECTIVE.....	15
1.9	SPECIFIC OBJECTIVES .....	16
<b>2</b>	<b>MATERIALS AND METHODS .....</b>	<b>17</b>
2.1	DESIGN STIMULATION SCHEME .....	18
2.1.1	BLOCK DIAGRAM.....	18
2.2	DEVELOPMENT OF ELECTRONIC INSTRUMENTATION SYSTEM .....	18
2.2.1	HARDWARE DESCRIPTION .....	19
2.2.2	MAGNETIC FIELD SOURCE.....	19
2.2.3	DEVICE CHARACTERIZATION .....	20
2.2.4	TESTING AND IMPROVING ELECTRONIC INSTRUMENTATION SYSTEM .....	24
2.3	SYSTEM FOR ELECTROCHEMICAL MEASUREMENT .....	24
2.3.1	ELECTROCHEMICAL SENSOR REDESIGN .....	27
2.3.2	DATA ACQUISITION.....	28
2.4	DEVELOPMENT AND IMPLEMENTATION OF THE CONTROL ALGORITHM.....	29
2.4.1	PID CONTROLLER VARIABLE INTERCONNECTABLE.....	29
2.4.2	HARDWARE DEVELOPMENT .....	31
2.5	CELL GROWN BEHAVIOR UNDERGOING RANDOM SEGMENTS OF OSCILLATING MAGNETIC FIELD .....	32

2.6 MAGNETIC EXPOSURE SYSTEM TO STIMULATE DOUBLE NUCLEI CELL DIVISION .....	34
2.6.1 CELL CULTURE AND DIFERENTIATION.....	34
2.6.2 MAGNETIC COIL.....	35
2.6.3 MAGNETIC STIMULATION SYSTEM.....	35
2.6.4 CELL STIMULATION .....	35
2.6.5 MEASUREMENT AND ANALSYIS.....	36
2.7 BIOLOGICAL EFFECT OF MF ON AMOEBIC SPECIES AND PERIPHERAL AND MONONUCLEARBLOOD CELLS .....	39
2.7.1 PERIPHERAL AND MONONUCLEAR BLOOD CELL PURIFICATION AND CARBOXYFLUORESC EIN SUCCINIMIDYL ESTER (CFSE) LABELING .....	39
2.7.2 IN VITRO STIMULATION WITH CONCANAVALIN A AND EXPOSITION TO MAGNETIC FIELD .....	39
2.7.3 GROWTH MEDIUM .....	40
2.7.4 CULTURE AND MAINTENANCE OF AMOEBIC STRAINS.....	41
2.7.5 MAGNETIC INDUCTION EQUIPMENT.....	41
2.7.6 MAGNETIC INDUCTION TRIALS .....	41
2.7.7 EFFECT OF MF ON AMOEBIC GROWTH.....	42
2.7.8 EFFECT OF MF ON AMOEBIC ERYTHROPHAGOCYTOSIS.....	42
2.7.9 EFFECT OF MF ON GADOLINIUM AND AMOEBIC AGGLUTINATION .....	42
2.7.10 DETERMINATION OF THE SUBCELLULAR DISTRIBUTION OF GD IN THE TROPHOZOITES.....	43
2.7.11 STATISTICAL ANALYSIS .....	43
2.8 PORTABLE DEVICE FOR MAGNETIC STIMULATION: ASSESSMENT SURVIVAL AND PROLIFERATION IN HUMAN LYMPHOCYTES.....	43
2.8.1 HARDWARE DESCRIPTION .....	43
2.8.2 SOFTWARE .....	44
2.8.3 MAGNETIC FIELD SOURCE.....	44
2.8.4 DEVICE CHARACTERIZATION .....	44
2.8.5 PERIPHERAL AND MONONUCLEARBLOOD CELL PURIFICATION AND FICOLL-HYPAQUE LABELING.....	46
2.8.6 IN VITRO STIMULATION WITH CONCANAVALIN A AND EXPOSITION TO MAGNETIC FIELD .....	48
2.9 INCREASING SURVIVAL IN KIDNEY HEK-293T CELLS IN PRESENCE OF MAGNETIC FIELD VORTICES AND NANO-FLUID .....	49
2.9.1 NANO-FLUID.....	49
2.9.2 MAGNETIC FIELD SOURCE.....	49
2.9.3 SOFTWARE .....	49
2.9.4 PROTOCOL.....	49
2.9.5 MAGNETIC FIELD STIMULATION .....	50

3.1	INSTRUMENTATION .....	50
3.2	CELL GROWN BEHAVIOR UNDERGOING RANDOM SEGMENTS OF OSCILLATING MAGNETIC FIELD .....	50
3.3	MAGNETIC EXPOSURE SYSTEM TO STIMULATE DOUBLE NUCLEI CELL DIVISION .....	53
3.3.1	EFFECT OF GD AND MF ON AMOEBIC GROWTH .....	55
3.3.2	EFFECT OF MF AND GD ON AMOEBIC ERYTHROPHAGOCYTOSIS .....	58
3.3.3	EFFECT OF MF ON GD AND AMOEBIC AGGLUTINATION .....	65
3.3.4	EFFECT OF SUGARS, GD AND AGGLUTINATION MF ON AMEBIC .....	67
3.4	PORTABLE DEVICE FOR MAGNETIC STIMULATION: ASSESSMENT SURVIVAL AND PROLIFERATION IN HUMAN LYMPHOCYTES.....	70
3.5	INCREASING SURVIVAL IN KIDNEY HEK-293T CELLS IN PRESENCE OF MAGNETIC FIELD VORTICES AND NANO-FLUID .....	71
3.6	APPLICATION OF INSTRUMENTATION FOR OTHER RESEARCH AREAS .....	73
3.6.1	DEVICE TO EVOKE THE BONE SYSTEM IN HIP DISLOCATION DIAGNOSIS .....	73
3.6.2	MEASURING GASTROESOPHAGEAL REGION FREQUENCIES: PRELIMINARY RESULTS .....	74
3.6.3	BIOMAGNETIC VALIDATION TO SKIN LEVEL FOR BLOOD PRESSURE CURVES AND VENOUS PRESSURE.....	75
3.6.4	EFFECT OF THE MICRO-MAGNETIC STIMULATION ELECTROENCEPHALOGRAPHIC PATTERNS.....	78
4	CONCLUSION AND DISCUSSION .....	79
4.1	EFFECT OF MF AND GD ON AMOEBIC CULTURES .....	79
4.2	DETERMINATION OF GD IN CELL SAMPLES .....	80
4.3	PORTABLE DEVICE FOR MAGNETIC STIMULATION: ASSESSMENT SURVIVAL AND PROLIFERATION IN HUMAN LYMPHOCYTES.....	80
4.4	INCREASING SURVIVAL IN KIDNEY HEK-293T CELLS IN PRESENCE OF MAGNETIC FIELD VORTICES AND NANO-FLUID .....	81
4.5	APPLICATION OF INSTRUMENTATION FOR OTHER RESEARCH AREAS .....	82
4.5.1	DEVICE TO EVOKE THE BONE SYSTEM IN HIP DISLOCATION DIAGNOSIS .....	82
4.5.2	MEASURING GASTROESOPHAGEAL REGION FREQUENCIES: PRELIMINARY RESULTS .....	82
4.5.3	BIOMAGNETIC VALIDATION TO SKIN LEVEL FOR BLOOD PRESSURE CURVES AND VENOUS PRESSURE.....	82
4.5.4	EFFECT OF THE MICRO-MAGNETIC STIMULATION ELECTROENCEPHALOGRAPHIC PATTERNS.....	83
5	PERSPECTIVES .....	84
6	BIBLIOGRAPHY .....	85

7	ANNEXES .....	90
7.1	APPLICATION OF INSTRUMENTATION FOR OTHER RESEARCH AREAS .....	90
7.1.1	ELECTRO-ACOUSTIC DEVICE FOR BONE DISEASE DIAGNOSIS .....	90
7.1.2	MEASURING GASTROESOPHAGEAL REGION FREQUENCIES: PRELIMINARY RESULTS .....	96
7.1.3	BIOMAGNETIC VALIDATION TO SKIN LEVEL FOR BLOOD PRESSURE CURVES AND VENOUS PRESSURE.....	97
7.1.4	EFFECT OF THE MICRO- MAGNETIC STIMULATION ELECTROENCEPHALOGRAPHIC PATTERNS.....	99
7.1.5	FARADAY EFFECT SENSOR.....	101
7.2	PATENTS AND PUBLICATIONS .....	103

## 1 INTRODUCTION

This thesis has the objective to determine the effect produced by weak magnetic field stimulation on the following types of cell cultures: *Entamoeba histolytica*, *Entamoeba invadens*, human lymphocyte, and HEK-293T. Changes in cell's proliferation and longevity without affecting their viability are thus studied. We intend to understand the effect produced by the magnetic field and gadolinium in the different levels of cell organization (organelle, macro molecules, and chemical reactions).

We are mainly interested in asserting the behavior of cells in a controlled manner, for example when applying oscillating magnetic fields at different frequencies and time intervals as well as the addition of certain concentrations of super-paramagnetic fluid in the growing medium.

Here I present effects on the cell motility of *Entamoeba invadens* cell cultures and the change in the natural cell behavior, such as controlled agglutination, cell movement velocity, membrane structural form. I also present the effects and dynamic responses on the growth of *Entamoeba* cells by applying an oscillating magnetic field in specific audio frequencies such as 100 Hz, 800 Hz, 1500 Hz, and 2500Hz, at six minutes time periodic intervals.

In addition to this I carried out experiments on human lymphocyte. The experiments have three steps. The first step was divided in three different tests. The first test consisted in a control cell culture. The second test consisted on a series of magnetic stimulation and the third one consisted on magnetic stimulation and super-paramagnetic fluid markers. In the second step cell cultures were incubated. In the last stage I have made a cytometry analysis. Now the interest was centered on cell division cycle. To analyze the test effect on cell division, a histogram was obtained from flow cytometry analysis, the cells being donated by volunteer patients. In spite of the application of magnetic fields and after incubation, cell viability was still observed.

The same technique of flow cytometry was used to analyze the growth effect on cell cultures of HEK-293T, a transformed mammalian cell line. It shows different effects done, while changing the magnetic field and super-paramagnetic fluid, without variation on other experiment conditions.

A study on the viability of cell line HEK-293T under the presence of oscillating magnetic fields is presented. It can be noticed that paramagnetic fluids were also present in the culture medium.

A characterization of the main parameters applied in the experiments was done. I also have theoretically estimated the sinusoidal magnetic field applied on the cell culture, and calculated the applied magnetic fields by the measurement of the electric current and the total impedance,  $|Z|$ , of the circuit. Concentration measurements of the used super-paramagnetic fluid Dotarem were also carried out obtaining the energy dispersive X ray fluorescence spectrum (EDXFS) to corroborate the quantity of gadolinium present on the contrast agent.

New specific instrumentation was designed, to give the proper cell culture environment conditions. It consist of controlling parameters such as temperature, proper space for the cell culture area, and efficient magnetic field distribution and form. This instrumentation is robust, so it can be used in other biomedicin areas (hip dislocation diagnosis, the measurement of gastroesophageal

region frequencies to understand the metabolism dynamic, the abstention of blood pressured curves at skin level, and the effect of micro magnetic stimulation as a therapeutic method against depression with a minimum of modifications.

I'm pleased to know that the technique developed during my thesis research that permits cell culture proliferation has been well received by other research groups.

## 1.1 THEORETICAL FRAMEWORK

In biomedical research, bio-electromagnetics is a determining factor for a better understanding of the fundamental mechanisms of communication and regulation levels ranging from the intracellular to the organic as all living things have, and to distribute these special effects through the nervous system so that they present throughout the body. A better understanding of the fundamental mechanisms of the interaction of electromagnetic fields (EMF) could lead directly to major advances in diagnostic methods and treatment of various diseases.

The bio-electromagnetics (BEM) is an emerging science that studies how living organisms interact with EMF; electrical phenomena are found in all living organisms. Moreover, there are electric currents in the body that produce magnetic fields that extend beyond the body. Consequently, Agents may also be influenced by external magnetic and electromagnetic fields. Changes in the bodies under natural fields may produce physical and behavioral changes. To understand how these fields can affect the body, it is useful to first discuss some basic phenomena associated with EMF.

The following studies have demonstrated accelerated healing of soft tissue wounds using direct current (DC), Electromagnetic fields, and electrochemical methods (1).

Pulsed electromagnetic field (PEMF) has been used clinically in the treatment of skin's venous ulcers. The results of double-blind studies demonstrated that PEMF stimulation promotes cell activation and proliferation through an effect on the cell membrane, particularly on endothelial cells (2).

Application of EMF and Radio frequency (RF) may accelerate wound healing (3). Under the skin, wounds have specific electrical potentials and currents. So EMF can aid in the healing process by inducing de-differentiation (*i. e.*, the conversion to a more primitive form) of neighboring cells, followed by rapid cell proliferation (4).

During the last two decades, the effects of exposure to EMF by the immune system and its components have been studied extensively. Although early studies indicated that long-term exposure to EMF could adversely affect the immune system, there are promising new studies indicating that applied EMF could modulate immune beneficial responses. For example, studies with human lymphocytes showed that exogenous EM and magnetic fields can cause changes in the calcium transport (5) and cause a mediated mitogenic response (*i. e.*, the stimulation of cell nuclei dividing certain types of immune system cells that begin to divide and multiply rapidly in response to certain stimuli, or mitogen). This discovery has led to conducting research about the potential increased by applying EMF from a population of immune cells, called natural killer cells (or NK cells), which have great importance in helping the body fight cancer and other viruses (6).

Some systems, like the magnetic coil stimulation circuit design and a mathematical analysis, show how the voltage increases proportionally with a membrane in the charging circuit of a typical electrical magnetic stimulator. The analysis shows how the membrane stress is related to energy, stamina, and the resonant frequency of the load circuit supply. There is an optimal resonance frequency for some nerve membrane depending on its time constant capacity time. The analysis also shows why greater membrane tension will be seen recorded in the second phase of a biphasic excitation pulse.

Limitations are in three typical level of voltage, current, and a silicon controlled rectifiers (SCR). The switching time is specified by key components, such as capacity and the choice of coil turns. Optimum resonant frequency occurs between the end of 4 kHz and 20 kHz, with a small monotonic decrease after 10 kHz. Kent R. Davey *et al.* US6527695 B1.

In this respect, it may be said that in this project the system used can cover frequency ranges of 15 Hz to 20 kHz, cover a broader spectrum to its application, and provide an oscillating sine wave, which is not affected in terms of power. In addition to the monotonous diminution of the invention mentioned above, by the power stage control is done using high current MOSFETs, which are used in half rang power electronics to produce an optimal switching. It is not necessary to force the circuit with other solid state devices for enabling the switching as is necessary when working with drivers such as SCR silicon.

The biological effects of magnetic fields have been extensively studied in recent years, however, information regarding cell abnormalities caused by magnetic frequencies remains controversial.

In this thesis, some cellular responses of *E. histolytica* *E. invadens* when exposed to magnetic fields are studied, in order to analyze the behavior of these pathogens and increase knowledge on the biology of these organisms.

Biological side effects in systems exposed to a magnetic field have been studied in the last decades. Many studies were published about the magnetic stimulation on the algal growth and its nutrition composition. Thus being, the ability of prokaryotic microorganisms to activate strategies in adapting themselves to the environmental stress induced by exposure to extremely low frequency electromagnetic fields, the growth of yeasts, and the magnetic field effect in children with acute lymphoblastic leukemia, among others (7,8).

The implementation of portable magnetic stimulating devices, for the evaluation of positive growth effects on cells, is presented. To evaluate this instrumentation there were several studies, like the evaluation of the effect that the magnetic field produces in human lymphocytes; the study made from healthy volunteer donors; the effect of magnetic field exposition by flow cytometry (proliferation and cell survival), which is an instrument largely used in biomedical applications to determine cell division; the clinical pathology in immunology; the analysis of bacteria; the mammalian sperm in the areas of reproductive toxicology; the identification of neoplastic marker probes for DNA-diploid disease; and so many other areas where cellular systems are involved (9–11).

The purpose of this work is to achieve an understanding of interactions produced between MF and biological systems. These depend on various factors, such as a) the duration of time that the



biological system is subjected to MF, b) the penetration of MF in biological tissues, c) the generation of heat in the tissue affected by the MF (which is related to the frequency and intensity of the MF), d) the type of MF, and f) the state in which cells are being exposed to MF (12).

## 1.2 MAGNETISM AND MAGNETIC FIELD (MF)

### 1.2.1 MAGNETIC FIELD

As the electric field, the magnetic field is a vector field, *i.e.*, vector quantity is associated with each point in space. The magnetic induction vector, or magnetic field  $\vec{B}$ , occurs when there are moving electric charges (current flows), unlike the electric field, that can occur in the presence of static charges. All magnetic fields can be represented by field lines. The field direction is indicated by the direction of the field lines and the magnitude of the field by its density.

Considering the direction of the field as the north pole of the needle of a compass, you can check that it meets the right hand rule: If you place your thumb in the direction of the current, the fingers that wrap the driver show the magnetic field lines.

### 1.2.2 BIOT - SAVART

After the discovery of Oersted in 1820, Jean Baptiste Biot and Felix Savart reported that a stable current conductor produces forces on a magnet. Experimental results from Biot and Savart reached an expression from the magnetic field obtained at a given point in space, this in terms of the current producing the field.

Biot Savart's law states that the magnetic field  $d\vec{B}$  produced at point named  $P$  by the current differential element  $I d\vec{l}$  is proportional to the product  $I d\vec{l}$  and the sine  $\alpha$  of the angle, between the element and the line joining  $P$  to the element, and is inversely proportional to the square of the distance  $R$  between  $P$  and element.

$$d\vec{B} \propto \frac{\mu_0 I d\vec{l} \sin(\alpha)}{R^2}, \quad (1)$$

Where  $\mu_0$  is the permeability of free space:

$$\mu_0 = 4\pi \times 10^{-7} = 12.6 \times 10^{-7} \text{ N/A}^2$$

Which means:

$$d\vec{B} = \frac{\mu_0 k I d\vec{l} \sin(\alpha)}{R^2}, \quad (2)$$

Where  $k$  is the proportionality constant  $k = 1/4\pi$ , then equation 2 becomes:

$$d\vec{B} = \frac{\mu_0 I d\vec{l} \sin(\alpha)}{4\pi R^2}, \quad (3)$$

From the definition of the cross product between two vectors, Equation 3 is expressed in vector form as:

$$d\vec{B} = \frac{\mu_0 I d\vec{l} \times \hat{a}_R}{4\pi R^2} = \frac{\mu_0 I d\vec{l} \times \vec{R}}{4\pi R^3}, \quad (4)$$

Let  $R = |\vec{R}|$  and  $\hat{a}_R = \frac{\vec{R}}{R}$ ,

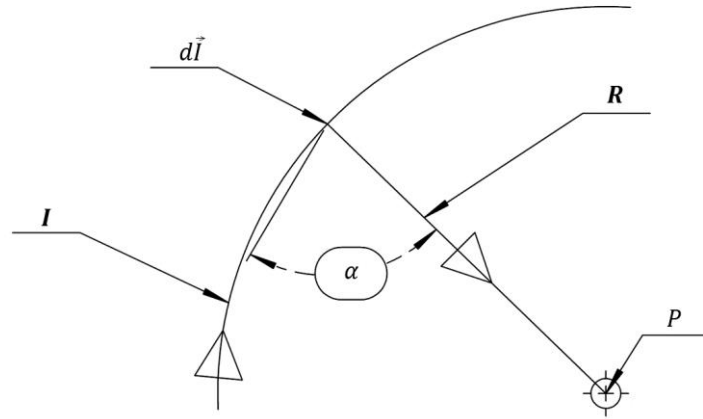


Figure 1.1 Magnetic field  $d\vec{B}$  in  $P$  due to the current distribution  $I d\vec{l}$

And due to current distributions, it can be defined  $\vec{K}$  as the superficial current density, and  $\vec{J}$  as

the volumetric current density. So it can be a relation in those elements as:

$$Id\vec{l} \equiv \vec{K}dS = \vec{J}dv, \quad (5)$$

In terms of sources of distributions of current, Biot-Savart law can be written in different ways.

Current lines:

$$\vec{B} = \int_L \frac{\mu_0 Id\vec{l} \times \hat{a}_R}{4\pi R^2}, \quad (6)$$

Current surface:

$$\vec{B} = \int_S \frac{\mu_0 \vec{K}d\vec{S} \times \hat{a}_R}{4\pi R^2}, \quad (7)$$

Volume of Current:

$$\vec{B} = \int_v \frac{\mu_0 \vec{J}d\vec{v} \times \hat{a}_R}{4\pi R^2}. \quad (8)$$

---

### 1.2.3 AMPERE'S LAW

Ampere's law states that the circulation of the magnetic field around a closed path is equal to the net current that runs along the way. Mathematically, Ampere's law can be expressed as follows:

$$\oint \vec{B} \cdot d\vec{l} = \mu_0 I_{enc}, \quad (9)$$

Expressing the current enclosed as the surface integral of the current density, then

$$\oint \vec{B} \cdot d\vec{l} = \int \mu_0 \vec{J} \cdot d\vec{S}, \quad (10)$$

Ampere's law is similar to Gauss's Law for the electric field, and is applied in a simple way to determine the magnetic field when current distributions are symmetric. In differential form it is expressed as:

$$\vec{\nabla} \times \vec{B} = \mu_0 \vec{J}, \quad (11)$$

This equation is only valid for stationary fields; when this ratio contain fields that vary over time errors are obtained. Maxwell corrected this equation to fit non-stationary fields:

$$\vec{\nabla} \times \vec{B} = \mu_0 \left( \vec{J} + \frac{d\vec{D}}{dt} \right), \quad (12)$$

Where  $\vec{J}_d = d\vec{D}/dt$  is referred to as displacement current density, while  $\vec{J}$  is the conduction current density.

## 1.2.4 APPLICATIONS OF THE BIOT - SAVART AND AMPERE

### 1.2.4.1 A TOROIDAL MAGNETIC FIELD

A toroid comprises  $N$  turns of wire around a hoop. To calculate the magnetic field within the toroid, Ampere's law applied to Equation 8. Note that the path encloses  $N$  turns, each of which carries current  $I$ , therefore the net current is enclosed  $NI$ , then taking,

$$\oint \vec{B} \cdot d\vec{l} = \mu I_{enc} \rightarrow B \cdot 2\pi r = \mu_0 NI, \quad (13)$$

$$B = \frac{\mu_0 NI}{2\pi r}, \quad (14)$$

where  $r$  is the mean radius of the toroid. This result demonstrates that the magnetic field varies within the toroid as  $1/r$ , therefore it is not uniform. However, if  $r$  is large compared to the radius of the cross section of the toroid, then the field is considered approximately uniform.

In the case that the torus is outside the net current enclosed by an amperian path:

$$NI - NI = 0 \rightarrow \vec{B} \quad (15)$$

Due to each toroid coil passing twice through the closed path carrying opposite currents.

### 1.2.4.2 MAGNETIC FIELD OF A STRAIGHT THIN THREAD

If the contribution of  $d\vec{B}$  in point  $P$  because of element  $d\vec{l}$

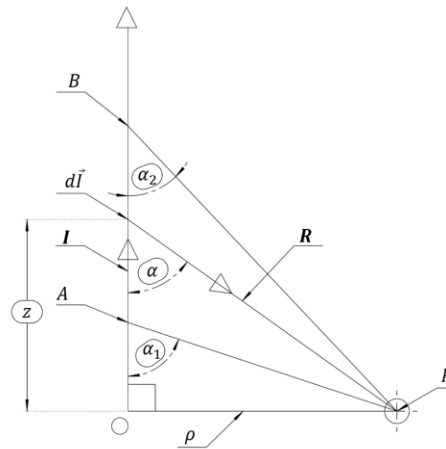


Figure 1.2 Magnetic field  $d\vec{B}$  in  $P$  in the straight of a thin thread

is considered and taken into account in the Biot-Savart equation 2.3, the result is:

$$d\vec{l} = \hat{a}_z dz \text{ and } \vec{R} = \rho \hat{a}_\rho - z \hat{a}_z, \quad (16)$$

Therefore  $d\vec{l} \times \vec{R} = \rho dz \hat{a}_\phi$ , so that:

$$\vec{B} = \int \frac{\mu_0 I \rho dz}{4\pi [\rho^2 + z^2]^{3/2}} \hat{a}_\phi, \quad (17)$$

Making a change of variable:  $z = \rho \cot(\alpha)$  y  $dz = -\rho \csc^2(\alpha) d\alpha$

$$\vec{B} = \int_{\alpha_1}^{\alpha_2} -\frac{\mu_0 I \rho^2 \csc^2(\alpha) d\alpha}{4\pi \rho^3 \csc^2(\alpha)} \hat{a}_\phi, \quad (18)$$

$$\vec{B} = -\frac{\mu_0 I}{4\pi \rho} \int_{\alpha_1}^{\alpha_2} \sin(\alpha) d\alpha \hat{a}_\phi, \quad (19)$$

$$\vec{B} = \frac{\mu_0 I}{4\pi \rho} (\cos(\alpha_2) - \cos(\alpha_1)) \hat{a}_\phi. \quad (20)$$

#### 1.2.4.3 MAGNETIC FIELD AT A POINT ON THE AXIS OF A CURRENT LOOP

Now to calculate the magnetic field at a point on the axis of a circular current loop.

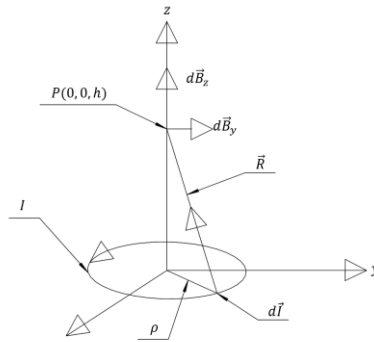


Figure 1.3 Magnetic field  $d\vec{B}$  in  $P$  in a circular current loop

Consider equation 3 again, then

$$d\vec{l} = \rho d\phi \hat{a}_\phi, \quad (21)$$

and  $\vec{R} = -\rho\hat{a}_\rho + h\hat{a}_z$  results in:

$$d\vec{l} \times \vec{R} = \rho h d\phi \hat{a}_\rho + \rho^2 d\phi \hat{a}_z, \quad (22)$$

$$d\vec{B} = \frac{\mu_0 I}{4\pi[\rho^2 + h^2]^{3/2}} (\rho h d\phi \hat{a}_\rho + \rho^2 d\phi \hat{a}_z), \quad (23)$$

By symmetry, contributions over  $\hat{a}_\rho$  are canceled and only taken into account contributions from  $\hat{a}_z$ , so what is obtained is:

$$\vec{B} = \int d\vec{B}_z \hat{a}_z = \int_0^{2\pi} \frac{\mu_0 I \rho^2 d\phi}{4\pi[\rho^2 + h^2]^{3/2}} \hat{a}_z = \frac{\mu_0 I \rho^2 2\pi}{4\pi[\rho^2 + h^2]^{3/2}} \hat{a}_z, \quad (24)$$

What finally remains as:

$$\vec{B} = \frac{\mu_0 I \rho^2}{2[\rho^2 + h^2]^{3/2}} \hat{a}_z. \quad (25)$$

---

### 1.2.5 FARADAY LAW

Faraday, Henry, and others' experiments demonstrated that if the magnetic flux through a circuit varies, an *emf* that is equal in magnitude to the variation per unit time of the induced flow in the circuit is induced. This statement is known as the Faraday induction law and can be expressed as:

$$\xi = -\frac{d\phi_m}{dt}, \quad (26)$$

where  $\phi_m = \int \vec{B} \cdot d\vec{S}$  is the magnetic flux.

The meaning of a negative sign of Faraday's law of induction is a consequence of Lenz's Law, which is expressed as the induced *emf* and current have a direction as tends to oppose the change that produces them. In its integral form, the induction law of Faraday has the following form:

$$\oint \vec{E} \cdot d\vec{l} = -\frac{d}{dt} \int \vec{B} \cdot d\vec{S}, \quad (27)$$

The electric field is not conservative; it varies with time and is generated by varying a magnetic field. The difference form of Faraday's Law can be obtained via the Stokes theorem:

$$\vec{\nabla} \times \vec{E} = -\frac{d\vec{B}}{dt}. \quad (28)$$

---

### 1.2.6 INDUCTANCE

By passing through a conductor an electric current, a magnetic field in its vicinity is produced, which is constant while the current is still flowing. In the case where  $I$  varies with time, it gives be a variable magnetic field, which would result in temporal variation of magnetic flux on the circuit itself and as a consequence, self-induced *emf*, which according to Faraday's Law gives:

$$\xi = -\frac{d\phi_m}{dt} = -\frac{d(LI)}{dt} = -L \frac{dI}{dt}, \quad (29)$$

The constant proportionality  $L = \frac{\phi_m}{I}$ , is the inductance of the circuit.

---

### 1.2.7 AC CIRCUITS

AC circuits are used in various systems for electric power distribution, communication systems, as well as in a variety of electric motors. In alternating current intensity, the direction in a conductor as a result of periodical change of polarity from the voltage applied at the ends of said conductor periodically changes. Although there are many types of signals which can be used in alternating current (AC) circuits, for instance, saw-tooth, square, and triangle, sinusoidal signals are the most used.

The sine wave voltage, or current, may be expressed as follows:

$$i(t) = i_0 \sin(\alpha), \quad (30)$$

$$v(t) = v_0 \sin(\alpha), \quad (31)$$

The angle is given by  $\alpha = \omega t$ , where  $\omega = 2\pi f$  the angular velocity in radians per second.

---

### 1.2.8 QUASI STATIONARY AC CIRCUITS

For very high frequencies, alternating current cannot be underestimated. The speed of propagation of electromagnetic fields and the displacement current (Ampere-Maxwell Law), mean that only conducting currents generates the magnetic field.

The main restriction to be imposed so that the current in the circuit can be called slow variations current, is that the circuit will not radiate an appreciable amount of power.

This constraint can be met by requiring the greatest linear dimension of the system, which is much smaller than the wavelength in free space associated with the exciting frequency, that is:

$$l_{\max} \ll \frac{2\pi c}{\omega}, \quad (32)$$

$$\omega \ll \frac{2\pi c}{l_{\max}}. \quad (33)$$

### 1.2.9 MAGNETIC FIELD IN A COPPER WINDING'S VORTEX-TYPE COIL

To calculate a first approximation of the magnetic field in the center of a Copper winding's vortex-type coil, first the magnetic field at the center of a regular polygon must be understood.

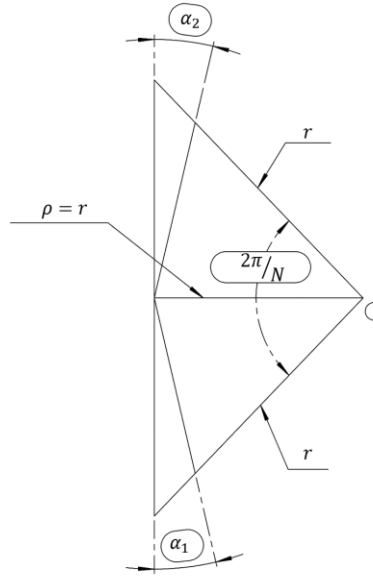


Figure 1.4 Circumscribe polygon of  $N$  sides

Considering that the magnetic field at the center of a regular polygon has a circumscribed circle of a polygon with  $N$  sides, what is obtained is:

$$\frac{360^\circ}{N} = \frac{2\pi}{N}, \quad (34)$$

And taking the result to the current thread like a conductor, Eq. (19) must be:

$$\alpha_2 = 90^\circ - \frac{\pi}{N}, \text{ and } \alpha_1 = 90^\circ + \frac{\pi}{N}. \quad (35)$$



Hence the magnetic field in the center of the polygon is expressed as:

$$\vec{B} = \frac{\mu_0 IN}{2\pi r} \sin\left(\frac{\pi}{N}\right). \quad (36)$$

#### 1.2.9.1 MAGNETIC FIELD AT THE CENTER OF A COPPER WINDING'S VORTEX-TYPE COIL

According to the coil geometry, a dodecagon approximation was performed to calculate the magnetic field at the center. Considering Equation 35, the field at the center of a dodecagon is expressed as:

$$\vec{B} = \frac{6\mu_0 I}{\pi r} \sin\left(\frac{\pi}{12}\right), \quad (37)$$

Taking in consideration that each side of the polygon has n turns it can be assumed that:

$$\vec{B}_1 = n \left[ \frac{6\mu_0 I}{\pi r} \sin\left(\frac{\pi}{N}\right) \right] \quad (38)$$

The copper winding's vortex-type coil is formed by two dodecagon shaped coils connected in series. Therefore by using the principle of superposition, the total magnetic field obtained is:

$$\vec{B} = \vec{B}_1 + \vec{B}_2, \quad (39)$$

### 1.3 MAGNETIC FIELD AND CONTRAST AGENTS

Since the commercialization of Magnevist Trademark in 1988, compounds of gadolinium (Gd) is used as contrast media for magnetic resonance imaging (MRI). Thanks to the para-magnetic properties of this chemical element, better and proper visualization and characterization of neoplastic and inflammatory processes are allowed by using this diagnostic technique. Gd increases the relaxation of hydrogen protons aligned by the magnetic field effect within the chamber of NMR equipment. This relaxation causes an increase in signal intensity at sites along where Gd is deposited. One of the advantages of the Gd is its ability to form organic compounds that decrease cellular uptake.

Gd belonging to the rare earth groups and being in the nature of gadolinium or gadolinium oxide (Gd<sub>2</sub>O<sub>3</sub>), also has eight isotopes. Its' name comes from the Swedish scientist, J. Gadolin. Para-magnetic metal is gadolinium and becomes strongly ferromagnetic at temperatures below 20°C.

## 1.4 CELL GROWN BEHAVIOR UNDERGOING RANDOM SEGMENTS OF OSCILLATING MAGNETIC FIELD

Entamoeba cells, caused from amoebic dysentery, are highly motile. This motility is an essential feature of the pathogenesis and morbidity of amoebiasis (13). Here, we present a method to reduce the cell motility on Entamoeba invadens cell culture and the change in the natural cell behavior, such as controlled agglutination, cell movement velocity, and membrane structural form by applying an oscillating magnetic field in specific audible frequencies at periodic time lapses to manage the cell dynamic response (14).

Table 1.1. Some properties of Gadolinium

Name	Gadolinium	Symbol	Gd
Atomic number	64	Atomic mass (g/mol)	157,25
Valence	3	Oxidation state	+3
Electro-negativity	1,1	Density (g/ml)	7,89
Covalent Radio (Å)	1,61	Ionic Radio (Å)	1,02
Atomic Radio (Å)	1,79	Curie point (°K)	16
Boiling point (°C)	3000	Fusion Point (°C)	1312

Amoeboid motility requires spatiotemporal coordination of biochemical pathways regulating force generation and consisting of the quasi-periodic repetition of a motility cycle that is driven by acting polymerization and actomyosin contraction.

Entamoeba motility and chemo-taxis have been studied by using relatively few methods, including haemocytometers, tube migration, and Boyden chamber assays. Under the first two conditions, cells have almost no resistance to their movement except substrate adhesion. During invasive disease, however, amoebae move in more restrictive conditions, similar to metastasis and extravasation. Under-agarose (under-agar) assays provide such an environment and have been used to study the motility and chemo-taxis of a variety of cells, including neutrophils, macrophages, and the free-living amoeba Dictyostelium, an evolutionary relative of Entamoeba. Under-agar assays have the added advantage of allowing moving cells to be visualized and parameters, such as cell shape, to be studied in detail.

Biomedical effects of low frequency electromagnetic fields (LEMF) on signal transduction have gained considerable interest, as shown in the results obtained from various point species' possible interaction between LEMF and ion transport mechanisms in the cell membrane (15,16).

Some of this LEMF is the Magnetic Field (MF), generated by copper coils and powered with alternating current energy in a specific oscillating frequency. Now, this technique is applied to study the cell movement behavior, working in ranges of audible frequencies, and the effects of this magnetic field stimulation; and to consider the results obtained to understand more of the cell behavior, specifically in their dynamics and cellular cycle.

Amoeboid cells moving on a planar substrate exhibit oscillations in cell velocity and shape. Cells protrude a pseudo-pod in the front that attaches to the substrate, forming new adhesions (17). The ensuing contraction breaks the adhesion at the back of the cell causing its retraction and the cycle repeats with a well-defined average period. This process is mainly driven by the coordinated turnover of the filamentous actin (F-actin), the F-actin directed non muscular myosin II complex (MyoII) Actin filament length that is regulated by capping proteins (18), and the mechanical properties of F-actin that are modulated by actin binding and cross-linking proteins.

## 1.5 MAGNETIC EXPOSURE SYSTEM TO STIMULATE HUMAN LYMPHOCYTE PROLIFERATION

Magnetic stimulation (MS), a non-invasive technique to stimulate different kind of cells by a sinusoidal magnetic signal through a coil put on the scalp, has been widely used in studies on clinical treatments on humans(19,20). A biophysical mechanism underlying its effect is, however, largely unknown. Magnetic fields can generate a potential action in the cell structure, such as the effects including a long inhibitory period. In this study, we develop a method for magnetic stimulation of human Lymphocytes (21).

A device's instrumentation for magnetic stimulation on human lymphocytes is presented. This is a new procedure to stimulate growing cells with ferro-fluid in vortices from the magnetic field. The stimulation of magnetic vortices was provided at five different frequencies of 100, 800, 1500, 2450, and 2500 Hz. To improve the stimulation effects, a para-magnetic ferro-fluid was added on the cell culture medium. The results suggest that the frequency changes and the magnetic field variation produce an important increase on the number of proliferating cells, as well as in the cellular viability. This new magnetic stimulation modality could trigger an intracellular mechanism to induce cell proliferation and cellular survival only on mitogen stimulated cells (22).

The magnetic stimulation is a technique that has been used in different study areas, such as nuclear magnetic resonance and biomagnetic signals in magneto-encephalography, thus like the effect of magnetic field on living organisms for the fermentation process and some biological self-organization studies (23).

Biological side effects in systems exposed to a magnetic field have been studied in the last decades. Many studies were published about the magnetic stimulation on the algal growth and its nutrition composition, the ability of prokaryotic microorganisms to activate strategies in adapting themselves to the environmental stress induced by exposure to extremely low frequency electromagnetic fields, the growth of yeasts *Saccharomyces cerevisiae* (23,24), and the magnetic field effect in children with acute lymphoblastic leukemia, among others (17,23).

The implementation of a portable magnetic stimulating device for growing cells presented in this work was tested in a human lymphocytes pilot study from healthy volunteer donors. The effect of magnetic field exposition was analyzed by flow cytometry (25) (proliferation and cell survival), which is an instrument largely used in biomedical applications to determine cell division, clinical

pathology in immunology, analysis of bacteria, mammalian sperm in the areas of reproductive toxicology, identification of neoplastic marker probes for DNA-diploid disease, and so many other areas where cellular systems are involved (20).

## 1.6 INCREASING SURVIVAL IN KIDNEY HEK-293T CELLS IN THE PRESENCE OF MAGNETIC FIELD VORTICES AND NANO-FLUID

The subject of study in this work is the cellular line HEK-293T, this cell line is originally derived from epithelial human embryonic kidney (HEK) cells. The 293-T variant of this cell line is a line derived from HEK-293T, that also contains the SV40-T antigen (large T antigen of SV40 virus), which allows replication.

Here is discussed the effect of magnetic field vortices on kidney cell cultures of line HEK293T, samples in which paramagnetic fluid is added, as well as a survival analysis by a flow cytometry technique.

## 1.7 JUSTIFICATION

The biological effects of magnetic fields have been extensively studied in recent years, however, information regarding cell abnormalities caused by magnetic frequencies remains controversial.

Recently, the use of magnetic fields has increased for diagnostic and therapeutic purposes. To date, its effect on biota, which is present in the host, has been reported. It was found that 28.1% (100/356) of the sampled population were infected with protozoans. Females showed a higher infection rate (29.7%; 56/182) than males (26.4%; 46/174) and there was a significantly ( $P < 0.001$ ) higher prevalence in rural areas (38.7%; 55/142) than in urban areas (21.0%; 45/214). The 6 to 12 years age group had a significantly ( $P < 0.05$ ) higher infection rate (42.9%; 30/70). The total prevalence of intestinal protozoans was as follows: *E. histolytica* (24.4%), *E. coli* (11.2%), and *G. lamblia* (0.6%). The most prevalent morbidity effects associated with intestinal protozoan infections were abdominal pains, dysentery, and body weakness.

This research analyzes some cell cultures when exposed to magnetic fields, to help understand their behavior and to increase the knowledge of the biology of these organisms. This is done to provide tools that can help to fight against the pathogenesis caused by some organisms (26,27).

## 1.8 GENERAL OBJECTIVE

This research aims at the design of the instrumentation needed to study the effects observed in the experiments performed in cell culture with the application of magnetic fields.

Various types of cell cultures that have been selected to meet a condition, which is that of simplicity in their metabolism, have been undergone throughout this research, in order to better understand the effects that may occur to the stimulation of varying magnetic fields.

## 1.9 SPECIFIC OBJECTIVES

1. The development of the appropriate instrumentation for creating a magnetic stimulation system for cell cultures.
2. The study of the magnetic field effect on cell differentiation of human lymphocytes.
3. The determination of the effect of magnetic field and gadolinium concentration on the growth of *E. Histolytica* and strain HM1-IMSS, *E. invadens*, and IP-1 NY.
4. The evaluation of the process of erythrophagocytosis in both species, after subjecting them to magnetic field and to gadolinium.
5. To analyze the effect of the magnetic field on the binding gadolinium trophozoites of *E. histolytica* *E. Invadens*.

## 2 MATERIALS AND METHODS

An instrument and a procedure for magnetic stimulation on human lymphocytes is presented. This is a new procedure to stimulate growing cells with ferro-fluid in magnetic field vortices. The stimulation of magnetic vortices was provided at five different frequencies from 100, 800, 1500, 2450 and 2500 Hz and intensities from 1.13 to 4.13 mT. To improve the stimulation effects, a paramagnetic ferro-fluid was added on the cell culture medium.

A new scheme that allows stimulation frequency ranges to exceed was used to date, which is based on frequencies in the order of 15-7000 Hz.

Moreover, micro-controllers were used, to try to minimize the size of the stimulation system, with the aim of replacing, at some point, the computer use.

Inter connectable card PID control, from a microcontroller, has also been developed, to maintain stability in the variables that can potentially cause an error in obtaining the information, or that may cause an additional effect that can alter the results of the experimentation.

To perform the design of the instrumentation, I have visited two synchrotrons facilities, to learn from the instruments they already use. In addition, biological experiments in the field were performed to have the necessary experience at the time, to study undergone cells treated with magnetic stimulation system.

The instrumentation for magnetic stimulation on human lymphocytes is also presented. This new procedure stimulates growing cells with ferro-fluid in magnetic field vortices. The stimulation of magnetic vortices was provided at five different frequencies from 100 to 2500 Hz and intensities from 1.13 to 4.13 mT. A paramagnetic ferro-fluid was added on the cell culture medium to improve the stimulation effects. The results suggest that the frequency changes and the magnetic field variation produces an important increase in the number of proliferating cells, as well as in the cellular viability. This new magnetic stimulation modality could trigger an intracellular mechanism to induce cell proliferation and cellular survival only on mitogen stimulated cells (23).

Also presented here is a study to understand the mechanisms of interaction between biological tissue and the magnetic field, pointing to a range of biological effects in the short and long term. However, some are positively affected cell types, while others are inhibited.

The effect of the magnetic field and Gadolinium on the viability, growth, adhesion, and erythrophagocytosis of human pathogenic amoebic strain (*E. histolytica*) and reptile's pathogenic (*E. invadens*) was analyzed. The results show that both Gd, as MF, differentially affect growth and adhesion of the two erythrophagocytosis amoebian strains.

## 2.1 DESIGN STIMULATION SCHEME

To achieve this, a study of the state of the art in profound ways is first undertaken to determine the best design in structure, to perform better in the field of action, and to have better distribution of each of the components, same sizes, schemes, and communication protocols suitable for easy application and use.

### 2.1.1 BLOCK DIAGRAM

Instrumentation is monitored and controlled through an algorithm performed in assembly language, and installed in a microprocessor. This algorithm was designed to generate sinusoidal oscillations at different frequencies, it worked at frequencies of 100, 800, 1500, 2450, and 2500 Hz, in segments of 360 s each one; this frequency cycle was repeated four times in a pilot work. So the experimental sample group was stimulated for 2 h, see Figure 2.1

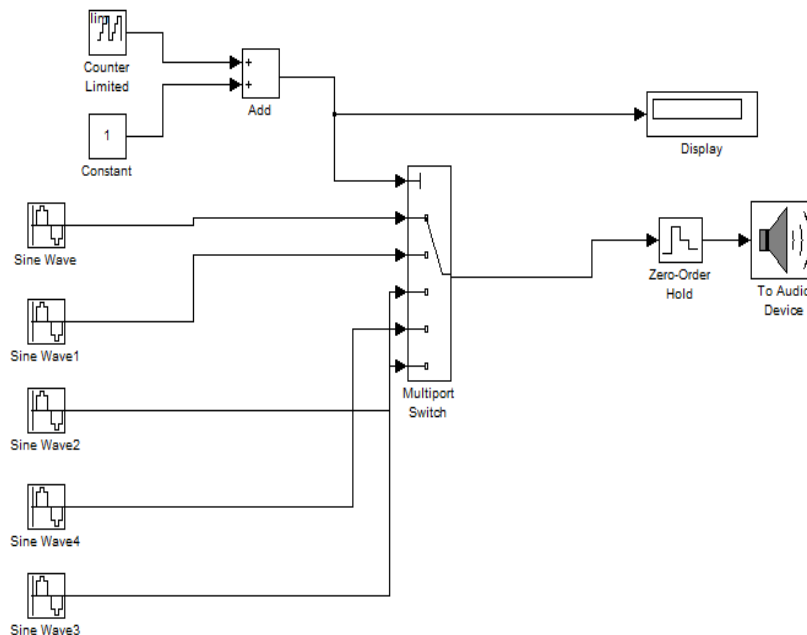


Figure 2.1 Signal generation block diagram, developed in MATLAB Simulink

## 2.2 DEVELOPMENT OF ELECTRONIC INSTRUMENTATION SYSTEM

Important parameters were considered in the system design to get an effective performance capable of providing strong security with regard to working conditions. The configuration shown be simple and miniaturized, representing a minimum cost for processing and having a modular design.

---

### 2.2.1 HARDWARE DESCRIPTION

There is a microprocessor containing an electronic stage for sine wave generation, which consists of a limited counter. Its design allows saving the parameters in an electronic memory, according to the frequency and the time intervals of the magnetic stimulation selected for the biological sample. Furthermore, the system permits setting different time intervals for each operating frequency previously designated. The switch exit is connected to a Fourier block diagram that converts a constant frequency value to an astern signal. In this block, other parameters can be established, such as the power, the central value for the signal, the RMS value, and the power of harmonics in sinusoidal signals. The output frequency generated is connected to an audio amplifier with the power of 1000 W and 12 V of amplitude, feeding a magnetic field source where the sample is deposited, see Figure 2.2.

---

### 2.2.2 MAGNETIC FIELD SOURCE

A coil system was assembled with two identical coils that have an average diameter of 22mm and winding of 21 turns. These two coils are plugged in series, allowing this arrangement of coils to have an electrical resistance of  $R = 6.83 \Omega$ . The geometry of this magnetic stimulating device is a 12-sided polygon. Furthermore, a particularity of coil geometry and its wire winding, is the magnetic vortices. Such an approximation of the magnetic field sample position was estimated by using the Biot-Savart Law:

$$\vec{B} = n \left[ \frac{6\mu_0 I}{\pi r} \sin\left(\frac{\pi}{12}\right) \right], \quad (40)$$

Where  $n$  is the number of coils,  $r$  is the distance from source to the sample center, and  $\mu_0$  is the magnetic permeability. Because this magnetic source is an assembly of two coils, the following expression was used for the theoretical magnetic characterization:

$$\vec{B} = \vec{B}_1 + \vec{B}_2, \quad (41)$$



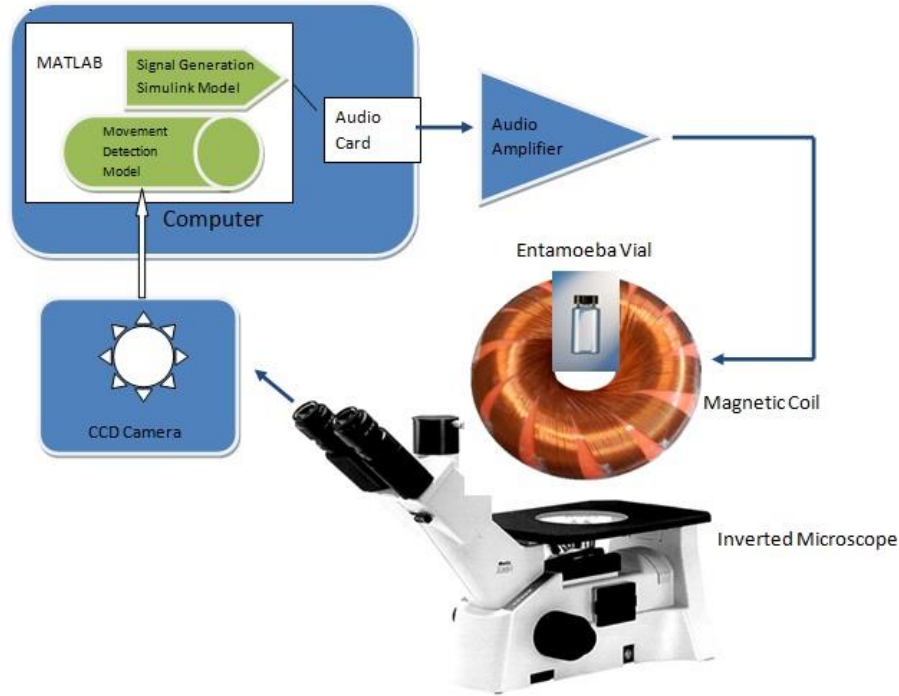


Figure 2.2: General diagram for the magnetic induction equipment. It shows the different components of the same: coil, amplifier, computer (from left to right on the top), fan, temperature control circuit, multimeter, and a magnet (from left to right on the bottom).

### 2.2.3 DEVICE CHARACTERIZATION

The sinusoidal signal generated for this device was amplified through the electronic stage, then the total impedance,  $|Z|$ , of the circuit was measured. This data was used to calculate the electric current and then, to have a theoretical estimation of the resource magnetic field. The magnetic field was also measured in the sample position with a scientific Gauss meter from Magnetic Instrumentation Inc.: Model 210 and sensibility from  $\mu\text{T}$  to T. All this information is summarized in Table 2.1.

The theoretical and experimental behavior of the coil magnetic field fitted to a first-order exponential function using Origin software. Where the, magnetic field depends on the frequency of the signal feed to the coil:

$$MF = -0.97 + 5.53^{-3.75 \times 10^{-4} f} \quad (42)$$

In order to have an evaluation of the workings of this magnetic exposure, the device was tested in a biological sample of cell culture (Human lymphocytes) according to the next procedure.



Figure 2.3: Magnetic field stimulation system to study the motility of *Entamoeba* cell cultures.

Table 2.1. Magnetic field stimulation system to study the motility of *Entamoeba* cell cultures magnetic field power characterization.

Signal	Frequency [Hz]	Voltage [Vpp]
1	110.60	40
2	846.63	44
3	1593.00	58
4	2601.00	54
5	2651.00	38

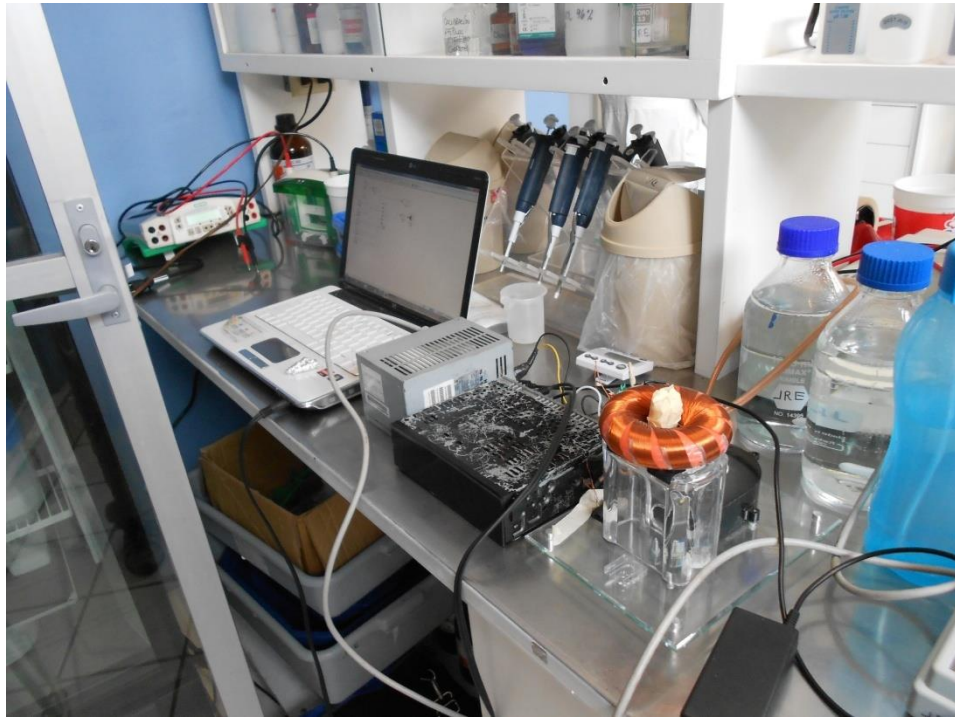


Figure 2.4: Magnetic system to stimulate Lymphocytes.

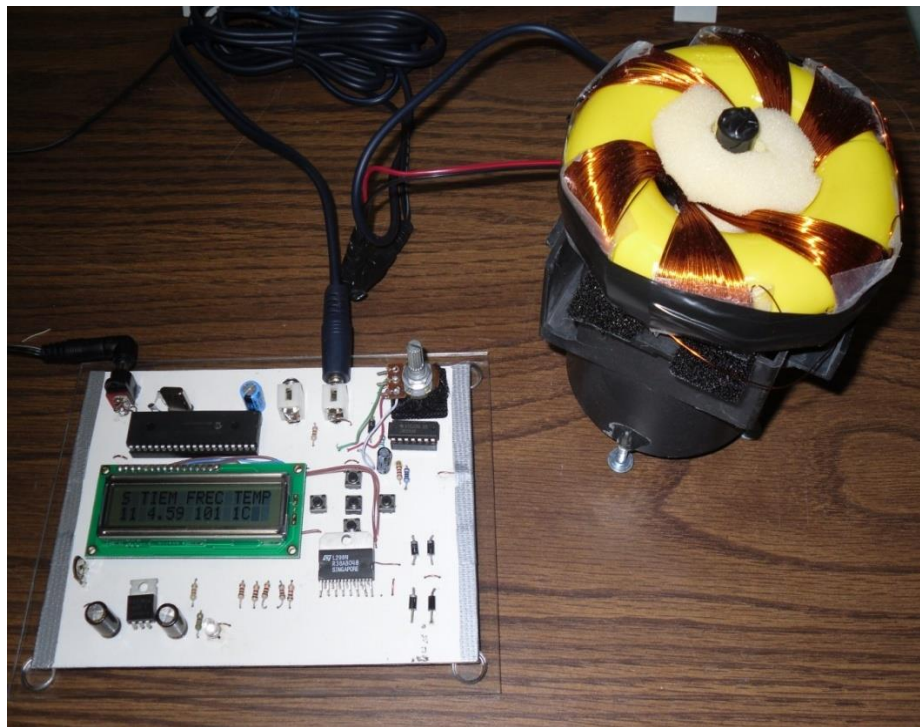


Figure 2.5 Portable magnetic field device to stimulate Human lymphocyte cell cultures



Table 2.2 Portable magnetic field device to stimulate Human lymphocyte cell cultures, coil voltage characterization.

Signal	Frequency (Hz)	Voltage (Vpp)
1	100	11.02
2	800	11.02
3	1500	11.02
4	2450	11.02
5	2250	11.02



Figure 2.6: Portable magnetic field device to stimulate Human lymphocyte cell cultures, coil voltage signal.



Figure 2.7 Helmholtz coil system to stimulate HEK-239T Cells

Table 2.3 Helmholtz coil system to stimulate HEK-239T Cells, coil voltage characterization.

Signal	Frequency (Hz)	Voltage (V <sub>pp</sub> )
1	100	37
2	800	37
3	1500	37
4	2450	37
5	2250	37

## 2.2.4 TESTING AND IMPROVING ELECTRONIC INSTRUMENTATION SYSTEM

Testing and essays will be conducted to bring the system to a working environment, where the behavior of the structure of the electronic components will be analyzed, to find holes in their functionality; it will be modified to be improved. Measurements will provide information on the final system behavior and performance once in the medium under study.

Analysis and adjustments to the control algorithm pacing system. After evaluating the capacity of the electronic system, the analysis of behavior of the control algorithm in a working environment has been carried out. The information obtained from the tests is analyzed and based on the results, adjustments will be made to the control system to generate an optimal operating point. Once this procedure has been achieved, the system will have the ability to solve the problems you face at a stage more robust of work

The system shown further is currently used for magnetic stimulation in cell culture. One of its main applications is the visible observation of cells behavior with a microscope. Visual information can be captured by a computer, using a camera, and be processed in real time, to determine motion parameters, cell clumping, and cell division, see figure 2.8.

## 2.3 SYSTEM FOR ELECTROCHEMICAL MEASUREMENT

Some effects linked to magnetic stimulation frequencies, were observed in initial experiments with amoeba motion. As the only data received did not provide adequate information on the effect caused in the cells, then a new electrochemical measurement system based on a bio-battery was developed. This measurement system could find any factor being potentially able to explain more accurately the effects on the dynamics of cell growth was developed. The system used is shown in the figure 2.9 scheme.

The designed circuit consists of schemes, such as instrumentation sensors, which may be suitable for measurement changes in electrical potential in the cell culture medium (35–37).

A series of experiments were conducted with this method, stimulating cell cultures for periods of 2 to 8 hours and altering the time duration of different frequencies. The following graph shows the voltage levels captured in a sampling period of 1 sample every two seconds, see figure 2.11.



Figure 2.8 System currently used for stimulation of Entamoeba cell cultures

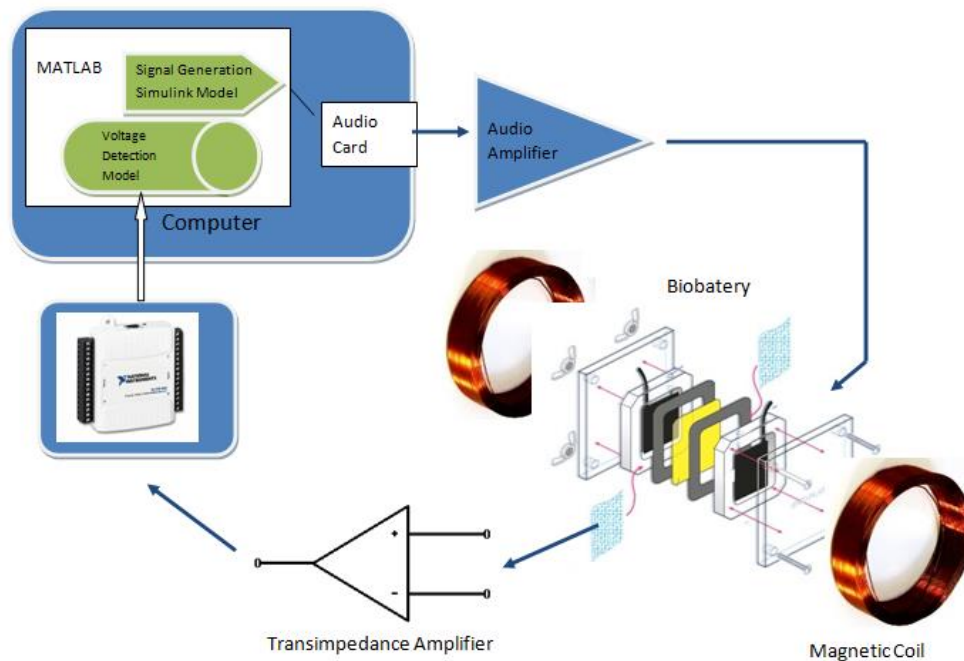


Figure 2.9: Magnetic stimulation system for measuring electrochemical parameters.



Figure 2.10: Bio-battery with air cooling system.

A clear effect caused by magnetic stimulation frequency can be noticed in Fig. 2. 11. The frequencies used were 60, 800, 2450.100, 1100, and 1700 Hz, each with duration of one hour.

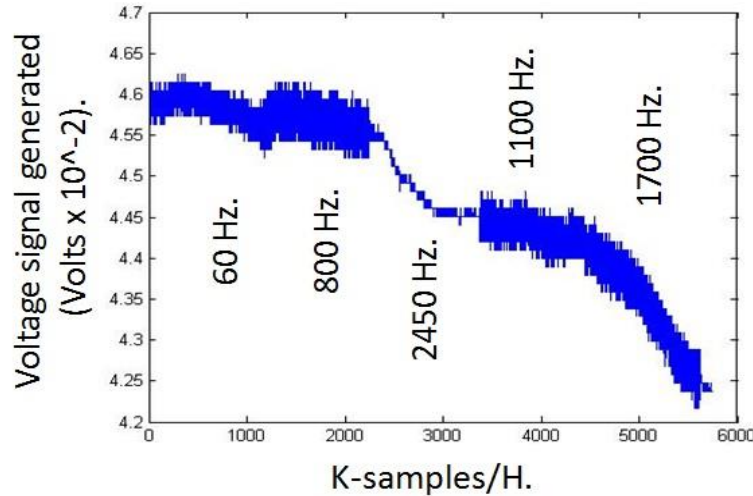


Figure 2.11: Voltage signal generated (VoltsX10-2) in the bio-battery from an Entamoeba cell culture electrochemical measurement captured in Matlab.

In concordance with this series of results, a suitable instrumentation has been developed to observe the electrochemical effects generated in the culture medium in real time.

### 2.3.1 ELECTROCHEMICAL SENSOR REDESIGN

The set of hardware and software technologies enable designing and develop tools that provide solutions to the problems that require remedy. In this respect an outline of the structure of a system of magnetic stimulation has been developed, in which a PID controller has been designed to maintain stable important variables in the cell culture medium.

The control process is stable with respect to variations in time. The control chart is the mechanism to detect irregularities which may be assignable causes adversely affecting the quality of results. Whenever a diagram shows a situation out of control, give notice so that an investigation can be initiated to identify the causes of the problem to take corrective action. This allows determining when action must be taken to adjust a process that has been affected by a special cause.

The design of this control system, implies primarily how much the microcontroller will be the basis of this circuit, this will take care of performing control tasks, with the mathematical algorithms that take the system to the desired levels of performance. Variables and desired levels of control parameters are stored in a microcontroller that is connected directly to the control microcontroller, and programming buttons, necessary for the user to set the appropriate parameters to control the process. To observe the status and parameters that the user is setting, a graphic display to have a dynamic and simple read-out function is used. In this way we guarantee interaction with the control system to communicate properly the graphic display. The microcontroller root adds a microcontroller between them, to take care of basic data interpretation system status, and transform for best performance in a graphical interface which will feature images, to have a friendly interface. To have communication between the control system and the plant to be controlled, in this case a



bioreactor, an input interface is added. This interface make the filters to adapt the signals from sensors, and to convert the digital analogous parameters to be interpreted by the control routine. The digital data acquire from the sensor is sent to the microcontroller who make the mathematical control operations to adjust the plant parameters, to make the changes on the plat it has been added an output interface comprising the microcontroller with a pulse width modulator, which is necessary for converting the digital outputs variable voltage signals to be applied to similar actuators of the plant, these signals be filtered and conditioned as required prior to its arrival to the actuators. It also will feature a digital output, which will be applied for on-off actuators.

---

### 2.3.2 DATA ACQUISITION

Data and signal acquisition, involves sampling the real world (analog system) to generate data that can be handled by a microcomputer or other electronic components (digital system). It consists of taking a set of physical signals, converting them at digitized voltages, so that it can be processed on a computer or PAC. It requires a conditioning step, which adapts the signal to levels compatible with the element that makes the transformation to a digital signal. The element that makes this transformation is the module or card scanning Data Acquisition (DAQ).

The components of the data acquisition systems have suitable sensors, which convert any measurement parameter of an electrical signal that the data acquisition hardware acquires. The acquired data is displayed, analyzed, and stored in a computer, either using the supplied software provider or other software. The controls and displays can be developed using various programming languages like Visual BASIC, C++, FORTRAN, and Java. Specialized programming languages used for the acquisition of data include DACs used in the construction of large data acquisition systems and the Matlab language that provides a programming environment optimized for data acquisition.

The National Instruments USB -6009, provides basic functionality for data acquisition applications such as simple data logging, portable measurements, and academic lab experiments, is used for computer data acquisition. It is accessible for student use and powerful enough for more sophisticated measurement applications. This has 8 analog inputs of (14 - bit, 48 kS / s) and 2 analog outputs (12 - bit, 150 S/s), 12 digital I / O, and 32 -bit spot.

For faster acquisition, it is suggested the use of data acquisition card USB-6210, which has a sampling frequency of 250,000 samples per second. This helps to capture important information and the variable in question and the most amount of voltage levels generated in the cell culture medium caused by chemical reactions.

## 2.4 DEVELOPMENT AND IMPLEMENTATION OF THE CONTROL ALGORITHM

To provide the basic strategy for the execution of the task, it is necessary to include the appropriate control schemes and computational algorithms, generating a structured pattern in which the environment and one or more agents are treated as separate schemes that can be coupled together. For this model, some rules to reduce the number of parameters are applied, reducing dependence on assumption transitions and cooperative behavior. Various strategies are designed to control each of the systems having the ability to independently control, adding to the design the ability to interface with other mechanisms of the system.

---

### 2.4.1 PID CONTROLLER VARIABLE INTERCONNECTABLE

At the moment, a type of PID controller is being worked on, to apply it in the system. The algorithm is designed in programming C and was developed in the MPLAB IDE program; implementing the equations of a proportional, integral and differential programming routine, that can be loaded into the microcontroller. The PID (Proportional Integral Derivative) is a feedback control mechanism that calculates the deviation or error between a measured value and the value to be obtained, useful to implement corrective action to adjust the process. The calculation algorithm of PID control is given in three different parameters: the proportional, integral, and derivative. The Proportional value determines the reaction of the current error. The Integral generates a correction proportional to the integral of the error, which ensures that applying a sufficient control effort reduces the tracking error to zero. Derivative determines the reaction time in which the error occurs.

The sum of these three actions is used to adjust the process via a control element and the position of a control valve, or the power supplied, to a heater for example. By adjusting these three variables in the PID control algorithm, the controller can be designed to provide the control required for the process to be performed. The response of the controller can be described in terms of the control response to an error, the degree to which the controller reaches the "set point", and the degree of system oscillation. Note that the use of the PID control does not guarantee optimal control system or stability. Some applications may require only one or two ways of providing this control system.

By implementing the PID controller, there are three terms that are based on the mistake of reading the sensor.

- Proportional Term:

$$u(t) = K_p e(t), \quad (43)$$

Where  $K_p$  is the proportional constant.

- Integral Term

$$u(t) = K_i \int E(\tau) d\tau \quad (44)$$

Where  $K_i$  is the integral constant

- Derivative Term:

$$u(t) = \frac{K_d de}{dt} \quad (45)$$

Where  $K_d$  is the derivative constant.

This generates the fundamental equation for use in the control algorithm, its output indicates that the proper level to be applied to the analog output controller was connected to one of the actuators of process:

$$u(t) = K_p e(t) + K_i \int e(\tau) d\tau + \frac{K_d de}{dt}. \quad (46)$$

This stage of the project involves physical proof of PID control algorithms, the controller. The mentioned test was made by incorporating the control algorithms in MPLAB IDE firm maker into microcontroller 16F84A, device that is intended to check the correct operation of a temperature controller. It uses a temperature and humidity sensor that has an I2C communication type. This sensor was interfaced to three microcontrollers, each in charge of one of the control steps: the proportional, integral, and derivative part. It also makes use of another controller which had the function of incorporating the desired control variable. There is another driver whose function is to establish the relationship of the control variable with the error signal, and finally a sixth driver to provide a PWM output, being the control signal sent to the power amplifier, that fed the temperature control actuator. We also used 2 sets of displays, to show the desired control variable and the temperature signal obtained.

## 2.4.2 HARDWARE DEVELOPMENT

The physical construction of the electronic circuit was tested in a breadboard. A voltage regulation stage to 5 volts, for the protection and adequacy of power microcontroller, was incorporated. A signal conditioning stage, from operational amplifiers, was also added; its function is to bring to them the signals obtained from sensors. As protection against overload, due to external signals that can cause some damage to the analog inputs of the microcontroller, a graphic LCD from the Atmel family display, as graphical interface, was incorporated. Some buttons were also incorporated for dealing with the communication interface between user and controller. In order to have a voltage output in either direct or alternating current, a power from an H-bridge, capable of operating in higher voltage ranges to feed the microcontroller and of having the ability to work in mode pulse width modulation PWM, was also added.

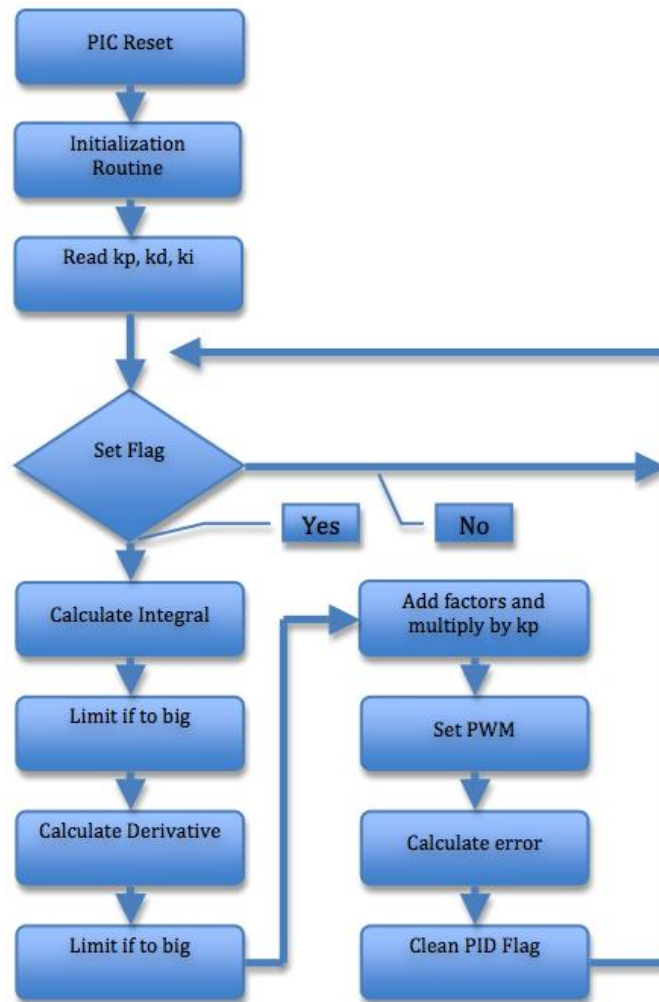


Figure 2.12. Block diagram of the structure of the PID control routine

## 2.5 CELL GROWN BEHAVIOR UNDERGOING RANDOM SEGMENTS OF OSCILLATING MAGNETIC FIELD

A Trophozoites of *E. invadens*, strain IP-1, was maintained and propagated under axenic conditions in TYI-S-33 medium at 26 °C. Ice-chilled trophozoites were harvested by centrifugation at 280 g and 4° C, counted in a Neubauer chamber and resuspended in TYI-S-33 at density of 50,000 cells/ml. One milliliter of previously prepared cells was placed in a 3 milliliter crystal vial, plus 2 ml of TYI-S-33 (13,15). Each vial was then sealed by a sterilized transparent tape on the upper side to let the microscope light go through.

All experiments were performed in the original culture media. A cylindrical observation chamber was made of Plexiglas (diameter 300 mm, depth 350 mm) with a Plexiglas plate on the lower side (15,16). For adaptation, cells were left undisturbed inside the crystal vial, and then put inside the chamber to start the measurements.

The observation chamber was placed in the center of the coil, with effective flux densities of 2.0 mT. The temperature was controlled by a liquid flux control system, using a PID controller to maintain the temperature at 26 °C. No significant temperature changes were measured within the observation area at flux densities that were registered, so changes in temperature has had no influence on the normal movement behavior of the cells.

An MF signal, implemented in a Simulink subsystem in Matlab, is determined to generate a sinusoidal signal in the frequency, by the slider gain block value. This frequency is given in hertz and the signal generated is send through the output of the computer audio card, via the audio device block in figure 2. A sinusoidal astern signal with low power, around 0.75 volts, is given by the computer audio output, which is connected to a power amplifier to increase the necessary voltage to power the coil. The power audio amplifier connected gives a 1000 watts power and is supplied with a 12 volts supply; the amplifier is in charge of giving it a peak-to-peak voltage of 20 Vpp to power the modified Copper windings vortex type coil.

To make the real time observation, the modified Copper winding's vortex type coil is mounted on an inverted microscope, which amplifies the image, then it is captured by a mounted web cam connected to the computer, which is in charge of doing the video recording. In this way it shows the real-time induced cell's image, and performs the image processing to make the cell movement analysis. The analysis is made taking an image frame capture every 0.72 seconds and doing a comparison of the actual taken image frame, and a frame captured one instant before; then different pixels are then added to obtain a total movement area, which is stored in a matrix with the cell stimulation frequency and the time value in the experiment.

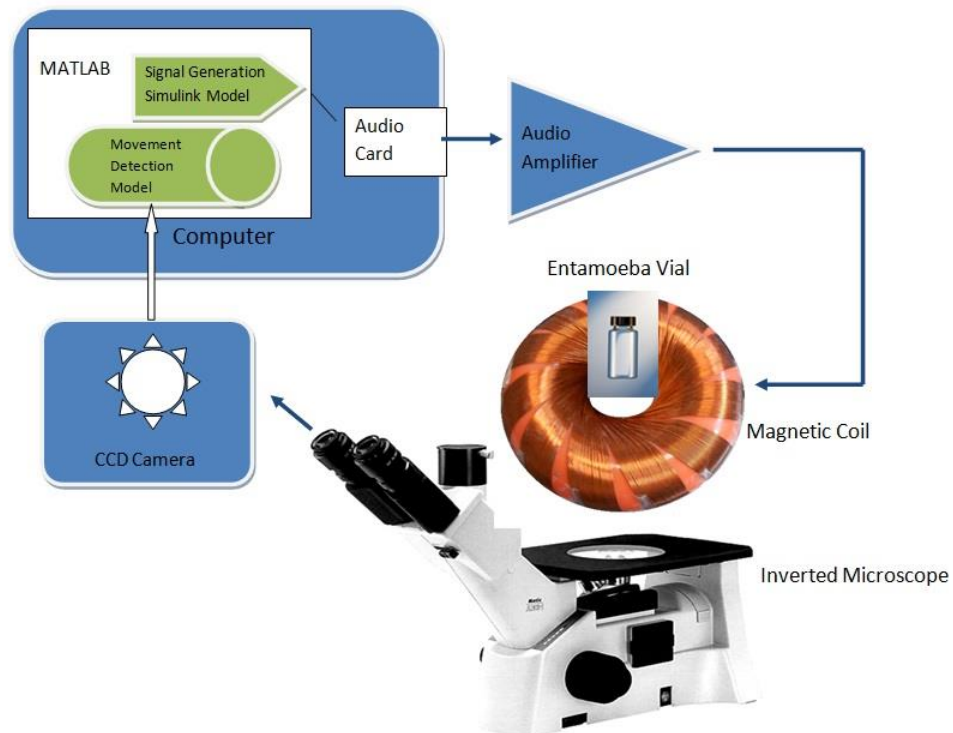


Figure 2.13. Blocks diagram of the stimulation system, to study the cellular behavior in the presence of the magnetic field.

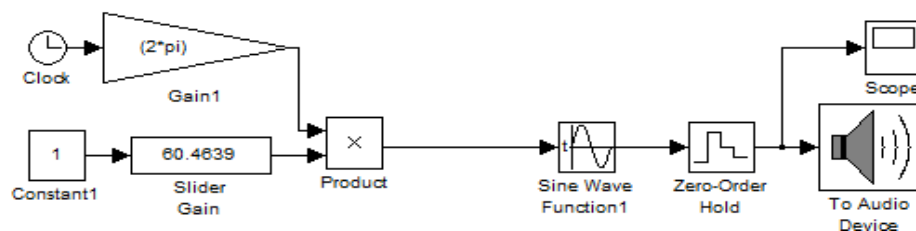


Figure 2.14. Blocks diagram for the oscillating signal generation in Simulink of Matlab.

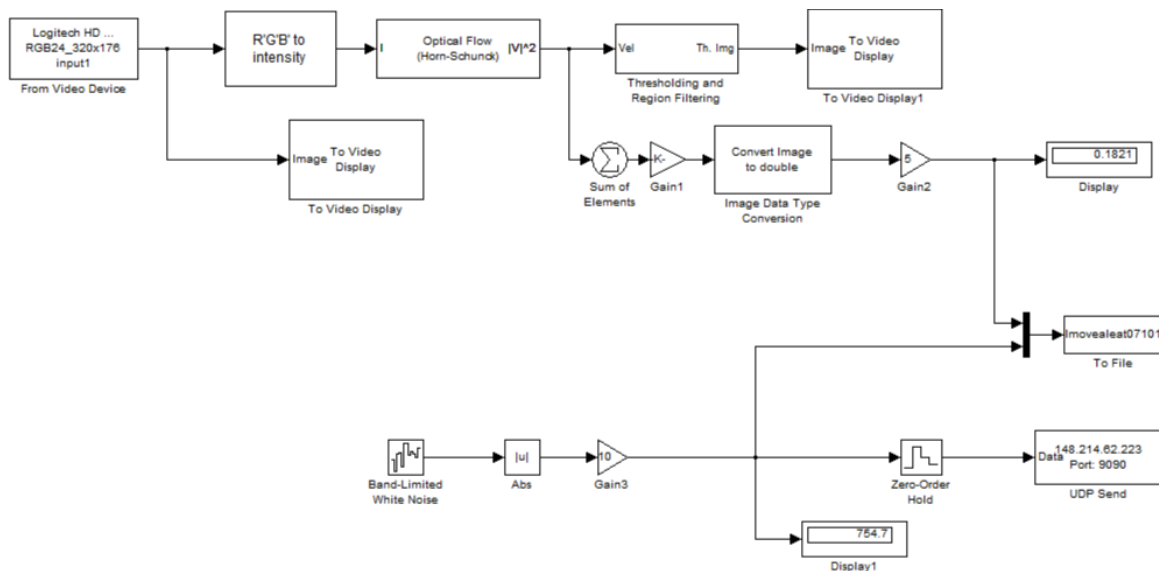


Figure 2.15. Blocks diagram for the movement monitoring in Simulink from Matlab.

## 2.6 MAGNETIC EXPOSURE SYSTEM TO STIMULATE DOUBLE NUCLEI CELL DIVISION

### 2.6.1 CELL CULTURE AND DIFERENTIATION

*Entamoeba invadens* is a protozoan parasite from reptiles that causes colitis, abscesses, and sometimes acute death in snakes. It's generally considered a commensal of chelonians but has also been implicated as a cause of colitis, diarrhea, and death in gopher (*Gopherus polyphemus*) (13) and leopard (*Geochelone pardalis*) tortoises. The diagnosis of *E. invadens* is currently made by detection of trophozoites and/or cysts upon direct fecal examination. *E. invadens* is used as a model for the study of amebic differentiation of the human enteric pathogen *Entamoeba histolytica*, because *E. invadens* form cysts in axenic culture opposed to *E. histolytica*.

For the experimentation, trophozoites of *E. invadens*, strain IP-1, were maintained and propagated under axenic conditions in TYI-S-33 medium, at 26 °C (15). Ice-chilled trophozoites were harvested by centrifugation, at 280g and 4°C, counted in a Neubauer chamber, and resuspended in TYI-S-33 at a density of 50,000 cells/ml. One milliliter of the cells was placed in a 3 milliliter vial, plus 2 ml of TYI-S-33 with 9 micro liters of medium or ferro-magnetic fluid. This experiment was made with a cell culture having an average population of approximately, 19.3 % of binuclear cells, 79.7 % of single nucleus cells, and 1. % cells with 3 to 5 nuclei's.

---

### 2.6.2 MAGNETIC COIL

To stimulate the cells, a copper winding's vortex type coil, which consists of a pair of wires wrapped around a doughnut-shaped core in a star pattern was used.

---

### 2.6.3 MAGNETIC STIMULATION SYSTEM

The magnetic stimulation system, consists of four main stages: a) signal generation stage; consisting in a Fourier block diagram that converts a constant frequency value in an astern signal, the parameters establish the amplitude of the signal, the center value for the signal, the RMS value, and the power amplitude for harmonics in sinusoidal or cosine signals. The parameters are saved in a register table, which are changed in time cycles to be able to generate different signal for the stimulation. b) a power stage; the signal generated is sent to the audio output device, which is connected to a 1000 watts 12 volts power audio amplifier, in charge of giving the signal power to the Copper winding's vortex type coil. c) the data analysis stage; to make the real time observation, the Copper winding's vortex type coil was mounted on an inverted microscope to amplify the image, one that is captured by a mounted web cam and connected to the computer in charge of doing the video recording, Figure 3 shows the real time induced cell's image; and to perform the image processing to make the cell counting culture approximation. d) an environmental control stage; to maintain the temperature stable and to provide the appropriate conditions for a good culture medium, the Copper winding's vortex type coil is submerged into a housing filled with antifreeze which is recirculated on a radiator cooling system.

---

### 2.6.4 CELL STIMULATION

The presence of magnetic fields allows the indefinite survival and replication of the cells hit by apoptogenic agents (26). In the case of this experiment, a sinusoidal varying magnetic field (SVMF) is applied to a cell culture to observe if the magnetic force induces changes in the dynamics of the plasma membrane, enhancing cell proliferation. The changes in membrane dynamics were typical to those observed in cell transformation. While the SVMF examined were (100, 800, 1500, 2500 & 7500 Hz), and performed at a magnetic field equal to 2.0 mT. A mechanism of excitation, relaxation, and stress, depends on the weak magnetic field frequency.

One of the most important aspects of the cell division cycle is cytokinesis, (the final process, which physically separates the two daughter cells with equal DNA content from each other). During cytokinesis, a contractile ring forms at the equator of the dividing cell. This ring is a contractile bundle of actin filaments similar to stress fibres. In response to specific signals, different proteins are recruited to modulate changes in the actin cytoskeleton producing this cellular process. In *Entamoeba*, homologues of actin, myosin, profilin, p21 Rho, p21 Rac, and diaphanous genes have been identified and fully characterized as important agents for cell cytokinesis; and an over-expression of a mutant RacG-V12 may occur as well, affecting the cell division cycle. The Eh Diaphanous gene product has



also been co-localized with polymerized actin at the site of cell division. This factors can not only deregulating the cell polarity, but also caused a defect in cytokinesis.

While scanty information is available on the molecular factors and mechanisms which regulate cytokinesis, an interesting report showed helper cells, also called 'midwives', assist in the division of trophozoites. It was suggested that extracellular factors, secreted by 'midwives', were required for the final separation of two daughter cells (20,27,38). The Cytokinetic processes in *E. histolytica* (this study) and *E. invadens* are similar. It was established that low frequency electromagnetic fields, such as the activities of some enzymes and the transcription of some genes, can affect biological functions (39).

Here, I generated the hypothesis that a magnetic field, with certain characteristics, promotes the necessary actin polymerization to end the division circle.

Entamoeba proteins may also affect the rate of cell division as deduced from the increased multi-nucleation in different mutants, this event appears to be largely controlled by extra-cellular factors. A random selection of cell division sites, coupled to a poorly controlled mechanical separation, can lead to the formation of a nucleate and multi-nucleated daughter cells.

---

#### 2.6.5 MEASUREMENT AND ANALYSIS

To determine an approximation of the cell culture, the cells were recorded with a Webcam assembled to a microscope, with a 20x lens for approximately 2 h stimulation; the data was stored in a computer and analyzed using a Matlab video routine analyzer. After each experiment, a cell counting, with a Neubauer chamber, was taken. At the beginning of each experiment, a control and a problem vial has been prepared, adding 50,000 Entamoeba cells for each one. At the end of the trial, remaining cells were counted in each vial. Were the results show an increase in the cells population in both control and experimental vials; corresponding to 12% and 65%, respectively.



Figure 2.16. Copper winding's vortex type coil that generates the magnetic stimulation field.

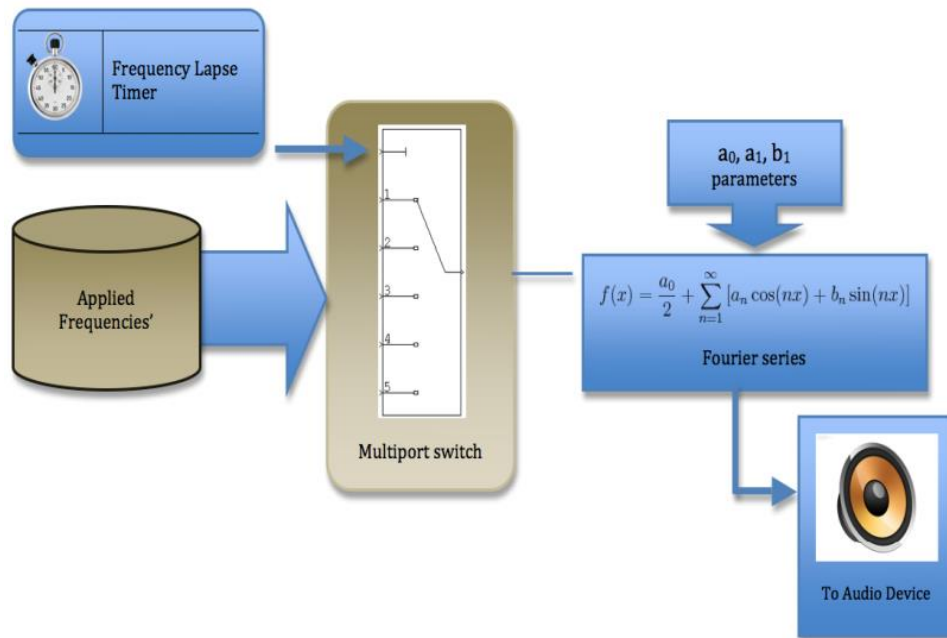


Figure 2.17. Diagram for the signal generation system in Matlab.

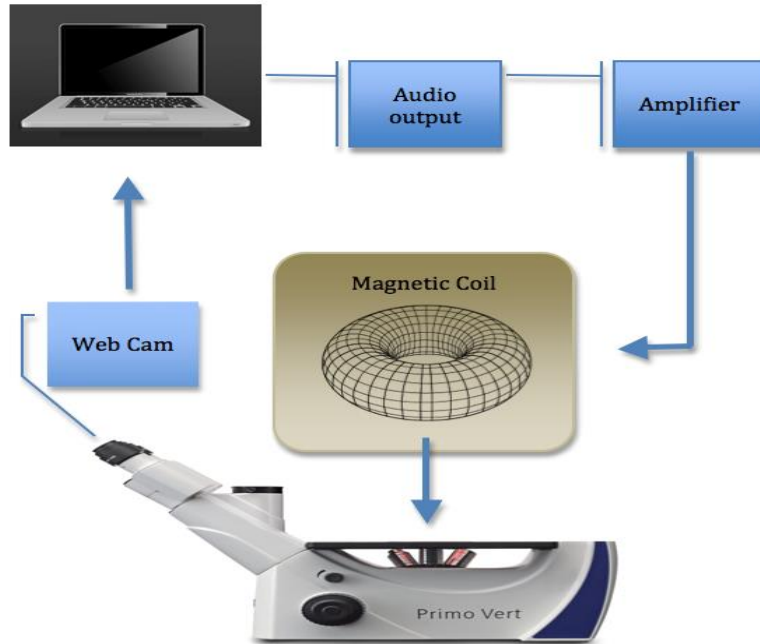


Figure 2.18. Magnetic stimulation system.

It is important to maintain the adequate cell culture medium conditions. One of the most important parameters to maintain stable is the temperature. Under the *E. invadens* stimulation experiments, heating occurred on the coil due to the transferred current. Indirectly the temperature can increase in the culture medium; to avoid this effect the coil is bean cooled by a water refrigeration system controlled with a proportional controller unit. The temperature sensor is placed in the area were the vial is placed, inside the toroidal copper winding's vortex type coil, to maintain the ideal temperature for the cells at 26 °C.

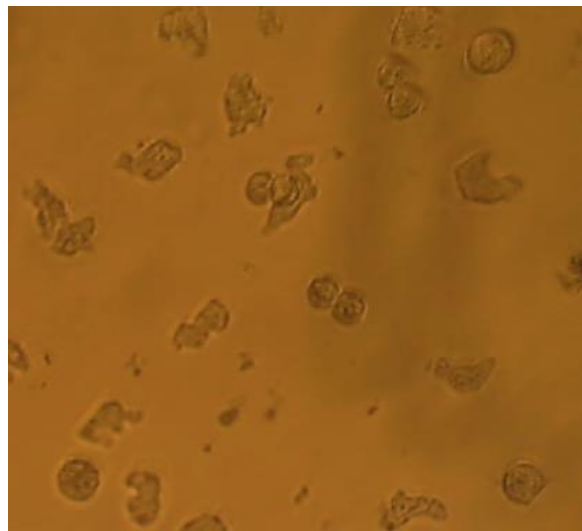


Figure 2.19. Cell division by magnetic stimulation.

## 2.7 BIOLOGICAL EFFECT OF MF ON AMOEBIC SPECIES AND PERIPHERAL AND MONONUCLEAR BLOOD CELLS

The local bioethics committee approved this study protocol; furthermore, a written informed consent was obtained from each volunteer. In basal conditions, each volunteer donated 20 ml of blood for the execution of these studies.

### 2.7.1 PERIPHERAL AND MONONUCLEAR BLOOD CELL PURIFICATION AND CARBOXYFLUORESCCEIN SUCCINIMIDYL ESTER (CFSE) LABELING

Blood samples were collected from 12 subjects of 24 to 35 years old. All individuals included in this study were healthy, non-smokers, and had no history of alcohol abuse or drug consumption. This study was made in the Department of Medical Sciences in the León campus of the University of Guanajuato.

The Peripheral Blood Mononuclear Cells (PBMC) were isolated from 20 ml of blood by conventional centrifugation in a density gradient of Ficoll-hypaque [16].

After centrifugation, PBMCs were collected from the Ficoll-histopaque interface. Then, the cells were washed twice with phosphate saline buffer. They were counted and the cell viability was detected by exclusion of trypan blue staining.

After that, PBMCs were loaded with cell tracker dye CFSE (0.5  $\mu$ M; Molecular Probes) to monitor proliferation. Next, CFSE staining, 5.71 micro L of Gadolinium, was added to the lymphocyte samples. Each sample was placed in a 2 ml Eppendorf tube containing the lymphocytes in RPMI-1640 medium.

### 2.7.2 IN VITRO STIMULATION WITH CONCAVALIN A AND EXPOSITION TO MAGNETIC FIELD

Two groups of samples from the same donor, control, and experimental groups were prepared.

The tubes containing the PBMC, plus 5.71 micro L of Gadolinium, were exposed to magnetic field at frequencies of 100, 800, 1500, 2450, and 2500 Hz. Each tube remained for 6 min, under the magnetic fields then, each one changed to other of the four frequencies; this frequency cycle was repeated four times, so the whole magnetic stimulation on the sample took 2 h. The magnetic field intensity was also changing from 1.13 to 4.13 mT; this was according to each frequency applied. Then, cells were adjusted at a concentration of  $1 \times 10^6$ /ml, in RPMI-1640 tissue culture medium (GIBCO, Eugene, OR); supplemented with 10 % fetal bovine serum: 2 mM L-glutamine, 50 U/ml penicillin, and 50 g/ml streptomycin; and cultured with or without 2.5  $\mu$ g/ml of concanavalin A (Con A, Sigma Aldrich) for 72 h, or 7 days at 37 °C, with a 100% humidity, and 5% CO<sub>2</sub> (in survival

experiments). The cells were cultured for 20 days, as will be indicated forward. The proliferation and cell survival were analyzed, with a FACS Canto II flow cytometer, by using the Diva software (Becton Dickinson, San Jose, CA).

Two species of *Entamoeba*, *E. histolytica* HM1-IMSS (maintained in the laboratory for over 15 years) and *E. invadens* IP1-NY (donated by Dr. Daniel Eichinger from the New York University) were used.

---

### 2.7.3 GROWTH MEDIUM

The medium used in the cultivation of both species was the TYI-S-33 (Diamond et al, 1978) under axenic conditions, this proportions are shown in table 2.4. All reagents were added and dissolved in the following order: in 500 ml of deionized water, diluting one by one, thereafter, deionized water was added to 800 ml, adjusted to pH 6.8 with 1N NaOH and finally dilute to 820 ml. The medium is packaged and sterilized at 121 °C for 15 min, cooled to room temperature, and stored at 4 °C until use. For amebic culture, 100 ml of medium were added to 20 ml bovine serum, and inactivated in a water bath at 56 °C for 30 min, supplemented with vitamins and special supplement Diamond (SED).

Table 2.4. Medium preparation.

Compound	Quantity
Biotriptasa peptone	30 g
Yeast extract	3 g
Dextrose	10 g
Sodium chloride	2 g
Monobasic potassium phosphate	0.6 g
Potassium phosphate dibasic	1 g
L-cysteine hydrochloride	1 g
ascorbic acid	0.2 g
Ferric ammonium citrate	0.0236 g
Deionized water	820 ml

---

## 2.7.4 CULTURE AND MAINTENANCE OF AMOEBIC STRAINS

Amoebic cultures were planted in a proportion of 10,000 complete and inoculated trophozoites / tube in sterile tubes of 16x150 mm, with screw cap, then 15 ml of culture medium TYI-S-33 were added. Then they were incubated for a period of 24, 72, 96, or 120 hours (exponential growth phase), the performance of reseeding the cell culture, consist of placing the tubes in an ice-water bath for 10 min to detach the amoeba cells from the tube wall. Once detached, they were mixed and counted to inoculate again 10,000 trophozoites / tube. The cultures were incubated at 36 ° C for *E. histolytica* and at 26 ° C for *E. invadens*.

---

## 2.7.5 MAGNETIC INDUCTION EQUIPMENT

For magnetic induction, a modified Copper winding's vortex type coil, calibrated to a constant flux of 2 mT and variable frequency, was used. The frequencies used were generated by a software program in MatLab and send out through speakers output. This output is connected to a SONY exploit amplifier that was connected to the coil which generate the magnetic field. The system comprises a consistent temperature control system and a magnetic coil that allows enough space to place three glass vials (13x30 mm) with a capacity of 4 ml on the center of the coil.

---

## 2.7.6 MAGNETIC INDUCTION TRIALS

Cells coming from tubes of 16x150 mm with 15 ml of TYI-S-33, and 10,000 trophozoites corresponding strains; incubated at 26 ° C and 36 ° C, as described above, were used for the experiments, which lasted 24 hours. The tubes were observed in an inverted microscope (Nikon), to ensure the formation of the cell monolayer. Those wherein the monolayer that were well formed, were placed in an ice-water bath for 10 min to detach trophozoites from the tube wall and stir them gently to mix the cells. An aliquot was taken and cells were counted on a Neubauer chamber. Glass vials were prepared in 13x30 mm and inoculated with 50,000 trophozoites in a final volume of 3 ml of TYI-S-33 that were added to the amount of Gd required for each test. A total of  $5 \times 10^4$  cells / ml were placed in glass vials, at a total volume of 3 mL, then added to the concentration of Gd required for the test, and finally placing the vials in the middle of the coil (for a maximum of 3 per assay). Then, the frequency generation program is started, with each induction protocol proceeding. In each experiment, control vials were used and similarly inoculated, but not subjected to MF, and others vials were not exposed to the effect of Gd or the MF. After each test, cell viability was determined with blue Trypan 0.2% v / v (final concentration) and the number of cells recovered after treatment was counted for all the cell vials.

---

### 2.7.7 EFFECT OF MF ON AMOEBIC GROWTH

To test the effect of MF on amoebic growth, a magnetic induction protocol was applied for two hours, every day, for 3 consecutive days in *E. histolytica* at a temperature of 36°C. A magnetic induction protocol was also applied for two hours, every day, for 5 consecutive days in *E. invadens* at a temperature of 26°C.

One protocol (protocol of fixed rate) consisted of subjecting the cells to MF produced by a frequency of 2,500 Hz for 6 minutes, a rest period of 6 min, and their respective repetitions by 2 hours of treatment.

A second protocol (protocol of variable frequency) consisted of subjecting trophozoites to the MF produced by a cycle frequency variation (6 min at 0 Hz, 6 minutes at 100 Hz, 800 Hz 6 minutes, 6 minutes at 1500 Hz, 6 minutes at 2500 Hz and repetition) for the first 2 hours of treatment. The experiments were used in the presence of Gd, containing 0, 0.8, 1.6, 3.3, 8.3 and 16.6 mM. These studies were made in the Department of Biology, campus León of the University of Guanajuato.

---

### 2.7.8 EFFECT OF MF ON AMOEBIC ERYTHROPHAGOCYTOSIS

To determine the effect of the MF on amoebic erythrophagocytosis, the samples were subjected to MF for two hours each day: *E. histolytica*, for 3 days and *E. invadens* for 5 days, using a fixed frequency of 800 Hz for 2h, or to variable cycle frequencies (6 min at each frequency: 0, 100, 800, 1500 and 2500 Hz) for 2h. The test was performed in both the absence and presence of Gd, at the concentrations listed (0, 0.8, 1.6, 3.3, 8.3 and 16.6 mM). Once the magnetic induction protocol was executed, the recovered trophozoites were used to determine their erythrophagocytosis ability, analyzing the quantity on erythrocytes absorbed by the *Entamoeba* cells in each population.

---

### 2.7.9 EFFECT OF MF ON GADOLINIUM AND AMOEBIC AGGLUTINATION

To test the effect of Gd and MF cell agglutination, amoebic behavior was analyzed during the development of the magnetic induction protocol by the direct observation of the cells through the microscope, and through photographs taken every 10 minutes. The cells (200,000 per well trophozoites inoculated in a volume of 300 ul) were cut and placed in wells of a box, ELISA, so that they could be introduced into the magnetic coil and subjected to MF for 2 hours, using the protocols described above. The frequency was fixed at 800 Hz, with cycles of 6 minutes and sleep induction, and variable frequencies with cycles of 6 minutes each, corresponding to 0, 100, 800, 1500 and 2500 Hz either in the presence or in the absence of the Gd concentrations mentioned (0.0, 0.8, 1.6, 3.3, 8.3 and 16.6 mM). The mounted camera in the microscope, took shots of the agglutination phenomenon trophozoites at the beginning of the magnetic induction and every ten minutes to complete two hours of each protocol. Appropriate controls were used taking into account the next considerations: Absence of MF, MF, absence of Gd added, and adding Gd but without subjecting the cells to MF.

---

#### 2.7.10 DETERMINATION OF THE SUBCELLULAR DISTRIBUTION OF GD IN THE TROPHOZOITES

To determine whether the Gd added in experiments was introduced to the cytoplasm or nucleus of the amoebae, washed and concentrated cells were analyzed, using a fluorescence spectrometer ray technique.

The samples subjected for 2 hours to MF ( variable frequency cycle, 6 min c / u: 0, 100, 800, 1500 and 2500 Hz ) in the presence of Gd ( 16.6 mM ) were recovered at the end of the treatment and centrifuged at 500 ×g for 10 minutes to separate the culture medium and the trophozoites. The culture medium was recovered and the cell pellet was re-suspended in 500 ul of deionized water and homogenized with a potter. The cell homogenate was recovered and diluted with 500 ul of sterile distilled water and centrifuged at 100,000 ×g for one hour in an ultracentrifuge (Beckman - Optima TLX) to separate the mixed fraction cytosol and amoebic membranes. The recovered cytosol and membranes were homogenized with a Potter after resuspension in 1 ml of bi-distilled water. Recovered samples (culture medium, mixed fraction cytosol and membrane) were stored at - 20 ° C, until analyzed by ray fluorescence spectrometer X. This analysis was performed at the Department of Engineering Physics León campus of the University of Guanajuato, using a spectrometer that allows accuracy in small samples. The system of photoelectric detectors detects the X-ray fluorescence, converting each radiation photon into an electrical pulse; all pulses are counted by the device, whose detectors work usually with dispersive energy.

---

#### 2.7.11 STATISTICAL ANALYSIS

All experiments were performed at least three times in duplicate. The results are representative values, and were submitted to an analysis of variance (ANOVA) by a factor ( $p = 0.05$ ).

### 2.8 PORTABLE DEVICE FOR MAGNETIC STIMULATION: ASSESSMENT SURVIVAL AND PROLIFERATION IN HUMAN LYMPHOCYTES

The magnetic assembled simulator system is a device that includes three parts: i) hardware, ii) software and iii) a magnetic field source.

---

#### 2.8.1 HARDWARE DESCRIPTION

The hardware uses a microprocessor and an electronic stage for sine wave generation, which consists of a limited counter. Its design allows saving the parameters in an electronic memory, according to the frequency and the time intervals of the magnetic stimulation selected for the biological sample. Furthermore, the system permits setting different time intervals for each operating frequency previously designated. The digital switch is connected to a Fourier block diagram that converts a constant frequency value to an altern signal; in this block, other parameters can be established, such as the power, the central value for the signal, the RMS value and the power of harmonics in sinusoidal



signals. The output generated frequency is connected to an audio amplifier with 1000 power watts and 12 volts of amplitude, this feeds a magnetic field source where the sample is deposited.

---

### 2.8.2 SOFTWARE

The instrumentation is controlled through an algorithm performed in assembly language and installed in a microprocessor. Such algorithm was designed to generate sinusoidal oscillations at different frequencies, in this work it operates at frequencies of: 100, 800, 1500, 2450 and 2500 Hz, in segments of 360 s each one; this frequency cycle was repeated four times in a pilot work. So, the experimental sample group was stimulated for two hours.

---

### 2.8.3 MAGNETIC FIELD SOURCE

A Copper winding's vortex system coil was assembled with two identical coils; they have an average diameter of 2.2 MF and winding of 21 turns; these two coils are plugged in series, so this arrangement of coils has an electrical resistance of  $R = 6.83 \Omega$ . The geometry of this magnetic stimulator device is a twelve-sided polygon; furthermore, a particularity of geometric coils and its wire winding create magnetic vortices (23). An approximation of the magnetic field's sample position was estimated by using the Biot-Savart Law.

$$\vec{B} = N \left[ \frac{6\mu_0 I}{\pi r} \sin\left(\frac{\pi}{12}\right) \right], \quad (47)$$

Where  $N$  is the number of coils,  $r$  is the distance from the source to the sample center and the magnetic permeability. Since the magnetic source is an assembly of two coils, then, for the theoretical magnetic characterization, this expression was used.

$$\vec{B} = \vec{B}_1 + \vec{B}_2. \quad (48)$$

Where  $\vec{B}_1$  states the magnetic field for the first coil and similarly  $\vec{B}_2$  is the magnetic field for the second coil.

---

### 2.8.4 DEVICE CHARACTERIZATION

The sinusoidal signal generated for this device was amplified through the electronic stage, then the total impedance,  $|Z|$ , of the circuit was measured. This data was used to calculate the electric current and then to have a theoretical estimation of the magnetic field source. The magnetic field was also measured in the sample position with a scientific Gauss meter possessing a sensibility from  $\mu T$  to T. this information is summarized in table 2.5.

The theoretical and experimental behavior of the coil magnetic field is shown in figure 2.31. As long as, the experimental data were fitting to a first-order exponential function by least squares using Origin™ software. Were the magnetic field can be calculated by the equation:

$$MF = -0.97 + 5.53^{-3.75 \times 10^{-4} f}, \quad (49)$$

Table 2.5. Theoretical and experimental data recorded in the Copper winding's vortex type coil characterization.

Frequency [Hz]	Z [Ω]	Intensity current [A]	Magnetic field intensity [mT]		Fem [V]
			Theoretical	Experimental	
100	6.86	1.60	3.80	4.13	0.20
800	8.78	1.25	2.97	3.05	0.85
1500	12.41	0.89	2.10	1.98	1.10
2450	18.26	0.60	1.42	1.16	1.14
2500	18.58	0.59	1.42	1.13	1.00

On the other hand, the magnetic field and electromotive force variation are affected by the frequency and impedance of the coil, these behaviors are shown in figure 2.32.

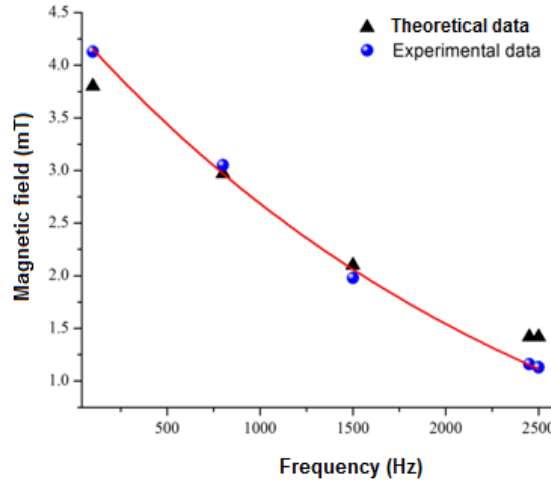


Figure 2.20. Frequency responses of the magnetic field in the Copper winding's vortex type coil according excitation frequency.

The coefficient of determination, denoted  $R^2$ , was used to indicate how well data fit the statistical model. Were in the next expression a data set has  $n$  values marked  $y_1 \dots y_n$

(collectively known as  $y_i$ ), each associated with a predicted (or modeled) value  $f_1 \dots f_n$  (known as  $f_i$ , or  $\hat{y}_i$ ). If  $\bar{y}$  is the mean of the observed data.

$$R^2 = \frac{\sum_i (\hat{y}_i - \bar{y})^2}{\sum_i (y_i - \bar{y})^2} \quad (50)$$

Adjusted correlation coefficient

The use of an adjusted  $R^2$  is an attempt to take account of the phenomenon of the  $R^2$  automatically and spuriously increasing when extra explanatory variables are added to the model. The adjusted  $R^2$  value can be calculated, given an observed (sample)  $n$ , the number of predictors  $p$  in the model, and the total sample size:

$$R^2_{adj} = 1 - \left(1 - R^2\right) \frac{n-1}{n-p-1} \quad (51)$$

The results obtained from the data calculated and measured were  $R^2 = 0.95789$  and  $R^2_{adj} = 0.9157$

---

#### 2.8.5 PERIPHERAL AND MONONUCLEAR BLOOD CELL PURIFICATION AND FICOLL-HYPaque LABELING

Magnetic exposure, was tested in biological samples of Human lymphocytes, to study the effects that their proliferation can cause according to the next procedure.

To obtain the lymphocytes samples, 20 ml of blood in basal conditions, were donated from different volunteers. The local bioethics committee approved this study protocol; furthermore, a written informed consent was obtained from each volunteer.

As explained before, the blood samples were collected from 12 subjects, from 24 to 35 years old. All individuals included in this study were healthy, non-smokers and had no history of alcohol abuse or drug consumption. Peripheral and mono nuclear blood cells (PBMC) were isolated from 20 ml of blood by conventional centrifugation in a density gradient of Ficoll-Hypaque (CFSE).

After centrifugation, PBMC was collected from the ficoll-hystopaque interface. Then, cells were washed twice with phosphate saline buffer. They were counted, and the cell viability was detected by exclusion of trypan blue staining. After that, PBMCs were loaded with a cell tracker dye CFSE (0.5  $\mu$ M; Molecular Probes) to monitor proliferation. After the CFSE staining, 5.71 ml of Gadolinium, were added to the lymphocyte samples. Each lymphocytes samples were placed in a 2 ml RPMI-1640 medium inside an Eppendorf tube.

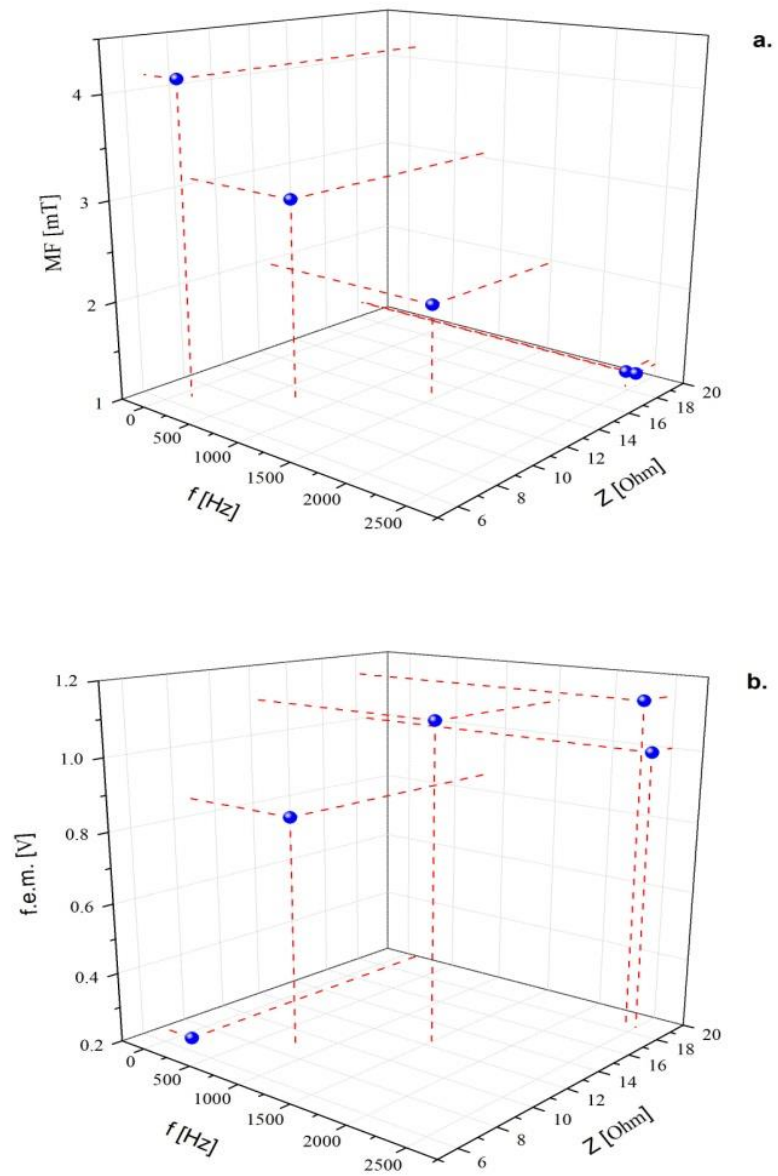


Figure 2.21. a) Magnetic field vs electrical impedance, depending on the frequency of the sinusoidal signal supplied.  
b) Electromotive force vs electrical impedance, depending on the frequency of the sinusoidal signal supplied.

#### 2.8.6 IN VITRO STIMULATION WITH CONCAVALIN A AND EXPOSITION TO MAGNETIC FIELD

Two groups of samples from same donor, control, and experimental groups were prepared.

The tubes containing the PBMC, plus gadolinium, were exposed to magnetic field at frequencies of 100, 800, 1500, 2450, and 2500 Hz. Each tube remained for 6 minutes in a single frequency, then, it switched to another of the four remaining frequencies. This frequency cycle was repeated four times, so that the whole magnetic stimulation on the sample took 2 hours. The magnetic field intensity was also changing from 1.13 to 4.13 mT, this was according to the power given by each of the applied frequency. After the stimulation, the cells were suspended to let them ready for incubation, at a concentration of  $1 \times 10^6$  / ml in RPMI-1640 tissue culture medium (GIBCO, Eugene, OR) and were supplemented with 10 % fetal bovine serum, 2 mM L-glutamine, 50 U/ml penicillin, 50 g/ml streptomycin; and finally cultured either with or without 2.5  $\mu\text{g/mL}$  of concanavalin A (Con A, Sigma Aldrich)(5) . They were incubated either for 72 h, or 7 days, at 37 °C, 100 % humidity and 5 % CO<sub>2</sub> (for survival experiments, the cells were cultured for 20 days, this is indicated at results section). The proliferation and cell survival was analyzed with a FACS Canto II flow cytometer and the software Diva (Becton Dickinson, San Jose, CA).

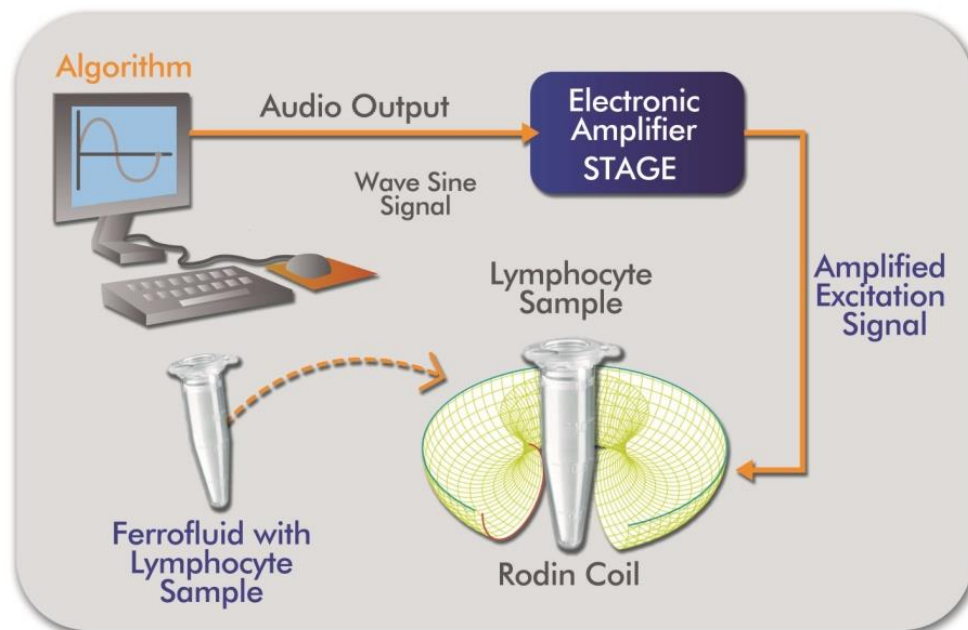


Figure 2.22. Schematic setup of the magnetic excitation system applied on the prepared Human lymphocytes.

## 2.9 INCREASING SURVIVAL IN KIDNEY HEK-293T CELLS IN PRESENCE OF MAGNETIC FIELD VORTICES AND NANO-FLUID

HEK-293T cells were grown in DMEM complete medium (Gibco-Invitrogen), with low glucose and glutamine, Sodium Pyruvate (110 mg / ml) and supplemented with 10 % fetal bovine serum, 100 U / ml penicillin, and 100 µg / ml streptomycin for 72 hours at standard conditions of temperature, humidity, and CO<sub>2</sub> concentration (37 ° C, 100% humidity and 5 % CO<sub>2</sub>).

### 2.9.1 NANO-FLUID

An Experimental group was prepared with Dotarem ® at a concentration of 0.5 mmol / ml. The dose used was 30 µl in a volume of 1.5 ml, at a concentration equivalent of 0.01 mmol / ml. taking in consideration the commonly used dose in patients is 0.1 mmol / kg, equivalent to 0.2 ml / kg.

### 2.9.2 MAGNETIC FIELD SOURCE

This was done with an assembly of copper winding's vortex-type coil, with the particularity of generation of magnetic vortices in the central region. So, the two coil windings follow a star model; they were plugged in series, each one has 21 turns, and a resistance  $R = 6.38 \Omega$ .

### 2.9.3 SOFTWARE

A computer algorithm, created in Matlab Simulink platform, was used to produce the sinusoidal signal; an electronic amplifier amplified this signal, in order to power the magnetic coil.

### 2.9.4 PROTOCOL

The monolayer formation of HEK-293T cells at the base of cell culture bottles was observed to select the culture for the experiment with better cell distribution. The cells were washed with NaCl at 9 % concentration. Then a process of trypsinization was applied, adding Trypsin-EDTA, 1x, 0.05%, GIBCO-Invitrogen on the monolayer to achieve its dissociation. DMEM complete medium was added to the culture, to neutralize the effect of trypsin, thus obtaining a cell suspension and cells being counted. The cell suspension was centrifuged and then cells were loaded with cell tracker dye CFSE (0.5 uM, Molecular Probes) to monitor proliferation. After staining with CFSE, each sample was placed in a 2 ml Eppendorf tube, containing HEK-293T cells in DMEM complete medium mixed with 30 µl of DOTAREM (paramagnetic solution) to enhance the effect of the magnetic field.

### 2.9.5 MAGNETIC FIELD STIMULATION

The samples of experimental group: nano-fluid plus HEK-293T, underwent in the magnetic field vortices at sinusoidal frequencies of 100, 800, 1500, 2450 and 2500 Hz; each sample was subjected 6 minutes during 2 h to a single frequency, with a magnetic field changing from 1.13 to 4.13 mT; the control group *i.e.* nano-fluid plus HEK-293T, did not undergo in the magnetic stimulation.

After the experiment,  $1 \times 10^6$  cells were inoculated in culture DMEM complete medium for 24, and 72 hours. The cell proliferation was analyzed by using of a flow cytometer, using as well the FACS Canto II Diva software (Becton Dickinson, San Jose, CA).

## 3 RESULTS

### 3.1 INSTRUMENTATION

The developed instrumentation was performed within the Laboratoire d'Ingénierie des Systèmes de Versailles de l'université de Versailles Saint-Quentin-en-Yvelines, in cooperation with the University of Guanajuato.

It consists of a continuously improved stimulation system finally operating automatically through the programming tools applied; it is based on installed hardware with either a microcontroller programming or FPGA's, something that is extremely useful for automation of applications required in the laboratory.

### 3.2 CELL GROWN BEHAVIOR UNDERGOING RANDOM SEGMENTS OF OSCILLATING MAGNETIC FIELD

The first experiment consisted of the stimulation of cell culture by applying magnetic oscillating frequencies in the range 15-2500Hz for time lapses of six minutes each. Then the form of the cell culture and its behavior is observed. The results showed that magnetic fields in a range frequency of 15-150 Hz maintained the cells with a normal behavior, what looks to be their natural culture conditions in terms of its pseudopod elongation and physical form, as shown in figure 3.1(A). In the experiment related to this figure, the cells were exposed to a magnetic field at a frequency of 100 Hz. In the case of stimulation with frequencies between 400-1000 Hz it was observed that the cells seem to be susceptible to the magnetic field. The cells tend to form agglutinations assuming a stressed behavior because of the round and rough form they take, (see figure 3.1(B)). At frequency ranges of 1000- 2500 Hz, the cell movement of the pseudopods is lower and the cells can be seen thicker than their normal way as shown in figure 3.1(C).

The second experiment consists of analyzing of the images obtained with the CCD camera with the frames being taken every 0.72 seconds. Then a comparison between the actual taken image

frame and the frame capture taken one instant before is carried on; the difference between pixels are then added to obtain a total movement area. A secondary video was made to show the pixels marking when there is a difference between the actual one and the previous one taken an instant before. The difference between pixels is then saved in a matrix to do the movement analysis. This shows that there may be changes in the cell movement behavior (see figure 3.2). When the magnetic field was applied, a control cell culture was observed, and it was determined that it maintained their movements at values of an average of 23 dimensionless unities. I built a comparative experiment applying an oscillating magnetic field with a frequency varying in the range of 10-750 Hz, changing in a random way during time lapses of six minutes and for duration of four hours. This experiment showed that the movement of the cells was in a range of, an average of 23.25 dimensionless unities. With this information we can obtain a movement difference between the stimulated cells and the control cells. It is obtained that; when frequencies lower than 100 Hz are applied a minimum of movement is obtained when frequencies are in ranges of 400-800 Hz; it is important to mention that when the magnetic fields are in ranges between 100-400 Hz, the cell movement tends to be from fast to normal.

The comparative graphic between the magnetic stimulation signal and the cellular movement average -at each six minutes time lapses- show that the effect of the magnetic field is reflected at the last minutes of each time lapse; therefore the first graphic in figure 3.3 shows, the frequency applied to the cell culture and the second graphic, shows how the cell culture is reacting to the stimulation.

We have therefore adapted this assay for studying *Entamoeba* chemotaxis. We have in the course of this study discovered that components of *E. invadens*-conditioned culture medium are key determinants of *Entamoeba* cell motility. The response to the conditioned medium (CM) includes an increase in both speed and negative chemotaxis (17).

This study clearly shows a direct effect of MFs in the behavior of different ciliates, the swimming velocity, and directional changes of the cell a magnetic field that can induce a behavior change phenomena in cell culture, and a possible effect on (F-actin) and (MyoII). Due to the observed mechanical variations, it can be considered that capping protein modulation changes.

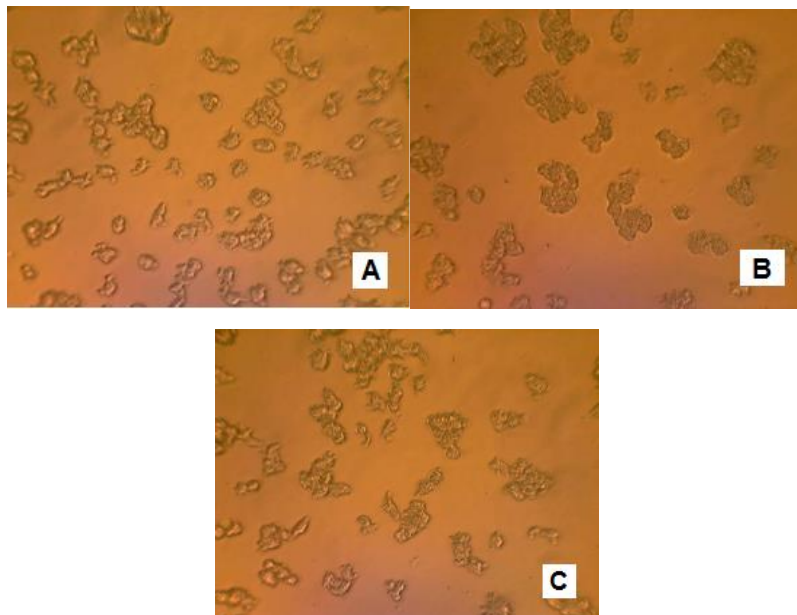




Figure 3.1. Images of the stimulated cell culture, with oscillating magnetic field in range frequencies of A) 100 Hz, B) 800 Hz, C) 1500 Hz, at the end of six minutes intervals.

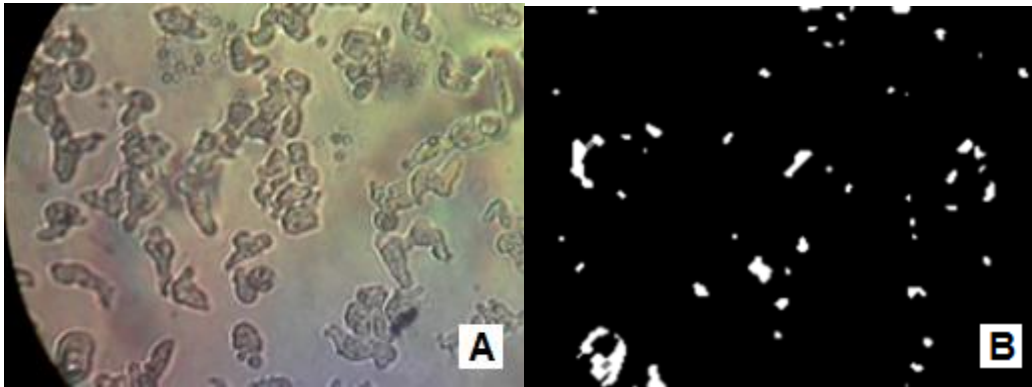


Figure 3.2. A) Obtained image with the CCD camera, B) pixels marked when there is a difference between the actual image and the image frame taken an instant before.

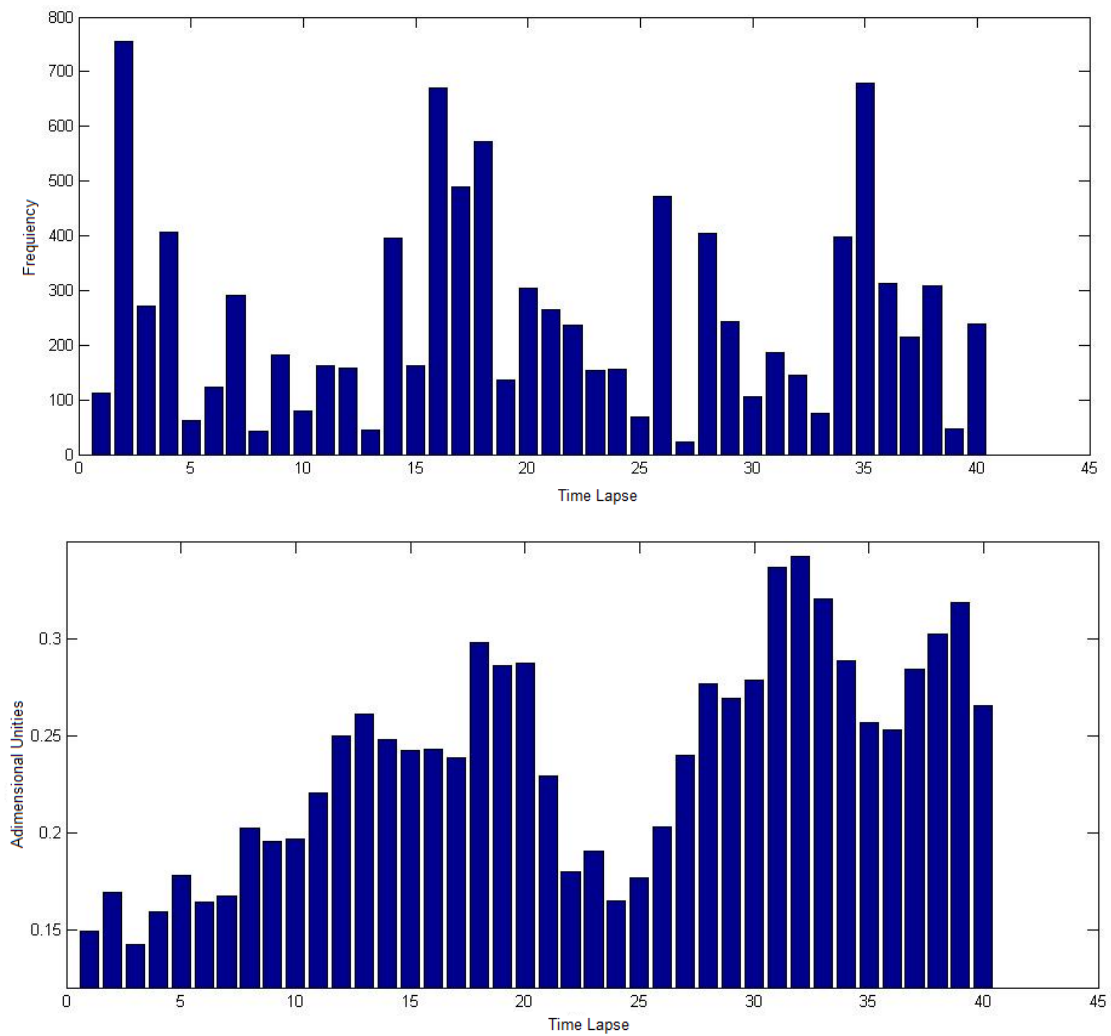


Figure 3.3: Comparative graphic between the magnetic stimulation signal and the cellular movement average, at each six minutes time lapse.

### 3.3 MAGNETIC EXPOSURE SYSTEM TO STIMULATE DOUBLE NUCLEI CELL DIVISION

It is demonstrated that a magnetic field reduced the number of protein nucleation and not only orientates the protein, but also it modified the habit of protein crystals (40). This suggests that a magnetic field can take place in the cell protein stabilization, promoting the cytofission (20,41).

We tested this hypothesis in the following experimental system: in the culture *E. Invadens*. Cells were exposed to SVMF of 5-7500 Hz / 2 mT for 2 h. Then we added ferromagnetic fluid and determined by test and error procedure the better frequencies necessary to stimulate cell division. This conducted us to consider as the best option a cycle of 30 minutes, stimulating by 6 minutes with each frequency mentioned above. It was noticed that a lower frequency is necessary at the beginning of each cycle, because the cells need to rest from the stressing frequencies; this will assure that the cells will be stimulated to promote mitosis, see figure 3.4.

A cell culture of Single nucleus, *Entamoeba histolytica* and *E. invadens* was exposed to the SVMF condition mentioned before, at a temperature of 36 °C. Using a real-time microscopy, we identified at least two modes of cytokinesis (42). Cytoplasmic constriction was initiated at random time, generating two dividing parts of a cell that pulled away one from each other and forming a thin cytoplasmic bridge that was eventually severed. In these cases, the connecting cytoplasmic bridges became unusually long and thin, but were not finally severed. Instead, the cytoplasmic bridge contracted and the two 'dividing halves' fused together without division. No significant increase in the number of dividing cells at any time after completion of the nuclear cycle was observed.

Another experiment was made with the cell culture of *Entamoeba invadens*. The experiment was made having a 20% of double nuclei cells, resulting in the double nuclei cell division before the 2h of magnetic exposure thanks to the magnetic stimulation, and at a temperature of 26 °C.

So it may be assumed that exposure to SVMF resulted in specific metabolic stress effects in *Entamoeba*, but it can be seen that there is a link, between the magnetic field when activating the SVMF enhanced cell proliferation of all cells, and division of the cells having more than one nucleus.

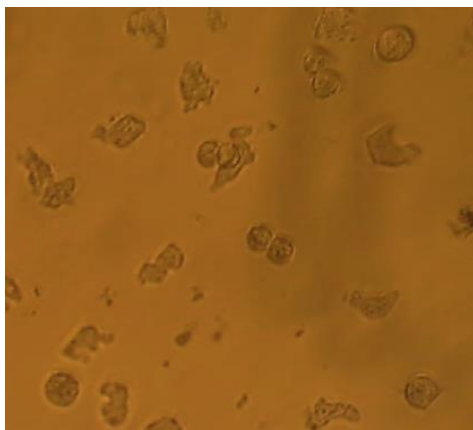


Figure 3.4: Cell division by magnetic stimulation.



### 3.3.1 EFFECT OF GD AND MF ON AMOEBIC GROWTH

#### 3.3.1.1 *E. Histolytica* HM1-IMSS

The growth of *E. histolytica* HM1 was determined in the vials used throughout the experiments done by Orlando Martinez from the research team in the University of Guanajuato, to observe whether amoebae grew to confluence in the vial. At time 0, 50,000 trophozoites / vial were inoculated and growth was determined every 24 hours. As seen in Figure 3.5, the optimum growth was at 72 hours and then there was a decline in the number of cells recovered, suggesting not-conducting experiments with longer times like 3 days of culture inoculated.

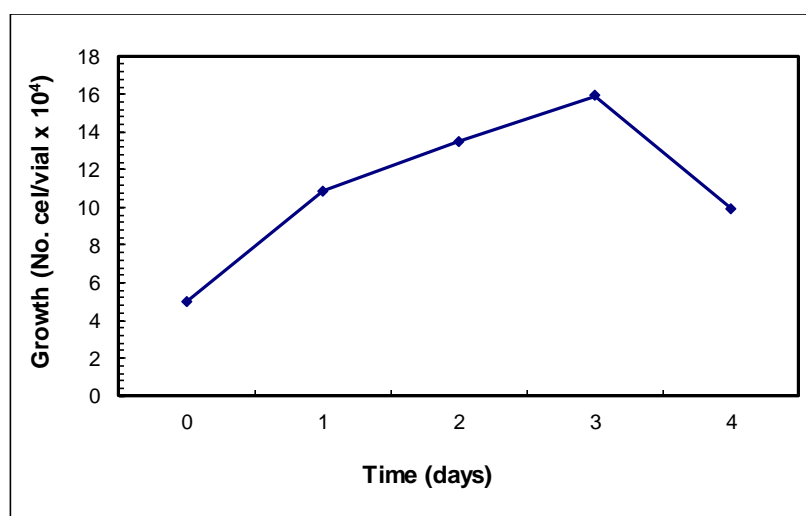


Figure 3.5: Growth curve of *E. histolytica* HM1-IMSS. 50,000 trophozoites / 3 ml vial were inoculated, containing TYI-S-33 complete, and counting every 24 hours the trophozoites present.

To analyze the frequency effect of the MF and Gd on the growth of *E. histolytica*, amoebae was exposed to a magnetic field of 2500 Hz, for 2 hours each day over three days. The MF itself has no effect on cell growth. As seen in Figure 3.6, Gd inhibits cell growth in the presence or absence of the magnetic field. Gd had an inhibitory effect on cell growth in both, the absence and presence of different concentrations of Gd tested (0, 0.8, 1.6, 3.3, 8.3 and 16.6 mM).

In each test, cell viability was determined, using trypan blue and 2% v / v; in all cases it was equal to, or greater than 95%. Each assay was performed at least three times for repeatability purposes.

### 3.3.1.2 E. Invadens IP-1-NY

Similarly to what was done with *E. histolytica* in *E. invadens*, amebic growth was evaluated to determine its growth in culture vials of  $13 \times 30$  mm, using an initial inoculum of 50,000 trophozoites / vial.

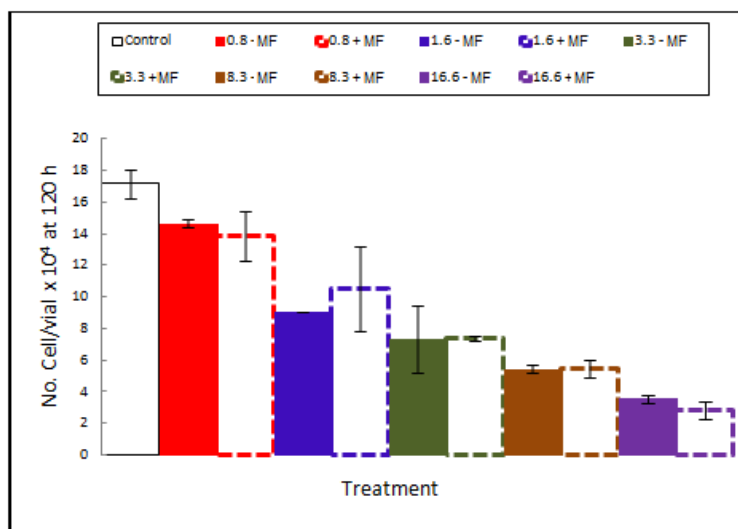


Figure 3.6: Effect of Gd and MF (fixed frequency) on the growth of *E. histolytica* HM1. The effect of Gd on the growth of *E. histolytica* in the presence and absence of a 2500 Hz varying field, applied MF for three days, for 2 hours each day. The white bar represents the control without Gd and without MF; the solid color bars represent the samples with different concentrations of Gd in the absence of MF, and the bars with dotted edges represent the samples with different concentrations of Gd and presence of MF.

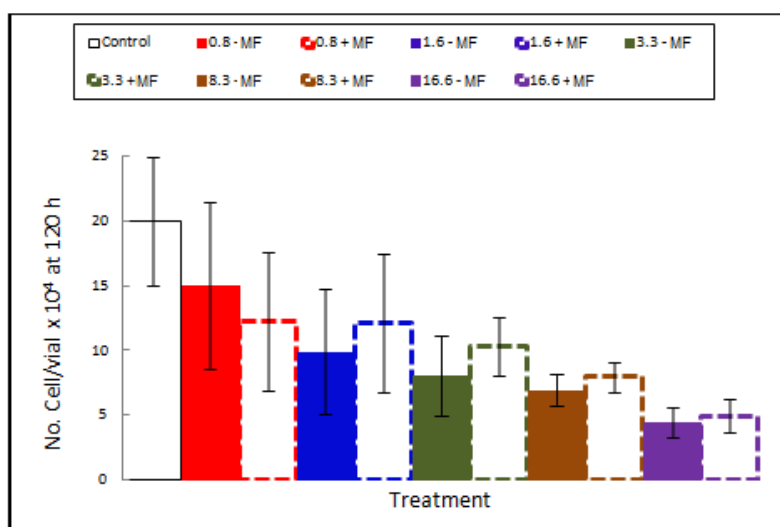


Figure 3.7 Effect of Gd and MF (frequency cycle) on the growth of *E. histolytica* HM1. The effect of Gd on the growth of *E. histolytica*, in the presence and absence of a MF and generated by a cycle frequency of every one of the next frequency values: 0, 100, 800, 1500 and 2500 Hz, for 6 minutes each, and applied for three days, for 2 hours each day. The white bar represents the control without Gd and without MF; the solid color bars represent the samples with different concentrations of Gd in the absence of MF, and the bars with dotted edges represent the samples with different concentrations of Gd and presence of MF.

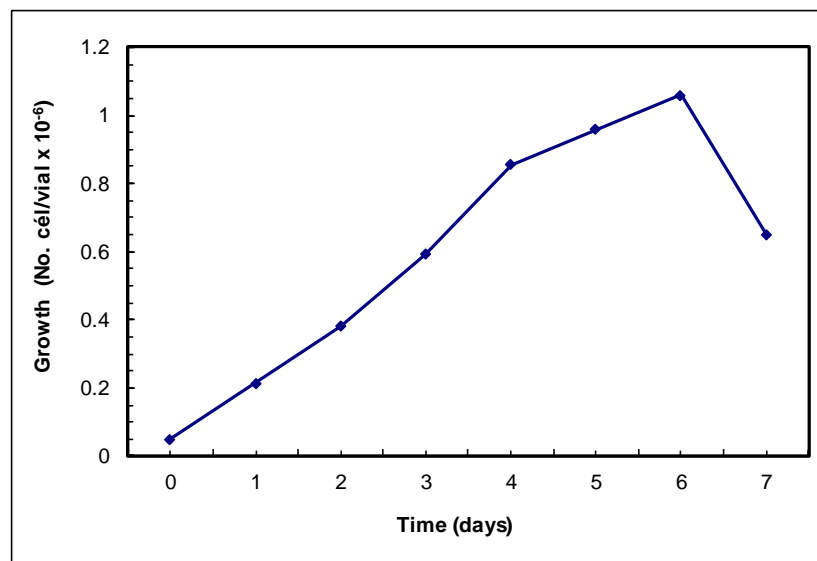


Figure 3.8 Growth curve of *E. invadens* IP-1-NY. 50,000 trophozoites / 3 ml vial -containing TYI-S-33 complete- were inoculated and counted every 24 hours, trophozoites present.

As seen in Figure 3.8, Gd inhibits the growth of *E. invadens*, showing greater inhibition by the increasing concentration.

Gd was added to the medium in proportions of 0.8, 1.6, 3.3, 8.3 and 16.6 mM in the absence of MF, but when the MF was applied, at a frequency of 2,500 Hz, less inhibition of cell growth was observed, yet statistically significant, ( $p < 0.05$ ), in the samples treated with a concentration of 3.3 mM Gd. A similar effect was observed when using the frequency cycle protocol of 0, 100, 800, 1500 and 2500 Hz; 6 min c / u and a concentration of 1.6 mM Gd.

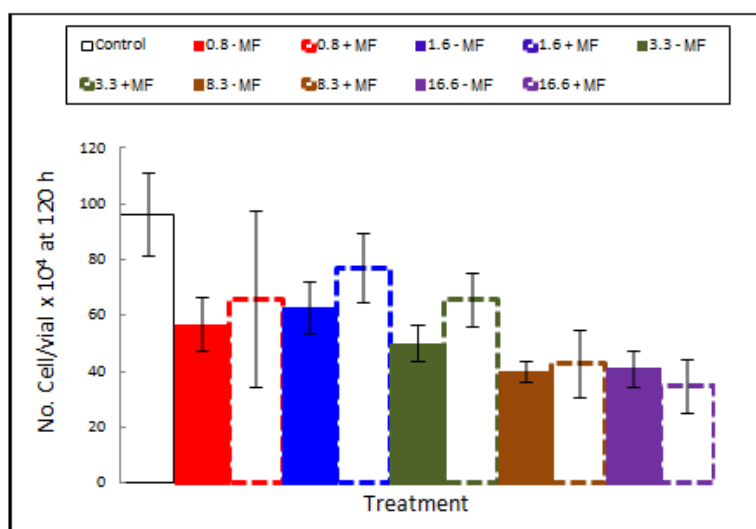


Figure 3.9. Effect of Gd and MF (fixed frequency) on the growth of *E. invadens* IP-1 NY. The effect of Gd on the growth of *E. invadens*, in the presence and absence of MF 2500 Hz, applied for five days, for 2 hours each day. The white bar represents the control without Gd and without MF; the solid color bars represent the samples with different concentrations of Gd in the absence of MF, and the bars with dotted edges represent the samples with different concentrations of Gd and presence of MF.

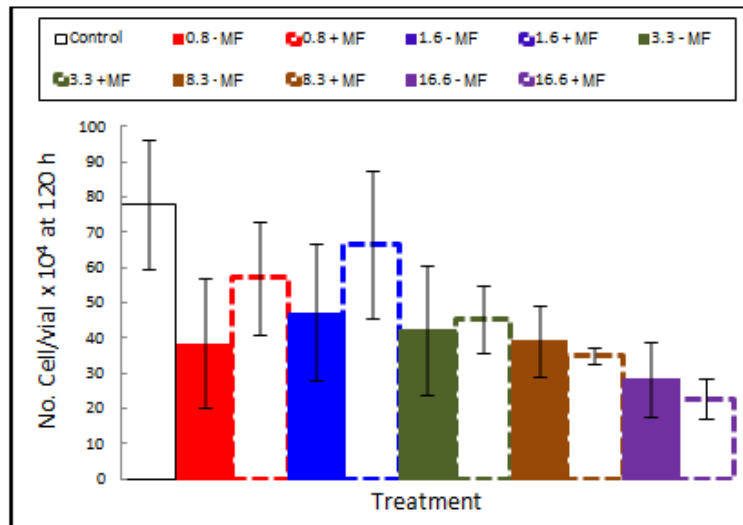


Figure 3.10. Effect of Gd and MF (frequency cycle) on the growth of *E. invadens* IP1 NY. The effect of Gd on the growth of *E. invadens*, in the presence and absence of a MF respectively and generated by cycle frequencies of 0, 100, 800, 1500 and 2500 Hz, lasting 6 minutes each, and applied for five days, 2 hours a day. The white bar represents the control without Gd and without MF; the solid color bars represent the samples with different concentrations of Gd in the absence of MF, and the bars with dotted edges represent the samples with different concentrations of Gd and presence of MF.

### 3.3.2 EFFECT OF MF AND GD ON AMOEBIC ERYTHROPHAGOCYTOSIS

We also studied the effect of the magnetic fields on the metabolism of the amebas. For this analysis the *Entamoeba* were fed with erythrocytes and a magnetic field was applied; it can be noticed that there is an impact of the cells when they absorbed the erythrocytes, and when the magnetic field is applied, a reduction on the phagocytosis can be observed.

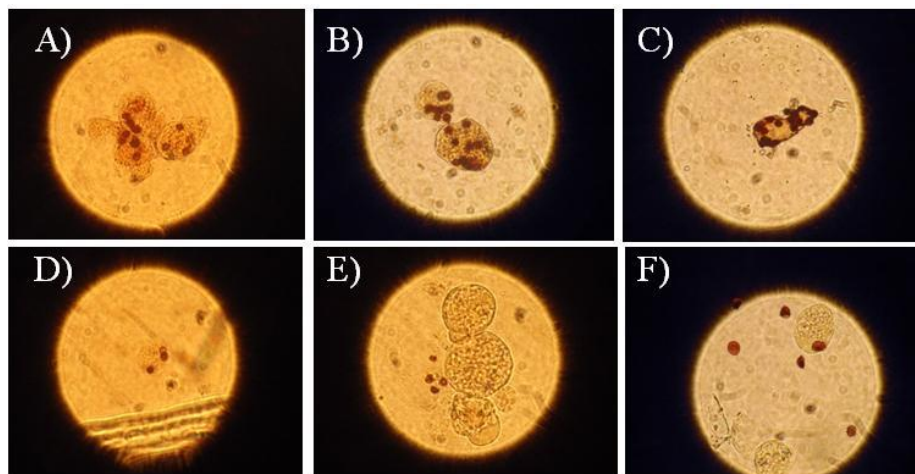


Figure 3.11. Gd effect on *E. histolytica* HM1, Erythrophagocytosis. Photographs of the amoebic erythrophagocytosis. Trophozoites that were incubated with *E. Histolytica* protozoans, every day for 2 hours in the presence of different concentrations of Gd: A) without Gd, B) 0.8 mM, C) 1.6 mM, D) 3.3 mM E) 8.3 mM and F) 16.6 mM.

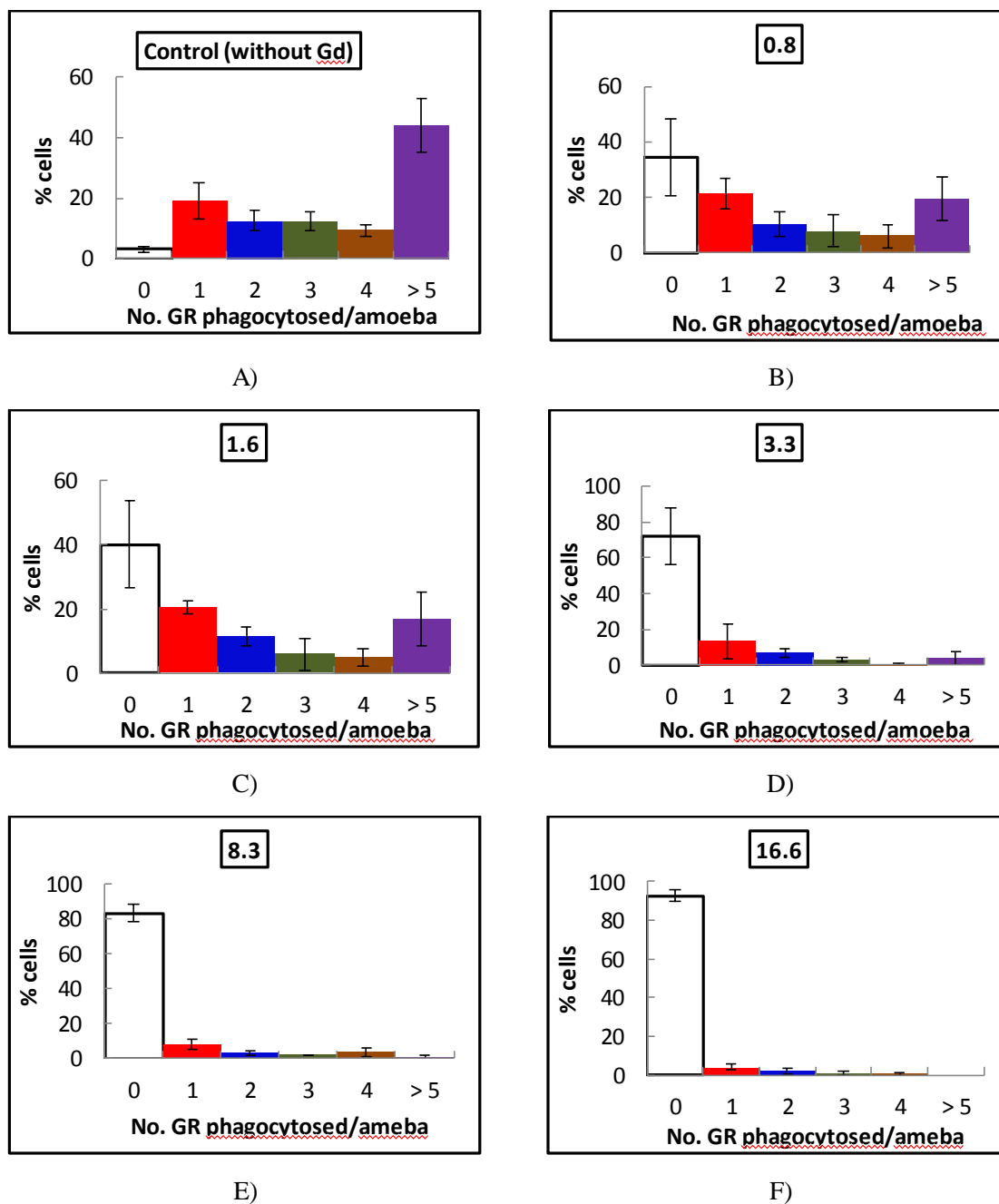


Figure 3.12. Gd effect on *E. histolytica* HM1, Erythrophagocytosis. Trophozoites that were incubated with *E. histolytica* protozoans every day for 2 hours in the presence of Gd concentrations noted in the figure, and subsequently change the culture medium by means without Gd. After three days of exposure; the trophozoites were used to perform the test using a 1:100 erythrophagocytosis (trophozoite / erythrocytes) during 10 minutes. Cells were stained and we counted the number of erythrocytes phagocytosed by amoeba. The concentration of Gd added in each test is presented in each graph, from A to 0 mM (control) to 16.6 mM F with Gd.



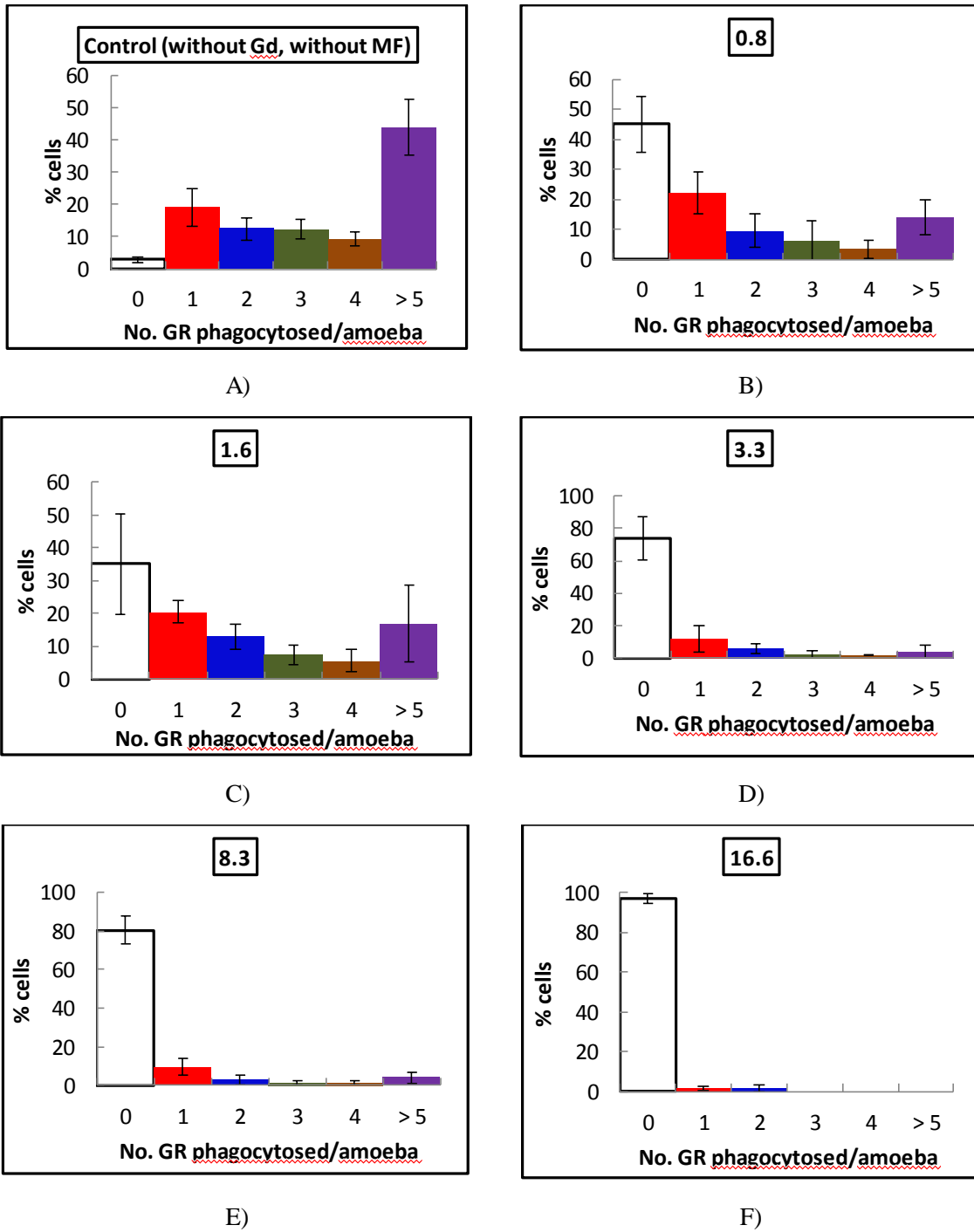


Figure 3.13. Effect of Gd and erythrophagocytosis MF on *E. histolytica* HM1. Trophozoites were incubated with *E. histolytica* protozoans, every day for 2 hours, in the presence of MF at a fixed frequency of 800 Hz and a Gd concentration of 0, 0.8, 1.6, 3.3, 8.3 and 16.6 mM respectively. After three days of exposure, erythrophagocytosis assay conducted for 10 minutes. Cells were stained and the number of erythrocytes, phagocytosed by amoeba, was counted.

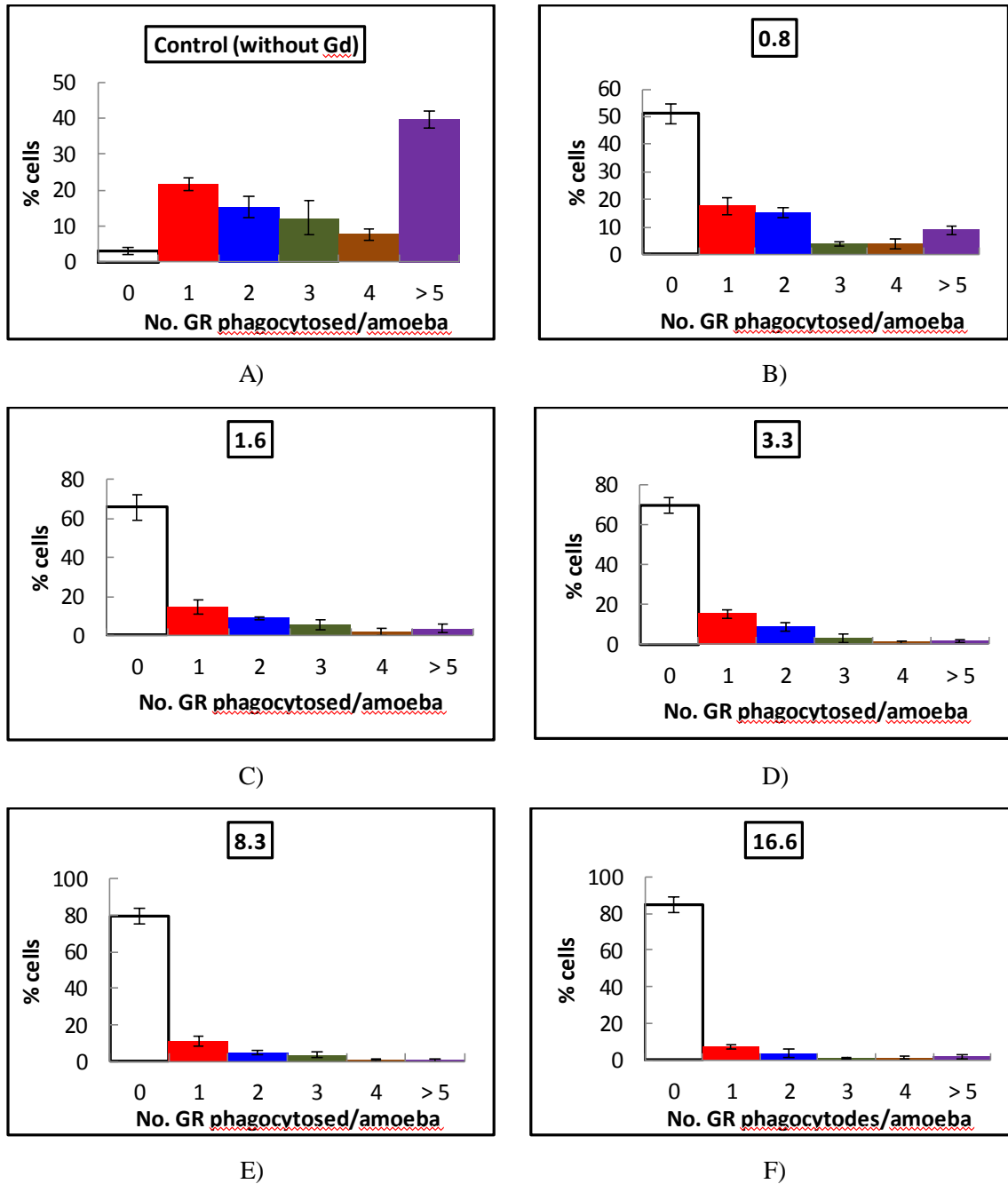


Figure 3.14. Gd effect on *E. invadens* IP-1 NY, erythrophagocytosis. Trophozoites were incubated with *E. invadens* protozoans, every day during 2 hours, in the presence of the Gd concentrations noted in the figure, and then changing the culture medium without Gd. After five days of exposure, the trophozoites were used to perform the test using a 1:100 erythrophagocytosis (trophozoite / erythrocytes) for 30 minutes. Cells were stained and the number of erythrocytes, phagocytosed by amoeba, was counted. The concentration of Gd added in each test is presented in each graph, from 0 mM (control) to 16.6 mM F with Gd.

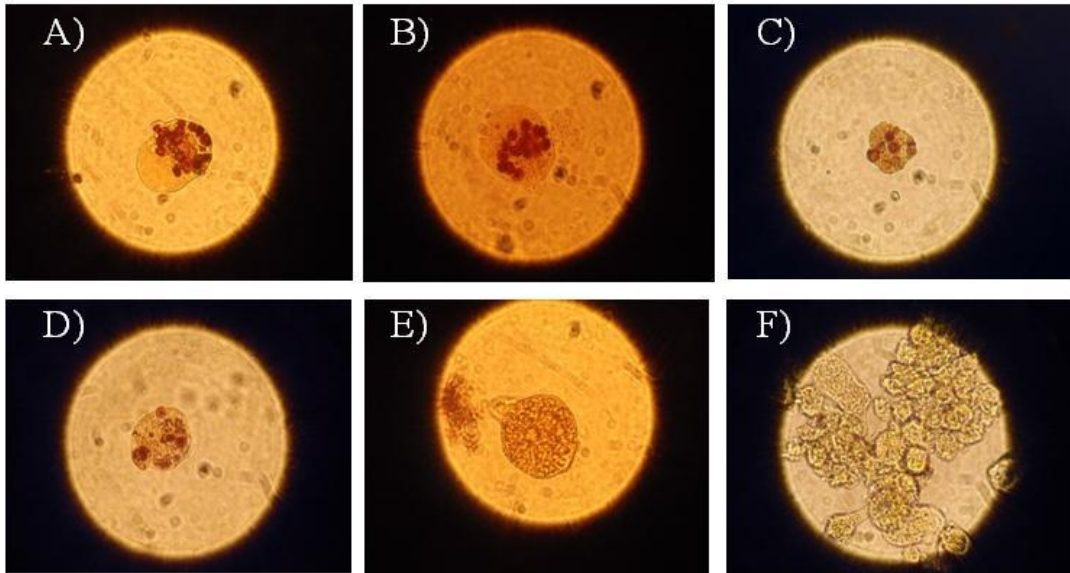


Figure 3.15 Gd effect on *E. histolytica* HM1, erythrophagocytosis. Photographs of the amoebic erythrophagocytosis. The trophozoites were incubated with *E. histolytica* protozoans, every day during 2 hours, in the presence of MF at a fixed frequency of 800 Hz, and at different concentrations of Gd as shown in figures A to F: A) without Gd, B) 0.8 mM, C) 1.6 mM, D) 3.3 mM E) 8.3 mM and F) 16.6 mM. After three days of exposure, the trophozoites were used to perform the test, using a 1:100 erythrophagocytosis (trophozoite / erythrocytes) during 10 minutes. Cells were stained and the number of erythrocytes, phagocytosed by amoeba, were counted.

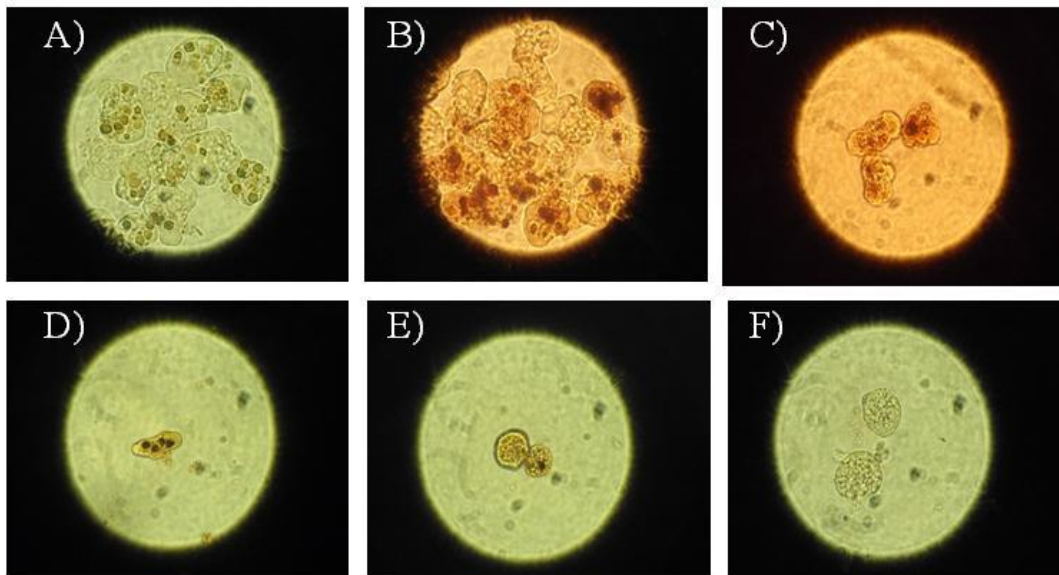


Figure 3.16. Gd effect on *E. invadens* IP-1 NY, erythrophagocytosis. Photographs of the amoebic erythrophagocytosis. The trophozoites were incubated with *E. invadens* protozoans, every day during 2 hours in the presence of different concentrations of Gd as shown in figures A to F: A) without Gd, B) 0.8 mM, C) 1.6 mM, D) 3.3 mM E) 8.3 mM and F) 16.6 mM. After five days of exposure, the trophozoites were considered apt for the test to be performed, using a 1:100 erythrophagocytosis (trophozoite / erythrocytes) during 30 minutes. The cells were stained and the number of erythrocytes, phagocytosed by amoeba, was counted.

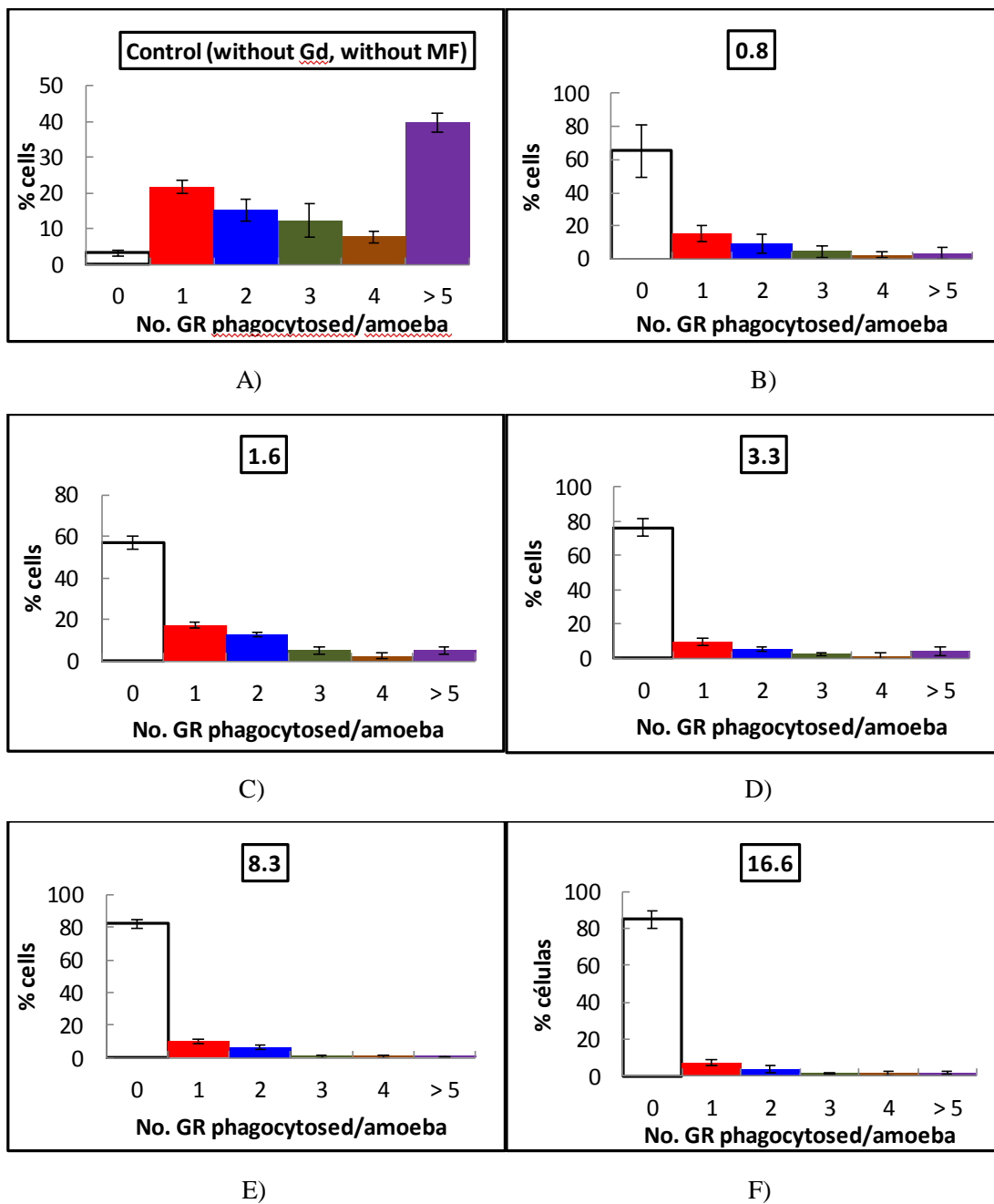


Figure 3.17. Effect of Gd and MF at a fixed frequency on erythrophagocytosis in *E. invadens* IP-1 NY. The trophozoites were incubated with *E. invadens* protozoans, every day during 2 hours, in the presence of MF at a fixed frequency of 800 Hz and different Gd concentrations: 0, 0.8, 1.6, 3.3, 8.3 and 16.6 mM from A to F respectively. After five days of exposure, erythrophagocytosis assay conducted during 30 minutes. The cells were stained and the number of erythrocytes, phagocytosed by amoeba was counted.

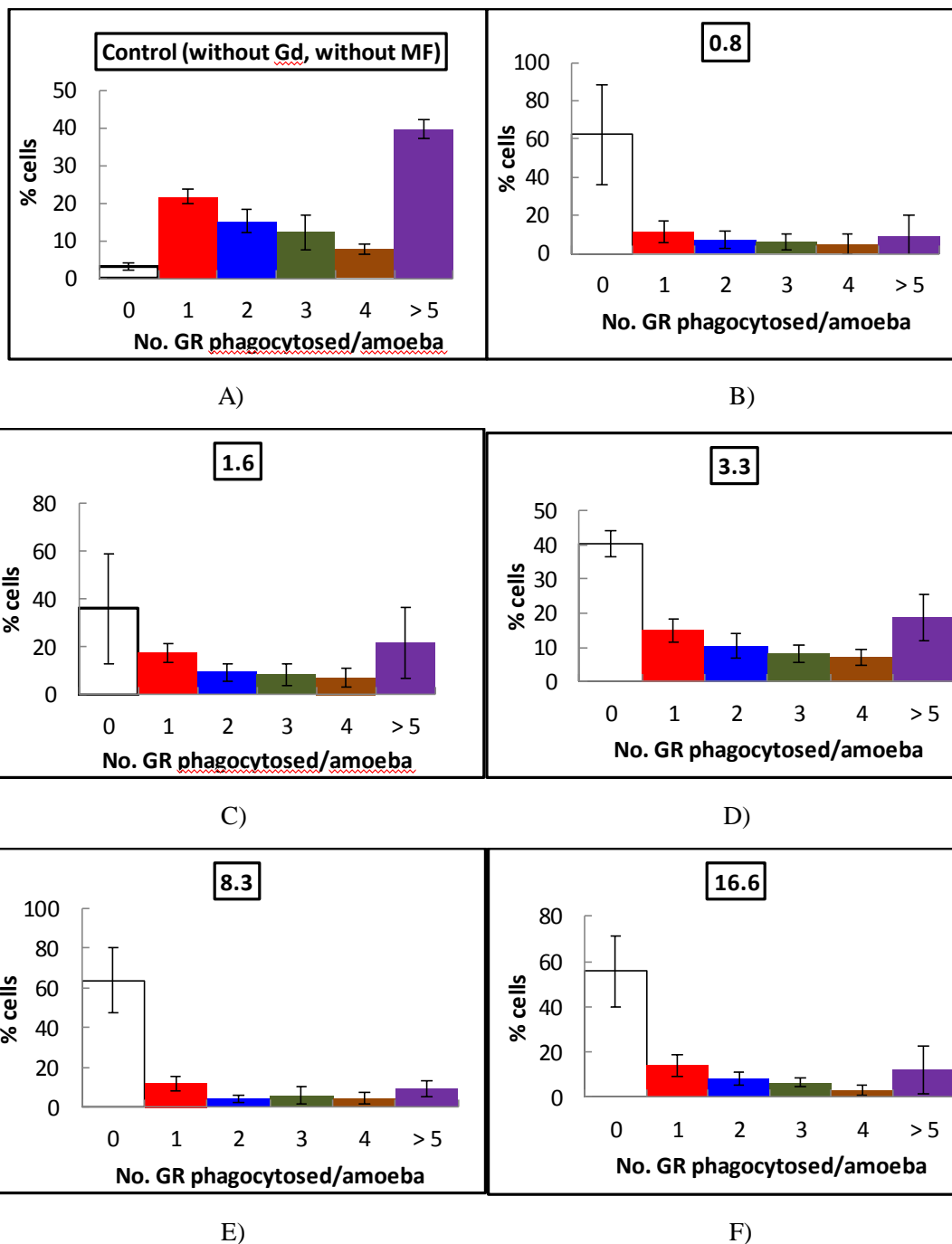


Figure 3.18. Effect of Gd and MF at variable frequencies on erythrophagocytosis in *E. invadens* IP-1 NY. The trophozoites were incubated with *E. invadens* protozoans, every day during 2 hours, in the presence of MF at frequency cycles of 0, 100, 800, 1500 and 2500 Hz, for 6 min each and Gd concentrations of 0, 0.8, 1.6, 3.3, 8.3 and 16.6 mM in figures A to F respectively. After five days of exposure, erythrophagocytosis assay were conducted during 30 minutes.

The cells were stained and the number of erythrocytes, phagocytosed by amoeba, was counted.

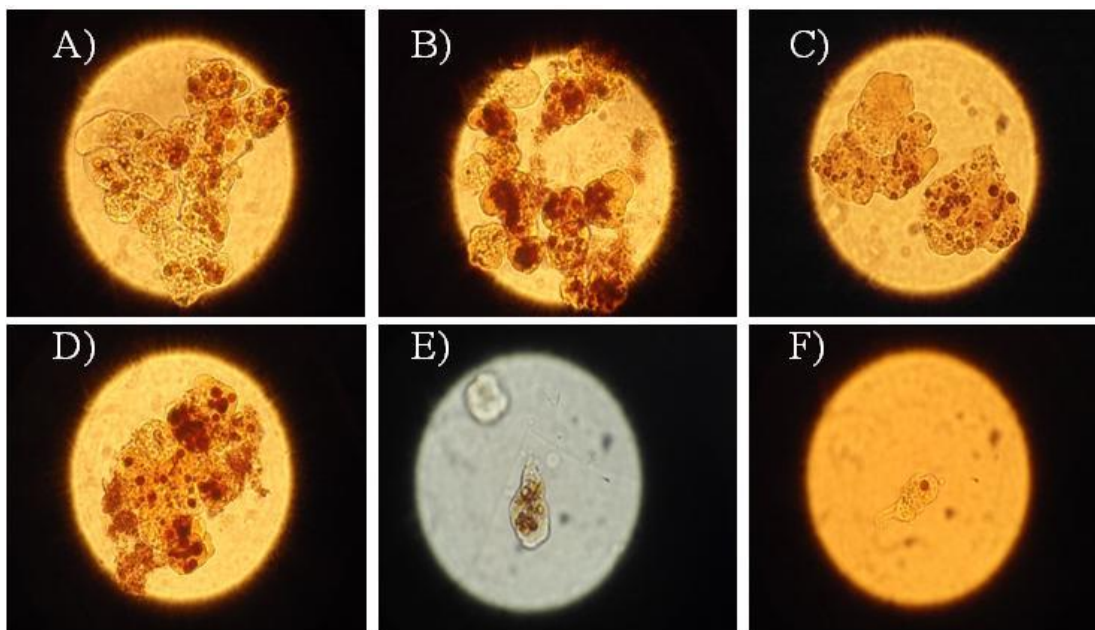


Figure 3.19. Effect of Gd and MF at variable frequencies on erythrophagocytosis in *E. invadens* IP-1 NY. From A to F photographs of the amoebic erythrophagocytosis are shown. Trophozoites were incubated with *E. invadens* protozoans, every day during 2 hours, in the presence of MF-frequency cycle of 0, 100, 800, 1500 and 2500 Hz, during 6 min each and Gd concentrations of 0, 0.8, 1.6, 3.3, 8.3 and 16.6 mM for snaps A to F respectively. After five days of exposure, the trophozoites were used to perform the test, using a 1:100 erythrophagocytosis (trophozoite / erythrocytes) during 30 minutes. The cells were stained and the number of erythrocytes, phagocytosed by amoeba, was counted.

### 3.3.3 EFFECT OF MF ON GD AND AMOEBIC AGGLUTINATION

#### 3.3.3.1 EFFECT OF GD AND MF IN *E. HISTOLYTICA* HM1-IMSS

It was determined that trophozoites aggregate formation subjectively, observing cells through an inverted microscope every 5 minutes for a duration of 2 hours of test. Agglutination was evaluated in the absence and presence of MF induced by a fixed frequency of 800 Hz and a series of frequencies of 0, 100, 800, 1500 and 2500 Hz during 6 min each, in the presence of the next different concentrations of Gd: 0, 0.8, 1.6, 3.3, 8.3 and 16.6 mM. If the table 3.1 is observed: The number in parentheses is the time in minutes, at which cell agglutination is made.

Table 3.1.Effect of Gd and the MF on cell agglutination *E. histolytica*.

Treatment	Concentration of Gd (mM)					
	0	0.8	1.6	3.3	8.3	16.6
Without MF	-	-	-	-	-	+
						(95)
Cycle of frequencies	-	+	+	+	+	+
		(35)	(35)	(45)	(20)	(15)
Fix frequency 800 Hz	+	+	+	+	+	+
	(65)	(35)	(25)	(25)	(20)	(15)

### 3.3.3.2 EFFECT OF GD AND MF IN *E. INVADENS* IP-1-NY

It was determined that trophozoites aggregate subjectively the formation by observing the cells with an inverted microscope every 5 minutes for a total time of 2 hours. Agglutination was evaluated in the absence and presence of MF induced by a fixed frequency 800 Hz and a series of frequencies equal to 0, 100, 800, 1500 and 2500 Hz, and for 6 min each in the presence of the next different concentrations of Gd: 0, 0.8, 1.6, 3.3, 8.3 and 16.6 mM. The number in parenthesis in table 3.2 represent the time in minutes at which cell agglutination initiated.

Table 3.2.Effect of Gd and the MF on cell agglutination *E. invadens*.

Treatment	Concentration of Gd (mM)					
	0	0.8	1.6	3.3	8.3	16.6
Without MF	-	-	+	+	+	+
			(105)	(55)	(45)	(35)
Cycle of frequencies	+	+	+	+	+	+
	(25)	(25)	(15)	(25)	(15)	(15)
Fixed frequency 800 Hz	+	+	+	+	+	+
	(35)	(15)	(15)	(15)	(15)	(5)

### 3.3.4 EFFECT OF SUGARS, GD AND AGGLUTINATION MF ON AMEBIC

It has been reported that in the agglutination process, amebic proteins, called lectins, were involved; these bind with high specificity sugars. The most studied are lectin, recognizing galactose residues and N-acetylgalactosamine (Gal / GalNAc). Based on this evidence it can be said that the effect of some sugars on amebic agglutination are induced by MF and / or Gd, several test were made to determine the involved sugars resulting in the fact that there were the lectins who were involved in cell agglutination. To perform these tests, the following sugars were used: galactose (Gal), lactose (Lac), glucose (Glc) and N-acetyl glucosamine (GlcNAc), and as a control normal culture medium, TYI-S-33, with no sugar added.

#### 3.3.4.1 EFFECT OF SUGARS, GD AND MF IN *E. HISTOLYTICA* HM1-IMSS

It was observed that in the presence of Gal and Gd, a cell monolayer was formed on the test wells on the first 15 min of addition, however, the formation of the monolayer was not complete, at the end of 2 hours of treatment, it was also observed a small cell aggregation; with Gd in the presence of MF. The monolayer formation and cell clusters were maintained for 85 min.

Table 3.3. Effect of sugars, Gd and MF on cell agglutination *E. histolytica*.

Treatment	Gd	Gd + MF	MF
Gal	(20)	(0)	(55)
	+	0	+
	(0)	(85)	(0)
Lac	(35)	(0)	(55)
	+	0	+
	(0)	(85)	(0)
Glc	(5)	(95)	(15)
	+	++	+
	(0)	(0)	(0)
GlcNAc	(5)	(25)	(5)
	+	++	+
	(0)	(0)	(0)
Medium	(95)	(15)	(35)
	+	+	++
	(0)	(0)	(0)

Table 3.4. Effect of sugars, Gd and MF on cell agglutination *E. invadens*.



Treatment	Gd	Gd + MF	MF
Gal	(0)	(0)	(0)
	0	0	0
	(5)	(15)	(5)
Lac	(0)	(0)	(0)
	0	0	0
	(5)	(15)	(5)
Glc	(5)	(15)	(25)
	++	++	+
	(0)	(0)	(0)
GlcNAc	(5)	(15)	(25)
	++	++	+
	(0)	(0)	(0)
Medium	(35)	(5)	(25)
	+	+	+
	(0)	(0)	(0)

++ Strong agglutination

+ Weak agglutination

0 No agglutination

#### 3.3.4.2 ANALYSIS OF GADOLINIUM INSIDE THE ENTAMOEBA MEMBRANE

To know if the gadolinium access the interior of the cell membrane, several vials containing 1 gram of total protein of ameba were measured with an XRay spectrometer. This can determinate the presence of gadolinium inside the membrane. It permits to observe the absorption of this paramagnetic fluid by the cell, giving the possibility of an atomical exchange between the molecules of the cell and the paramagnetic fluid, enforced by the oscillating magnetic field. As it has been observed in many non-equilibrium processes that go through a radical pair intermediate, the magnetic field is thought to influence the spin dynamics in the pair and thereby, to determine the branching ratio between singlet recombination and triplet dissociation. Here, I propose a qualitatively new mechanism by which magnetic nanostructures can significantly enhance the effect of magnetic fields on radical pair processes. The essence of the argument is that the field, due to a magnetic nanostructure, may vary significantly over the extent of a single radical pair, causing the two spins to process at different rates and about different axes. Relative reorientation of two spins leads to intersystem crossing (ISC). Homogeneous magnetic fields, in contrast, are forbidden by symmetry from achieving this relative reorientation, and only affect spin dynamics through higher order processes. Field gradients, near physically realistic magnetic nanostructures, are strong enough to dominate all other processes that lead to ISC. Nanostructures that may enhance ISC include magnetic nanocrystals, ferromagnetic domain boundaries, and surfaces exhibiting antiferromagnetism, or spin density wave order (43–48).

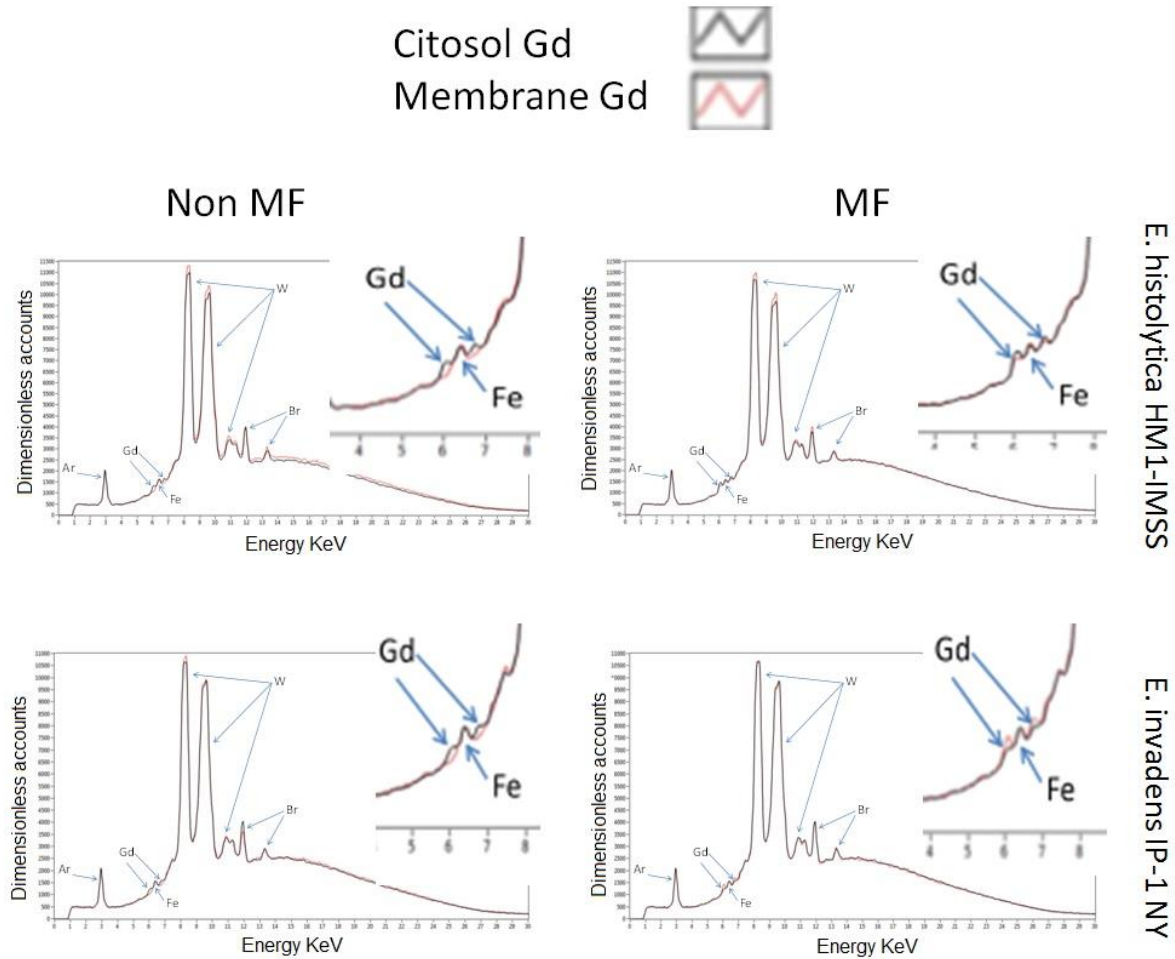


Figure 3.20. Determination of the subcellular distribution of Gd in *E. histolytica* HM1-IMSS and *E. invadens* IP-1 NY.

In Figure 3.20 Fluorescence spectra of X-ray determination was made to observe the subcellular distribution of gadolinium in the ameba culture, where mixed fraction cytosol and membranes both parasites in the presence of Gd is shown in (Panel A and C) and comparing the cytoplasmic concentration of Gd in the presence and absence of MF amoebian, the two species (Panel B and D). The peaks that appear are Ar, due to air; W, the X-ray tube; Br, to the measuring table; and Fe, its presence in the environment. The Gd has two peaks with energies of 6.07 keV and 6.71 keV.

### 3.4 PORTABLE DEVICE FOR MAGNETIC STIMULATION: ASSESSMENT SURVIVAL AND PROLIFERATION IN HUMAN LYMPHOCYTES

A non-invasive device for stimulation with magnetic vortices in cells growing was presented. The vortices of magnetic field were programmed to work in random segments at frequencies of 100, 800, 1500, 2450 and 2500 Hz. As far as it is known, this is the first time that magnetic vortices and suspension of Gadolinium were added to the PBMC samples to improve the effect of magnetic field.

In order to determine the effect of the magnetic field stimulation, a primary culture of human lymphocytes isolated from healthy donors was tested. After 72 h there were no changes in cell proliferation or cell survival when the PBMC were co-stimulated with magnetic field and concanavalin A, in comparison with those PBMC treated only with concanavalin A (data not shown). However, after 7 days of culture, it was found that magnetic field stimulation did not induce any change on human lymphocytes without mitogenic treatment (Fig. 3.21c). When human lymphocytes were co-stimulated with magnetic field and concanavalin A, an important increase on proliferating cells was detected (Fig. 3.21d), thus, when lymphocytes were treated with concanavalin A but not stimulated with a magnetic field, the proliferation was observed in a lesser extent (Fig. 3.21.c). In Fig. 3.21 the representative plots for the CFSE dilution there are shown. In vitro concanavalin A, induced T cell proliferation was evaluated in healthy donors. The CFSE-labeled PBMCs were alternately stimulated or not stimulated under a magnetic field, then they were cultured either with or without concanavalin A for 7 days and finally the percentage of divided cells was determined by flow cytometry.

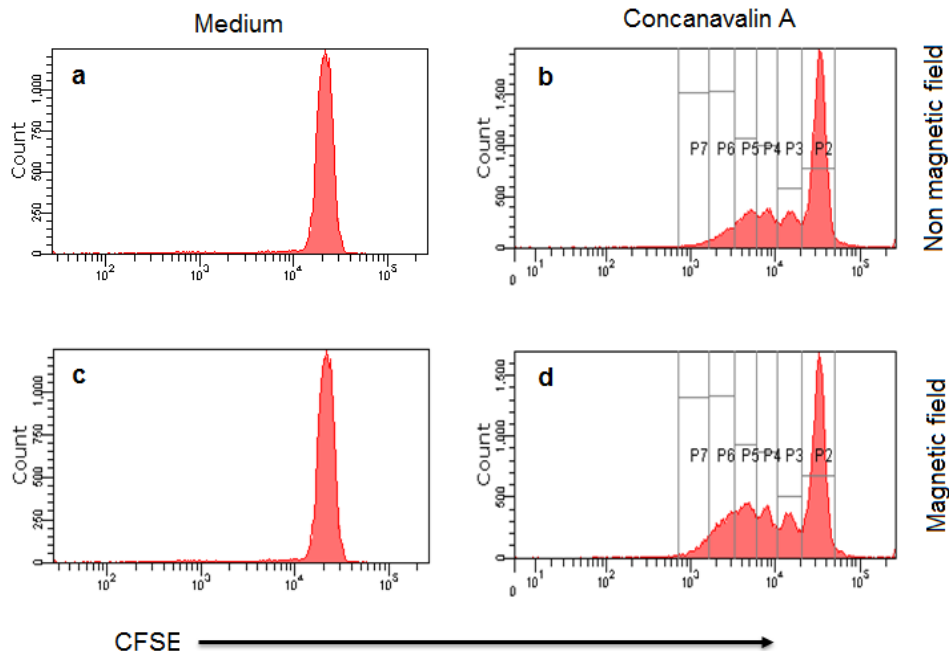


Figure 3.21. Proliferation of human T cells stimulated with concanavalin A and magnetic fields: a) PBMC cultured in RPMI with no concanavalin A, nor magnetic fields; b) PBMC stimulated with concanavalin A but not magnetic fields; c) Concanavalin A stimulated cells with any magnetic field; and d) cells stimulated with both concanavalin A and magnetic

fields. Average of cells reaching 2 (P4), 3 (P5), 4 (P6) and 5 (P7); the cell divisions were significantly higher in cells stimulated with concanavalin A under magnetic fields, than those stimulated with concanavalin A and no magnetic fields.

On the other hand, when 20 days cultures of human lymphocytes were analyzed, an important increase in the number of surviving cells was detected on lymphocytes co-stimulated with magnetic fields and concanavalin A (Fig. 3.22.d), while only few lymphocytes treated with concanavalin A, but not stimulated with a magnetic field, were viable after 20 days on culture (Fig. 3.22.b). It must be remarked that cells stimulated under a magnetic field, but not treated with concanavalin A, had a higher surviving ratio than those stimulated with concanavalin A alone (Fig. 3.22.c).

### 3.5 INCREASING SURVIVAL IN KIDNEY HEK-293T CELLS IN PRESENCE OF MAGNETIC FIELD VORTICES AND NANO-FLUID

Figure 3.24 shows the experimental and the control group HEK-293T cell culture, in addition of Dotarem ® nano-fluid (concentration 0.01 mmol / ml), in which only the stimulation has a different magnetic. Different parameters were evaluated like the cell size (forward side scatter-SSC) against the cell granularity (-FSC), 72 h after magnetic exposure, using a flow cytometry technique.

Figure 3.23 shows an increase in the survival of the samples exposed to magnetic stimulation, compared to control samples with a difference of 12.89 %, with a  $P < 0.05$ , by using Student's normalization method.

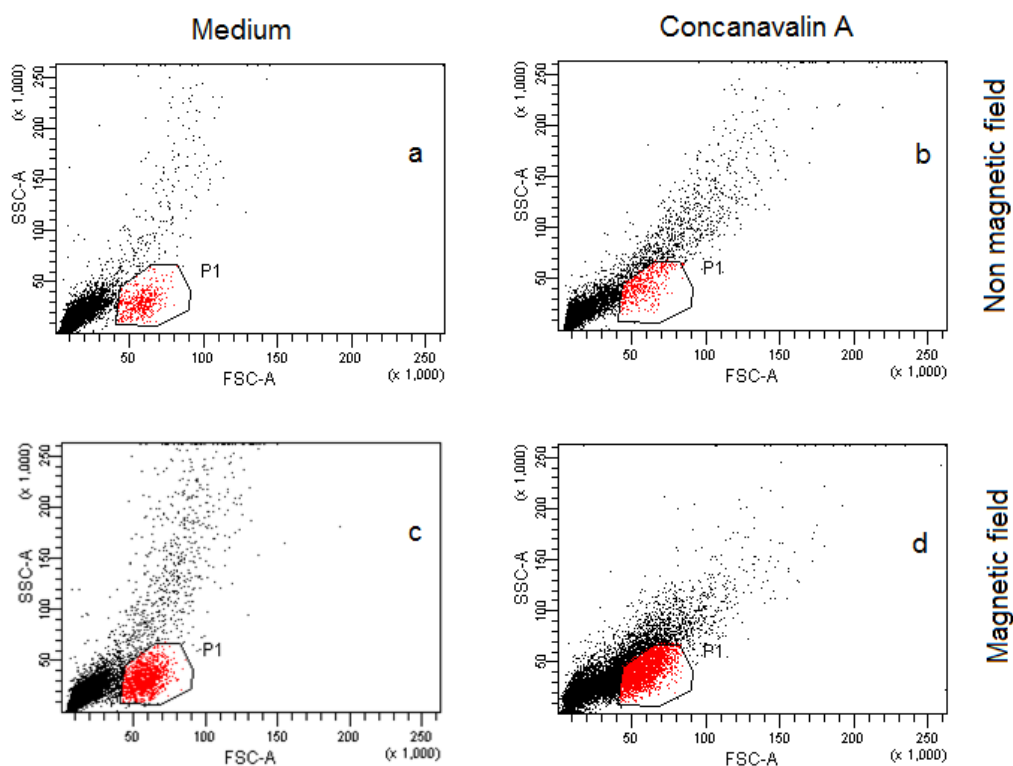


Figure 3.22. Histogram obtained from flow cytometric analysis of a magnetic field that excites samples from volunteer patients. P1 represents proliferating cells and the black spot near the origin represents dead cells. a) Cell divisions unstimulated with concanavalin A, b) Stimulated cell division with concanavalin A, c) Cell population unstimulated with concanavalin, and d) Cell divisions with concanavalin and magnetic stimulation. Forward Scatter Counts (FSC), Side Scatter Counts (SSC).

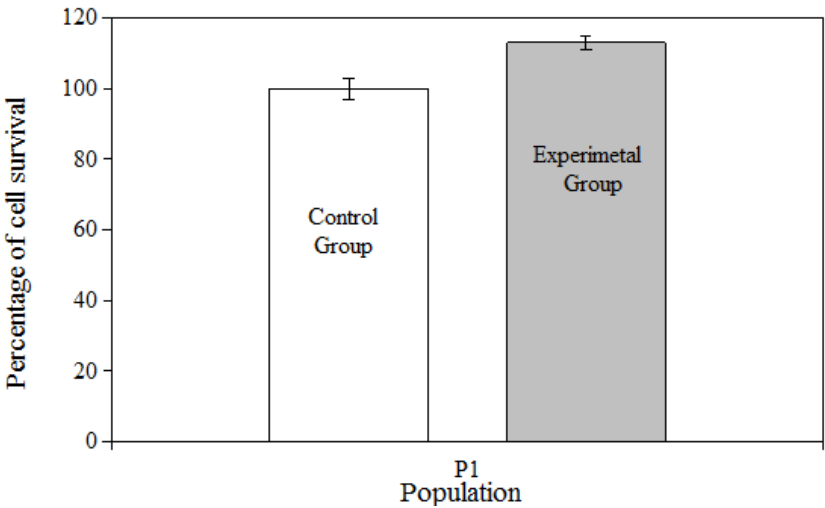
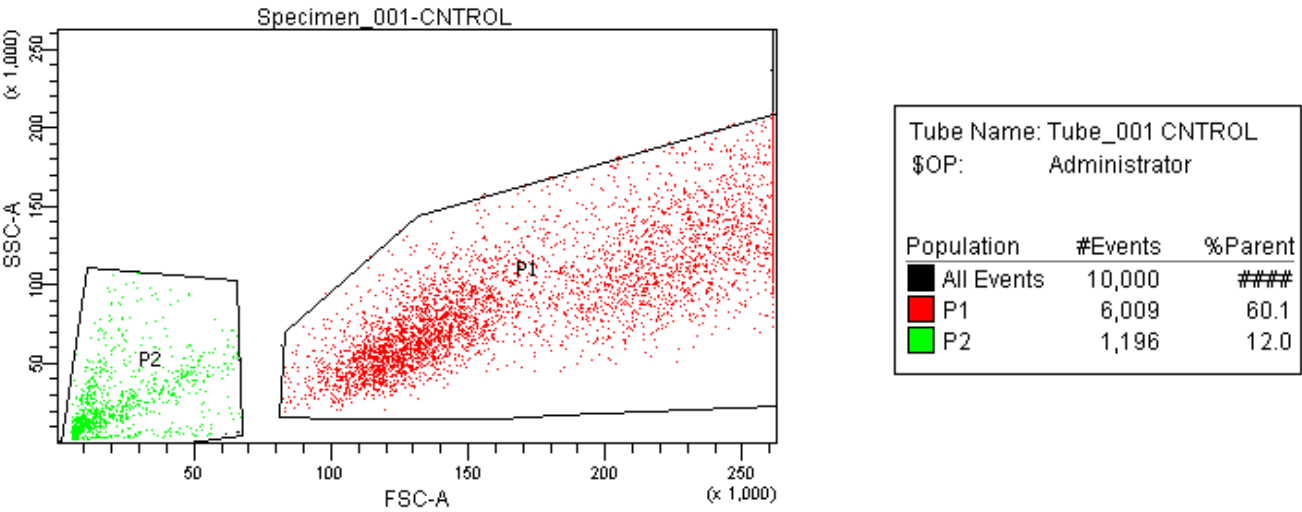


Figure 3.23. The survival of control samples and samples exposed to the magnetic field is shown here. HEK-293T line cell was prepared with nano-fluid. P1 shows the population (survival) of 3 independent experiments performed in triplicate ( $P < 0.05$ ), where a 12.89 % is the increase in cell survival.



a

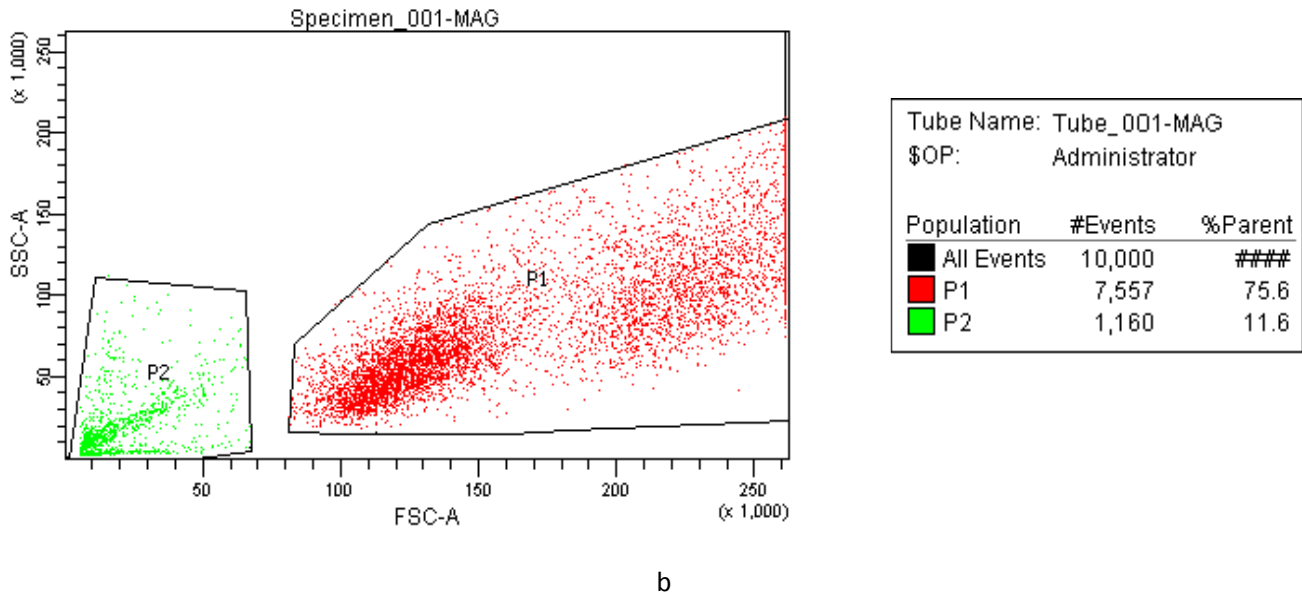


Figure 3.24. Histograms of the control group (a.) and the experimental group (b.). There are two known populations P1 and P2, which represent the cell survival and cell in the death process.

### 3.6 APPLICATION OF INSTRUMENTATION FOR OTHER RESEARCH AREAS

#### 3.6.1 DEVICE TO EVOKE THE BONE SYSTEM IN HIP DISLOCATION DIAGNOSIS

This device can be used as a sound transmission test to diagnose congenital hip dislocation in newborns of affected parents, or in some cases, whole families. For its usage it is recommended that the diagnosis must be made by a specialist medical doctor.

Commonly hip dislocation problems are detected or diagnosed usually when the infant is older. Then it could be necessary to make a risky intervention. This is the main reason to make an early diagnosis at young age. This device is then recommended for this specific purpose due to its easy usage and low price.

For its usage the device emits a sound that is transmitted mostly through the bone and its microphone is placed on the iliac crest, located on the same side of the femur. Extending the foot of the subject in analysis, the value brand for powerful sound is observed in the instrument display. The whole operation is repeated on the other side of the individual and the values are compared. If the powers are very similar, it means that probability of a hip dysplastic lesion is low but if there are variations greater than 10 percent, it means that there is a break and it must be addressed promptly. As a second analysis, the same operation is performed by flexing the leg of the individual being tested, toward his chest at an angle of 90 degrees. Next power comparisons –consisting in matching the powers– help to determine any damage of dysplasia.

By applying this principle, this device can detect the existence of fractures and low levels of calcium, if the sound transferred by the transmission medium is affected, the signal will be partially truncated at the point where the medium is interrupted.

The bone is a material with a certain hardness and therefore, a good sound transmitter. If at some point a transmitter is placed at a particular frequency, it is expected that at a known distance, a power level of sound has to be detected. With this approach, it is possible to establish a relationship in the breakpoint of sound and at the point where a fracture or injury is located. The amplitude of the signal captured through the receiver indicates if there is any suffering from dysplasia of the hip; this means that a rate analysis from input/output signal, determines if there is a dislocation of bone in the femur or in the hipbone.

In the first experiment (at a fixed position), the recorded reference audio signal is compared with the incoming signal from the opposite end of the bone; if the measured signal is smaller than a hysteresis test value, then it means that the hip is affected, otherwise, it can be considered as an unaffected hip bone. Furthermore, for the flexural test two signals were recorded; the first in a fixed position (0 degrees) and the second in flexion (90 degrees). Comparing the two audio signals, some of which resulted in greater amplitude, means the hip bone has had involvement. Otherwise, the hip is considered healthy.

These encouraging results do not replace standard clinical maneuvers, however, this technique can be considered as an alternative for the detection of disease in a developing dysplastic hip.

---

### 3.6.2 MEASURING GASTROESOPHAGEAL REGION FREQUENCIES: PRELIMINARY RESULTS

The registered signals shown in the majority of the subject's registries of contractile activity, in the different sections from the gastro esophageal tract the following:

- Basal activity

The contractile activity for this relaxed state of bloat was between the 1,5 and 3 cpm (cycles/minute).

- Postprandial activity

The contractions are better defined by less noisy signals, with the frequencies that went from the 1,5 to 3 cpm, being the more recurrent frequencies of 2,5 cpm or greater. Unlike the shown activity in the basal state, in the after-lunch state there are fewer overtones for the main frequency of contractions in the different sections from the stomach.

- Esophageal activity

The predominant activity of this region was around the 1,5cpm, although, in some subjects, there were harmonic frequencies of around 3 cpm. In figure 3.26, the behavior of the main frequencies of contraction for a subject can be observed in each one of the gastric bloat states (basal and postprandial) and for each of the regions (stomach and gullet). In figure 3.26, the variation of the main contraction

frequencies can be appreciated, as well as how they change depending of the GI section; and the distention states in which it is. Finally, a summary is presented in figure 3.27.

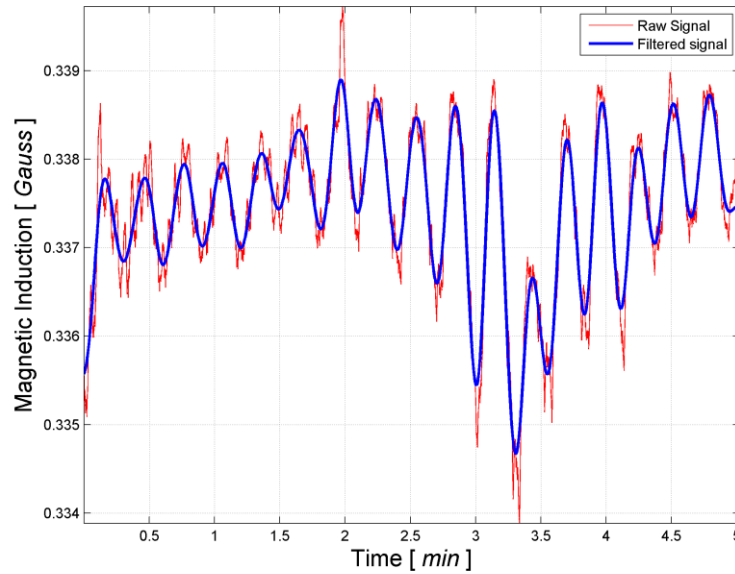


Figure 3.25: Contractile activity of the stomach after the food ingestion.  
The contractions in the stomach are around three contractions per minute can be observed.

### 3.6.3 BIOMAGNETIC VALIDATION TO SKIN LEVEL FOR BLOOD PRESSURE CURVES AND VENOUS PRESSURE

The first part of the measurements performed with the PPC device shows an excellent behavior of the pulse waves from arterial and venous pressure; it is a stage of apnea, where the wave morphology of the artery and the pulses of the vein are shown in accordance with the physiological theory of the cardiac cycle. This test was performed in healthy subjects.



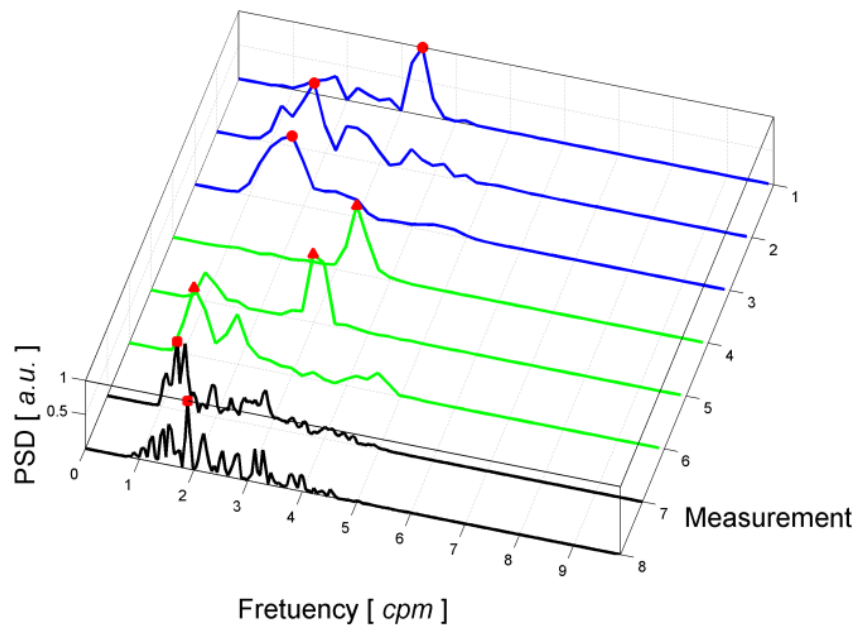


Figure 3.26. Graphic of the spectral densities indicating the main frequencies in the different regions from the GE tract, from the antrum region (measurement 1), to the middle esophagus (last measurement). This graphic contains all the measurements realized in a subject. The blue lines show the measurements in basal state. In these measurements it can be observed how the contractions' frequency was slowing down while the stomach went away relaxing. The green lines show the frequencies after the subject ingested food. It is easily perceivable that as the stomach has more luminal containing, the gastric activity returns smoother, and when the stomach is empty, the activity becomes noisy.

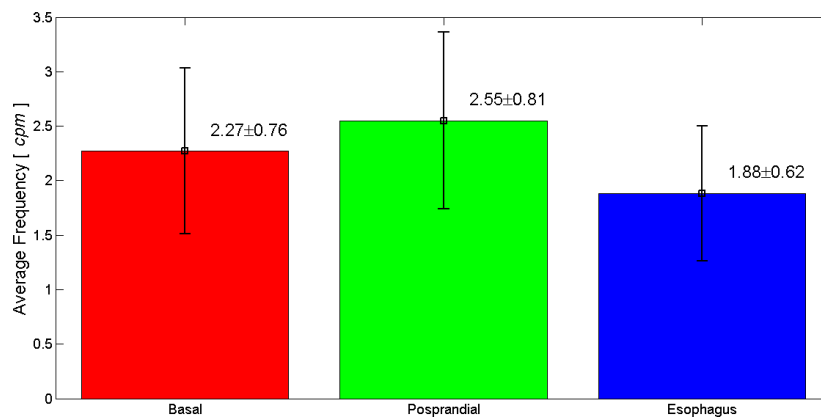


Figure 3.27. Averages of the contraction frequencies of all measured subjects, for every one of the different distention states.

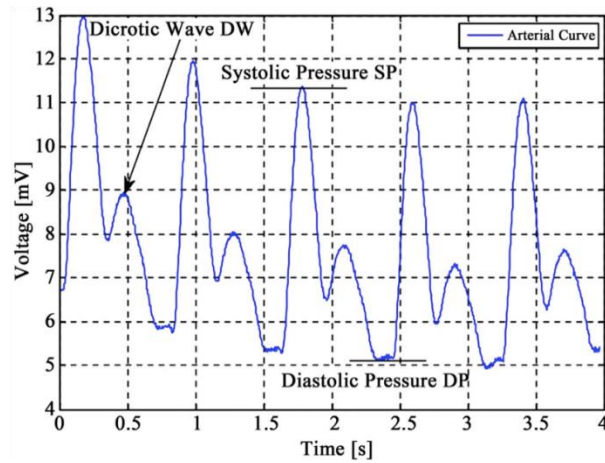


Figure 3.28. Typical pressure wave recorded, using a PPC device, on suprasternal zone and in supine position with breathing noise. The curve is reached, clearly distinguishing three points of interest: dicrotic waves, due to backflow of blood; as well as maximal and minimal, corresponding to the systolic pressure (SP); and diastolic pressure (DP), as the cardiac cycle.

The positive waves of venous pulse coincide with a delay or with the reverse of the flow, while each depression indicates an acceleration of venous return.

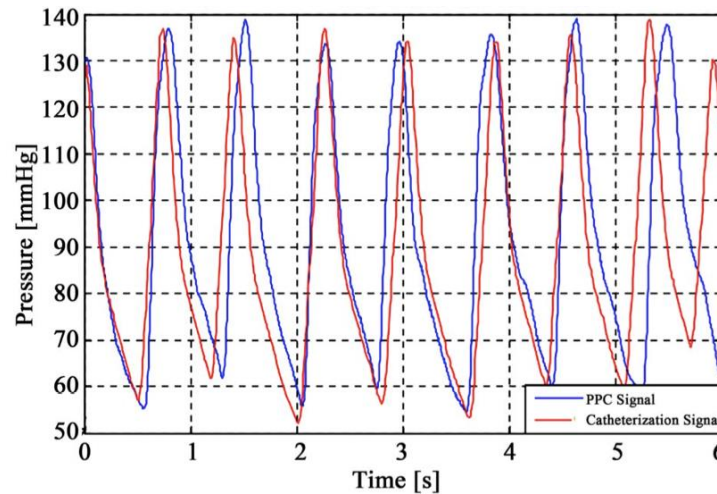


Figure 3.29. Superposition of signals obtained with the PPC and polygraph and the switch made from units of volts to millimeters of mercury in the PPC signal.

A statistical analysis was performed to determine the correlation between the measures of pressure differences (Pd) in mmHg -obtained with the digital sphygmomanometer standardization in healthy subjects- and voltage differences (Vd) for the PPC. At the same time, there is the correlation for values of PPC and cardiac catheterization. Using the correlation coefficient model of Pearson, Spearman, and Kendall, a linear fit for both cases can be performed.

---

#### 3.6.4 EFFECT OF THE MICRO-MAGNETIC STIMULATION ELECTROENCEPHALOGRAPHIC PATTERNS

---

We can speak of Resistant Depression in the current episode either, when there is no response, or when there is a poor response to one or more doses of therapeutic attempts methods, in appropriate times. One of the problems is the minimum time required for a failed particular treatment to be declared. Some studies suggest that, at least for the Monoamine Oxidase Inhibitors (MAOIs) and imipramine, therapeutic response makes its appearance in a more delayed way, reaching 50% at 10 weeks and 75 % at 17 weeks of treatment. Another study with fluoxetine, also points to a more delayed response. These observations suggest that it is necessary to be very cautious with the classic model of 4-6 weeks of treatment with no response to declare it definitively failed.

In a human study under optimal conditions, patients were exposed to 0.5-3 mT of magnetic stimulation for a period of 2 hours. The application of the stimulation signal occurred, creating a cycle in which sinusoidal signals stimulated at frequencies of 1, 8, 15, 24, 7.5 Hz, each one for periods equal to 6 minutes and lasting 2 h. SVMF exposure resulted in specific effects via stimulation of the neuronal brain's reward system, with a set of coils and a deeper level of magnetic penetration of about five to six centimeters into the cerebral cortex. In this way depression can be treated. It is also capable of stimulating other brain areas associated with other mental illnesses.

Some studies suggest that, at least for the MAOIs and imipramine, therapeutic response at a later point, reaching 50% at 10 weeks and 75 % at 17 weeks of treatment. Another study with fluoxetine also points to a more delayed response. These observations suggest that it is necessary to be very cautious with the classic model of 4-6 weeks of treatment with no response to declare it definitively failed.

## 4 CONCLUSION AND DISCUSSION

The aim of this study was to evaluate the effect of MF and Gd on different cellular activities of *E. histolytica* HM1-IMSS and *E. invadens* IP-1 NY. The specific objectives were the evaluation of amoebic growth, erythrophagocytosis, and cellular clumping effects of Gd and MF (fixed rate or variable).

### 4.1 EFFECT OF MF AND GD ON AMOEBIC CULTURES

A new noninvasive instrumentation has been described, this is a magnetic stimulating device, in which vortices of magnetic field are generated by a magnetic source assembly with an arrangement of Copper winding's vortex coils, through a sinusoidal signal. This device was programmed to work at frequencies of 100, 800, 1500, 2450, and 2500 Hz. It is important to point out that these frequencies were selected after doing a pilot study and finding that the effects of proliferation were evident. The effect of sinusoidal varying magnetic fields was tested on amoebic cultures such as *E. histolytica* and *E. invadens*.

The multiple studies performed around the side effects of electromagnetic field on biological models, to date, there are still not enough conclusive results that indicate whether a malignant or beneficial effect is induced through EM fields. Therefore, additional experiments are being carried out in our laboratory and in other laboratories all around the world in order to elucidate the intracellular mechanisms induced after electromagnetic field stimulation.

Here it was determined that Gd inhibits cell growth of *E. histolytica* depending on the concentration achieved without the MF affecting this behavior. However, this inhibitory effect manages to be reversed in *E. invadens* to apply a concentration of 3.3 mM Gd at a fixed frequency of 2,500 Hz, or at a concentration of 1.6 mM, with a cycle frequency. At the end of the trial, the trophozoites show a viability equal to or greater than 95% being inhibited in *E. erythrophagocytosis histolytica*, depending on the concentration of Gd used, and apparently the MF does not affect it; but when applied to a MF protocol cycle frequencies in *E. invadens*, Gd concentrations of 1.6 and 3.3 mM, were observed in significant erythrophagocytosis.

Most MF Gd accelerates cellular agglutination, especially when applying a fixed frequency of 800 Hz, this effect is clearer in *E. invadens*. In the absence of Gd binding stimulates the ameba with MF for longer times. Sugars that are involved in cell binding, are those containing Glc, since there is allowed a more rapid and greater consistency in the formation of cell aggregates, best observed in *E. invadens*.

By spectrometric analysis of X-ray fluorescence, an evaluation for the presence of Gd (49) within samples established that an approximately 65% remains in the culture medium and the other 35% is internalized within the cell, specifically within the cytosol. Also, the MF differentially affects both amoebae causing Gd increase or decrease, depending on the amoebic species cytoplasm.

A more stable instrumentation was then made, for researchers to study the effect of magnetic fields on living beings can further apply it. There have been systems which have the capability of quick response, with order to have a wide range of working frequency and to generate a signal as clean as possible, so that one day it can be applied in medicine or industry.

## 4.2 DETERMINATION OF GD IN CELL SAMPLES

*E. invadens* and *E. histolytica* species, exhibit similar behavior with the addition of Gd in the absence of MF, however, when applying the MF in *E. Invadens*, cytoplasmic concentration increases, and when applying the MF in *E. Histolytica*, the opposite effect is observed. This behavior could be explained based on differences in the two lectin amoebic species, suggesting that the differential effects observed at erythrophagocytosis cell agglutination, may have a direct relationship with amoebic lectin and Gd. Additionally, one could speculate that Gd amoebas internalize a very similar way as internalized iron (Fe), to perform its essential metabolic functions, so that it may recognize the Gd amoebae by surface lectin once bound to the receptor, giving start pinocytosis processes and mediated clathrin (a unique protein associated with intracellular transfer of membrane by coated vesicles, or covered vesicles). Once inside, the amoeba initiate degradation in the endosome and finally Gd reach amoebic lysosomes, where they could be degraded by active cysteine proteases at acidic pH, (Sicairos Leon et al., 2010).

## 4.3 PORTABLE DEVICE FOR MAGNETIC STIMULATION: ASSESSMENT SURVIVAL AND PROLIFERATION IN HUMAN LYMPHOCYTES

A new noninvasive instrumentation has been described; this is a magnetic stimulating device, in which vortices of magnetic fields are generated by a magnetic source assembly. The device has an arrangement of Copper winding's vortex type coils, through a sinusoidal signal; and it was programmed to work at the next frequencies: 100, 800, 1500, 2450 and 2500 Hz. It is important to point out that these frequencies were selected after doing a pilot study and found that the effects of proliferation were evident. The effect of sinusoidal varying magnetic fields was tested on fresh human mononuclear cells and stimulated in vitro for 7 and 20 days with a mitogen. The PBMC were collected from healthy donors to avoid any possible alteration on cells, as consequence of diseases or infections, because it is well known that different diseases and infections could alter the proliferation capacity of human cells.

This data had shown that after 72 hours of culture, the magnetic stimulation did not have any effect in both cell proliferation and survival. However, it has been reported that exposition to electromagnetic field decreases the proliferation after mitogenic stimulation (21), nevertheless, the very low frequency (3 Hz) and time of exposition used in other experiments were different than those used here. Controversially, other groups have reported an important increase of cell proliferation after electromagnetic stimulation. Therefore, it is clear that the effect of exposition to electromagnetic field could be influenced by several experimental conditions such as, biological model, exposure system, exposure length, intensity, frequency, and pulse width.

On the other hand, it has been reported that a minimum of 6 h of exposure to electromagnetic field is necessary to induce any effect but, in most cases, a single frequency of exposure was used [(27); also, effects of electromagnetic fields have been observed as soon as 24 h. Here, PBMC was stimulated for 2 h, in intervals of 6 minutes with five different frequencies, and after 5 days of culture. An important increase in the cell proliferation on cells, co-stimulated with mitogen, and electromagnetic field was observed, but not on those PBMC stimulated with mitogen alone.

Moreover, the effect of electromagnetic fields and mitogen also increased the survival after 20 day of cell culture. Thus, some mechanisms of cell survival have been reported to be activated by exposure to electromagnetic fields, such as the increase in the synthesis of RNA (50) and  $\text{Ca}^{+2}$  influx and efflux being observed (23); in the same way, previously, it has been reported that cell exposition to magnetic fields increases cell survival by inhibiting apoptosis via modulation of  $\text{Ca}^{2+}$  influx (50).

#### 4.4 INCREASING SURVIVAL IN KIDNEY HEK-293T CELLS IN PRESENCE OF MAGNETIC FIELD VORTICES AND NANO-FLUID

As far as known, this is the first time that is studied the effect of magnetic stimulation through magnetic vortices, in audible frequency segments from 100 to 2500 Hz and in a magnetic intensity from 1.13 to 4.13 mT, in kidney cell line HEK-293T.

It was shown that 72 h later the magnetic stimulation of cells immersed in nano-fluid, the population was increased on survival and cell viability by 12.89 %.

In the literature, a large number of papers tested the effect of magnetic fields, giving qualitatively and quantitatively different results, depending on the characteristics of the field. Some of these investigations show conflicting results, reporting that as the human lymphocyte exposure to electromagnetic fields decreases proliferation by using a frequency of 3 Hz (21). Conversely, it is also reported that the use of low frequency magnetic fields (60 Hz and 100 Gauss) and using a Helmholtz coil as a magnetic stimulator, accelerate the healing process of the skin in Balb-C mouse (51). Similarly, Cossariza reported that exposure to pulses of low frequency electromagnetic fields increases the lymphocyte proliferation in young and elderly subjects (6). The aforementioned experiments were conducted under conditions different from those of this study: biological model, frequency, field strength, magnetic field generating coil, and exposure time, among some other conditions. However, similar results of this investigation, where exposure to magnetic fields decreases the degree of apoptosis in different human cell systems (52), have also been reported. As it has been seen, the task was to determine the effect of electromagnetic radiation in different biological systems and their potential benefits or damages to them.

The results open a new modality for determine the mechanisms that induce or inhibit the cellular level, mechanisms that cause an increase in proliferation survival, due to stimulation with controlled vortices of magnetic fields and samples in touch with nano-fluid. Due to the similarities and characteristics shared by different cell types, basic principles performed in this study can be applied and extrapolated to other human or animal cells under the same standardized conditions, to determine the behavior of the same.

## 4.5 APPLICATION OF INSTRUMENTATION FOR OTHER RESEARCH AREAS

### 4.5.1 DEVICE TO EVOKE THE BONE SYSTEM IN HIP DISLOCATION DIAGNOSIS

This patented procedure. Bases its operation through a transmitter and a receiver in surface contact, just over the bone to be evaluated, the bone density parameters can be observed on a LCD screen; there is also possible to storage measurements for subsequent assessments. Preliminary measurements determined that the dominant frequency for evaluated femoral bones in several subjects is around 160 Hz, this procedure can be used as a proposed assessment to determine hip dislocation in neonates (babies in the first 3 week of life) (28).

It is important to point out that this is a diagnosis technique proposal for the evaluation of bone density and mainly, for hip dislocation. Traditional techniques for performing these evaluations use ionization radiation, in this case, sound in the audible range is used, as far as known, side effects will be unexpected in these studies, so the babies will have a better quality of treatment.

### 4.5.2 MEASURING GASTROESOPHAGEAL REGION FREQUENCIES: PRELIMINARY RESULTS

The frequencies of contraction for the different distention states, presented a wide rank of frequencies, in particular in the stretched state. This is clearly due to the fact that the particles move throughout the Gastro esophageal (GE) tract in proximal direction, the frequencies are mixed, which means there is a high influence in the esophageal activity. Besides this phenomenon, other factors can be considered to have influence in the results. Some of them are those concerning the characteristic frequency consideration as the frequency that correspond to the maximum tips in our spectral densities of power, and since the stomach behaves in different forms for different subjects, in particular in the state to base, the characteristic tips in this state of bloat are not always the same.

Different modalities to measure gastro esophageal activity have been used, among them is emphasized the manometry and the Radionuclide Imaging, magnetic resonance (to secure references of these techniques), with which registries have been obtained. On the other hand, measurements were made during the food ingestion; hopefully, the sharp alteration of the magnetic direction moments of the markers, originates a great change in the amplitude of the magnetic induction. This shows the potential to register gastro esophageal region frequencies (30).

### 4.5.3 BIOMAGNETIC VALIDATION TO SKIN LEVEL FOR BLOOD PRESSURE CURVES AND VENOUS PRESSURE

The Pulse Pressure Cardiac gauge (PPC) device has shown an excellent signal, which describes qualitatively and unequivocally form elevations and depressions corresponding to waves of arterial and venous pressure by noninvasive methods. However, it is affected by characteristics of the medium



and particularly by respiration; although, the gold standard in measuring blood pressure has proven to be highly correlated with pressure points of a digital sphygmomanometer.

It has more meaning to find the magnitude under the curve, to relate maximum and minimum to a coordinate of voltage, as the device shows a wide variability in its measurements if used at different times with a variation period of 24 h. These result in a descriptive curve, outdated even for the same subject, with the same values of pressure (31).

It cannot be used in individuals with Body Mass Index (BMI), indicating a degree of obesity, because both the suprasternal area and the lateral neck show no oscillatory motion of venous pressure and arteries by the large amount of fatty material, which causes it to lose the spread of the movement of vasodilation.

It can be used for pressure measurement; two scales are needed depending on the type of vessel to measure, because biologically, both vessels show pressure values and curved very characteristic, for the PPC measuring in (voltage-time), and which is already associated with a curve (mmHg-time).

For the venous study, it is proposed to carry out more measurements comparing the signal acquired by the PPC *versus* the cardiac catheterization, like the Doppler echocardiography and oscillometric methods; a larger sample is needed.

---

#### 4.5.4 EFFECT OF THE MICRO-MAGNETIC STIMULATION ELECTROENCEPHALOGRAPHIC PATTERNS

Approximately 30 % of the patients with major depression do not respond adequately to treatment with serotonergic agents and 60-70 %, do not achieve complete remission within 6 weeks. While applying the magnetic micro-stimulation, intervention helped to reduce symptoms associated with major depression and to increase alpha waves in the EEG measurement.

Now mind the protocol used in this research, it is to analyze the effect of magnetic micro-stimulation intervention in people with treatment-resistant depression. The Beck Depression Inventory is applied to evaluate the intensity or severity of symptoms and depression-related behaviors before and after the intervention period with magnetic micro-stimulation. EEG patterns are evaluated before and after the intervention period with magnetic micro-stimulation, to know the type of brain wave that dominates the person, and to apply the magnetic micro-stimulation to people with treatment-resistant depression for a period of time.



This research was concerned to understand the effects that can cause magnetic fields in different kind of cell cultures. Generally summarizing, it is a method of stimulating the viability, proliferation, and cell longevity, using magnetic fields in the range of human audible frequencies; and to improve the outcomes. A paramagnetic fluid has been added to the cell culture to promote a direct stimulus in the cell.

Further analysis of MF and Gd on the structure of the cytoskeleton should be studied, since some reports indicate that the MF fails to produce certain changes in other different models:

- To confirm the subcellular distribution of Gd and characterize the protein that enables fixed and internalization.
- To evaluate the effect of MF and Gd on amoebic protein pattern, *i.e.*, whether there is a change in the number or type of protein in the cell membrane, and
- To analyze the effect of different magnetic frequencies on cells, in order to increase the understanding of the biology of these treated species. Currently known equipment capable of achieving higher magnetic frequencies will be used.

Finally, this is an instrumentation description of the implemented device, where segments of frequencies, in periods of time, were supplied in a biological sample. Despite of this work and multiple studies performed around side effects of electromagnetic fields on biological model, it has to be mentioned that while using this technique, additional experiments are being carried out in collaboration in several laboratories and other labs in the world in order to elucidate the intracellular mechanisms induced after electromagnetic field stimulation.

## 6 BIBLIOGRAPHY

1. Pilla AA. MECHANISMS AND THERAPEUTIC APPLICATIONS OF TIME-VARYING AND STATIC MAGNETIC FIELDS. *Handb Biol Eff Electromagn Fields*. 2006;3:1–79.
2. Markov MS. Pulsed electromagnetic field therapy history, state of the art and future. *Environmentalist* [Internet]. 2007 Sep 6 [cited 2013 Nov 3];27(4):465–75. Available from: <http://link.springer.com/10.1007/s10669-007-9128-2>
3. Sunkari VG, Aranovitch B, Portwood N, Nikoshkov A. Effects of a low-intensity electromagnetic field on fibroblast migration and proliferation. 2011;30(2):80–5.
4. Chow K, Tung WL. Magnetic field exposure enhances DNA repair through the induction of DnaK/J synthesis. *FEBS Lett* [Internet]. 2000 Jul 28;478(1-2):133–6. Available from: <http://www.ncbi.nlm.nih.gov/pubmed/10922484>
5. Perez-Olivas H, Cordova-Fraga T, Gómez-Aguilar F, Rosas-Padilla E, Lopez-Briones S, Espinoza-García a. a., et al. Magnetic exposure system to stimulate human lymphocytes proliferation. *AIP Conf Proc* [Internet]. 2012 [cited 2013 Nov 2];146(1):146–8. Available from: <http://link.aip.org/link/APCPCS/v1494/i1/p146/s1&Agg=doi>
6. Cossarizza a., Monti D, Bersani F, Cantini M, Cadossi R, Sacchi a., et al. Extremely low frequency pulsed electromagnetic fields increase cell proliferation in lymphocytes from young and aged subjects. *Biochem Biophys Res Commun* [Internet]. 1989 Apr [cited 2013 Nov 3];160(2):692–8. Available from: <http://linkinghub.elsevier.com/retrieve/pii/0006291X89924881>
7. Zhang W-J, Chen C, Li Y, Song T, Wu L-F. Configuration of redox gradient determines magnetotactic polarity of the marine bacteria MO-1. *Environ Microbiol Rep* [Internet]. 2010 Oct [cited 2013 Oct 7];2(5):646–50. Available from: <http://www.ncbi.nlm.nih.gov/pubmed/23766250>
8. Wendla Paile, Kari Jokela, Armi Koivistoinen SS. Effects of 50 Hz sinusoidal magnetic fields and spark discharges on human lymphocytes in vitro. *Bioelectrochemistry Bioenerg*. 1995;36(1):15–22.
9. Potenza L, Cucchiaroni L, Piatti E, Angelini U, Dachà M. Effects of high static magnetic field exposure on different DNAs. *Bioelectromagnetics* [Internet]. 2004 Jul [cited 2013 Oct 13];25(5):352–5. Available from: <http://www.ncbi.nlm.nih.gov/pubmed/15197758>
10. Torgomyan H, Kalantaryan V, Trchounian A. Low intensity electromagnetic irradiation with 70.6 and 73 GHz frequencies affects *Escherichia coli* growth and changes water properties. *Cell Biochem Biophys* [Internet]. 2011 Jul [cited 2013 Oct 13];60(3):275–81. Available from: <http://www.ncbi.nlm.nih.gov/pubmed/21229332>
11. Sakurai T, Kiyokawa T, Narita E, Suzuki Y, Taki M, Miyakoshi J. Analysis of Gene Expression in a Human-derived Glial Cell Line Exposed to 2.45 GHz Continuous Radiofrequency Electromagnetic Fields. *J Radiat Res* [Internet]. 2011 [cited 2013 Oct

13];52(2):185–92. Available from:  
<http://joi.jlc.jst.go.jp/JST.JSTAGE/jrr/10116?from=CrossRef>

12. Cifra M, Fields JZ, Farhadi A. Electromagnetic cellular interactions. *Prog Biophys Mol Biol* [Internet]. Elsevier Ltd; 2011 May [cited 2013 Nov 3];105(3):223–46. Available from: <http://www.ncbi.nlm.nih.gov/pubmed/20674588>
13. Heredia-Rojas JA, Torres-Flores AC, Rodríguez-De la Fuente AO, Mata-Cárdenas BD, Rodríguez-Flores LE, Barrón-González MP, et al. *Entamoeba histolytica* and *Trichomonas vaginalis*: trophozoite growth inhibition by metronidazole electro-transferred water. *Exp Parasitol* [Internet]. Elsevier Inc.; 2011 Jan [cited 2013 Nov 10];127(1):80–3. Available from: <http://www.ncbi.nlm.nih.gov/pubmed/20603119>
14. Fojt L, Strásák L, Vetterl V, Smarda J. Comparison of the low-frequency magnetic field effects on bacteria *Escherichia coli*, *Leclercia adecarboxylata* and *Staphylococcus aureus*. *Bioelectrochemistry* [Internet]. 2004 Jun [cited 2013 Nov 10];63(1-2):337–41. Available from: <http://www.ncbi.nlm.nih.gov/pubmed/15110299>
15. Perez HA, Villagomez JC, Cordova T, Sosa M, Bernal JJ. Cell Behavior Undergoing Random Segments of Oscillating Magnetic Field. *IFMBE Proc.* 2013;39:654–6.
16. Hemmersbach R, Becker E, Stockem W. Influence of extremely low frequency electromagnetic fields on the swimming behavior of ciliates. *Bioelectromagnetics* [Internet]. 1997 Jan;18(7):491–8. Available from: <http://www.ncbi.nlm.nih.gov/pubmed/9338630>
17. Zhang D, Pan X, Ohno S, Osuga T, Sawada S, Sato K. No effects of pulsed electromagnetic fields on expression of cell adhesion molecules (integrin, CD44) and matrix metalloproteinase-2/9 in osteosarcoma cell lines. *Bioelectromagnetics* [Internet]. 2011 Sep [cited 2013 Oct 13];32(6):463–73. Available from: <http://www.ncbi.nlm.nih.gov/pubmed/21480303>
18. Vranckx L, De Buck E, Anné J, Lammertyn E. *Legionella pneumophila* exhibits plasminogen activator activity. *Microbiology* [Internet]. 2007 Nov [cited 2013 Oct 13];153(Pt 11):3757–65. Available from: <http://www.ncbi.nlm.nih.gov/pubmed/17975084>
19. Ueno S. Studies on magnetism and bioelectromagnetics for 45 years: from magnetic analog memory to human brain stimulation and imaging. *Bioelectromagnetics* [Internet]. 2012 Jan [cited 2013 Oct 13];33(1):3–22. Available from: <http://www.ncbi.nlm.nih.gov/pubmed/22012916>
20. Miyakoshi J. Effects of static magnetic fields at the cellular level. *Prog Biophys Mol Biol* [Internet]. 2005 [cited 2013 Oct 13];87(2-3):213–23. Available from: <http://www.ncbi.nlm.nih.gov/pubmed/15556660>
21. Conti P, Gigante GE, Cifone MG, Alesse E, Ianni G, Reale M, et al. Reduced mitogenic stimulation of human lymphocytes by extremely low frequency electromagnetic fields. *FEBS Lett* [Internet]. 1983 Oct 3;162(1):156–60. Available from: <http://www.ncbi.nlm.nih.gov/pubmed/6617888>

22. Falzone N. Response to comment on “In vitro effect of pulsed 900 MHz GSM radiation on mitochondrial membrane potential and motility of human spermatozoa” by Falzone et al. *Bioelectromagnetics* [Internet]. 2011 Sep 15 [cited 2013 Oct 13];32(6):510–510. Available from: <http://doi.wiley.com/10.1002/bem.20673>
23. Pérez H, Cordova-Fraga T, López-Briones S, Martínez-Espinosa JC, Rosas EF, Espinoza a, et al. Portable device for magnetic stimulation: Assessment survival and proliferation in human lymphocytes. *Rev Sci Instrum* [Internet]. 2013 Sep [cited 2013 Oct 7];84(9):094701. Available from: <http://www.ncbi.nlm.nih.gov/pubmed/24089844>
24. Muniz JB, Marcelino M, Motta M, Schuler A. Influence of Static Magnetic Fields on *S. cerevisiae* Biomass Growth. *BRAZILIAN Arch Biol Technol A*. 2007;50(May):515–20.
25. Lyons AB. Determination of lymphocyte division by flow cytometry. *J Immunol Methods*. 1994;171(1):131–7.
26. Cifra M, Fields JZ, Farhadi A. Electromagnetic cellular interactions. *Prog Biophys Mol Biol* [Internet]. Elsevier Ltd; 2011 May [cited 2013 Oct 1];105(3):223–46. Available from: <http://www.ncbi.nlm.nih.gov/pubmed/20674588>
27. Kesari KK, Kumar S, Behari J. Effects of radiofrequency electromagnetic wave exposure from cellular phones on the reproductive pattern in male Wistar rats. *Appl Biochem Biotechnol* [Internet]. 2011 Jun [cited 2013 Oct 13];164(4):546–59. Available from: <http://www.ncbi.nlm.nih.gov/pubmed/21240569>
28. Perez HA, Cordova T, Padilla N, Sosa M. Device to Evoke the Bone System in Hip Dislocation Diagnosis. *IFMBE Proc*. 2013;39:1386–8.
29. Holen KJ, Tegnander a, Bredland T, Johansen OJ, Saether OD, Eik-Nes SH, et al. Universal or selective screening of the neonatal hip using ultrasound? A prospective, randomised trial of 15,529 newborn infants. *J Bone Joint Surg Br*. 2002;84(6):886–90.
30. Cordova T, Sosa M, Mendosa A. Measuring Gastroesophageal Region Frequencies for Long time : Preliminary Results. *Int J Bioelectromagn*. 2011;13(4):245–8.
31. Cordova-Fraga T. Biomagnetic Validation to Skin Level for Blood Pressure Curves and Venous. *Open J Appl Sci* [Internet]. 2012 [cited 2013 Oct 7];02(03):128–34. Available from: <http://www.scirp.org/journal/PaperDownload.aspx?DOI=10.4236/ojapps.2012.23018>
32. Blazer, D. G., Kessler, R. C., McGonagle, K. A. and Swartz MS. The prevalence and distribution of major depression in a national community sample: The National Comorbidity Survey. *Am. J. Psychiatr. Natl Comorbidity Surv Am J Psychiatr*. 1994;151:979–86.
33. Arroll, B., Khin, N., y Kerse N. Screening for depression in primary care with two verbally asked questions: Cross sectional study. *Br Med J*. 2003;327:1144–6.
34. Beck A, Ward C, Mendelson M, Mock J EJ. An inventory for measuring depression. *Arch Gen Psychiatr*. 1961;4:561–71.

35. Bo M, Lipus LC, Kokol V. Magnetic Field Effects on Redox Potential of Reduction and Oxidation Agents. 2008;81(3).
36. Bund a., Koehler S, Kuehnlein HH, Plieth W. Magnetic field effects in electrochemical reactions. *Electrochim Acta* [Internet]. 2003 Dec [cited 2013 Oct 7];49(1):147–52. Available from: <http://linkinghub.elsevier.com/retrieve/pii/S001346860300714X>
37. Kim D, Kim J, Choi W. Effect of magnetic field on the zero valent iron induced oxidation reaction. *J Hazard Mater* [Internet]. Elsevier B.V.; 2011 Aug 30 [cited 2013 Oct 7];192(2):928–31. Available from: <http://www.ncbi.nlm.nih.gov/pubmed/21689884>
38. Jiménez-García MN, Arellanes-Robledo J, Aparicio-Bautista DI, Rodríguez-Segura MA, Villa-Treviño S, Godina-Nava JJ. Anti-proliferative effect of extremely low frequency electromagnetic field on preneoplastic lesions formation in the rat liver. *BMC Cancer* [Internet]. 2010 Jan;10:159. Available from: <http://www.pubmedcentral.nih.gov/articlerender.fcgi?artid=2873390&tool=pmcentrez&rendertype=abstract>
39. Mukherjee C, Majumder S, Lohia A. Inter-cellular variation in DNA content of *Entamoeba histolytica* originates from temporal and spatial uncoupling of cytokinesis from the nuclear cycle. *PLoS Negl Trop Dis* [Internet]. 2009 Jan [cited 2013 Nov 17];3(4):e409. Available from: <http://www.pubmedcentral.nih.gov/articlerender.fcgi?artid=2659751&tool=pmcentrez&rendertype=abstract>
40. Perez H, Rosas E, López S, Espinosa A. Magnetic exposure system to stimulate human lymphocytes proliferation. 2008;13:6–7.
41. Blackman CF, Benane SG, House DE. The influence of 1.2 microT, 60 Hz magnetic fields on melatonin- and tamoxifen-induced inhibition of MCF-7 cell growth. *Bioelectromagnetics* [Internet]. 2001 Feb;22(2):122–8. Available from: <http://www.ncbi.nlm.nih.gov/pubmed/11180258>
42. Rojas JAH, Rodr AO, Velazco-campos MR, Leal-garza CH, Rodr LE. Cytological Effects of 60 Hz Magnetic Fields on Human Lymphocytes InVitro : Sister-Chromatid Exchanges , Cell Kinetics and Mitotic Rate. *Bioelectromagnetics*. 2001;149(May 1999):145–9.
43. Cohen AE. Nanomagnetic control of intersystem crossing. *J Phys Chem A* [Internet]. 2009 Oct 15;113(41):11084–92. Available from: <http://www.ncbi.nlm.nih.gov/pubmed/19725575>
44. Anders J, Angerhofer A, Boero G. K-band single-chip electron spin resonance detector. *J Magn Reson* [Internet]. Elsevier Inc.; 2012 Apr [cited 2013 Oct 7];217:19–26. Available from: <http://www.ncbi.nlm.nih.gov/pubmed/22405529>
45. Kaila VRI. Theoretical Studies on Coupled Electron and Proton Transfer in Cytochrome c Oxidase. 2009.
46. Krishna MC, Devasahayam N, Cook J a, Subramanian S, Kuppusamy P, Mitchell JB. Electron paramagnetic resonance for small animal imaging applications. *ILAR J* [Internet]. 2001 Jan;42(3):209–18. Available from: <http://www.ncbi.nlm.nih.gov/pubmed/11406720>

47. Lyons MEG, Brien RO, Kinsella M, Gloinn C Mac, Scully PN. Magnetic Field Effects in Ferrocenealkane Thiol Self Assembled Monolayer Modified Electrodes. 2010;5:1310–41.
48. Lipps F. Electron spins in reduced dimensions : ESR spectroscopy on semiconductor heterostructures and spin chain compounds. 2011;
49. Available N, Booklet OXD. X-RAY DATA BOOKLET. Lawrence Berkeley Natl Lab Univ Calif. 2000;
50. Goodman R, Chizmadzhev Y, Shirley-henderson A. Electromagnetic Fields and Cells. J Cell Biochem. 1993;44:436–41.
51. Afanasyev VN, Korol B a, Matylevich NP, Pechatnikov V a, Umansky SR. The use of flow cytometry for the investigation of cell death. Cytometry [Internet]. 1993 Jan [cited 2013 Oct 13];14(6):603–9. Available from: <http://www.ncbi.nlm.nih.gov/pubmed/8404366>
52. Fanelli C, Coppola S, Barone R, Colussi C, Gualandi G, Volpe P, et al. Magnetic fields increase cell survival by inhibiting apoptosis via modulation of Ca<sup>2+</sup> influx. FASEB J [Internet]. 1999 Jan;13(1):95–102. Available from: <http://www.ncbi.nlm.nih.gov/pubmed/9872934>

## 7.1 APPLICATION OF INSTRUMENTATION FOR OTHER RESEARCH AREAS

## 7.1.1 ELECTRO-ACOUSTIC DEVICE FOR BONE DISEASE DIAGNOSIS

Device and procedure for detecting irregularities in the bone system are presented here. They can assess fractures, lesions, osteoporosis or irregularities in vivo. The resonance system is found, or a system characteristic frequency is transmitted, in order to determinate bone density or its sound propagation. This patented procedure bases its operation through a transmitter and a receiver with surface contact, just over the bone, evaluated by simultaneously observing it on a screen; it also makes it possible to store measurements for subsequent assessments. Preliminary measurements determined that the dominant frequency for evaluated femoral bones in several subjects is around 160 Hz, this suggests that this procedure is powerful enough for the proposed assessments in neonates (28). Around one hundred thousand new patients of osteoporosis and bone metastases diseases are related to bones. According to several studies, it was found that universal ultrasound screening of newborn infants was more effective at detecting CDH/DDH than at targeting ultrasound screening of only high-risk infants. The randomized controlled trial conducted by Holen et al (2002) screened 15,529 infants who were randomized to either clinical screening or ultrasound of all hips, or clinical screening and ultrasound of only high-risk infants. The rate of late dysplasia detection was found to be 0.13 and 0.65 per 1000, respectively ( $p=0.22$ )(29). So early diagnosis of this pathology is suggested for a new born, in order to have the opportune medical attention on time. In congenital hip dislocation, a clinical diagnosis was made with traditional maneuvers from Ortolani, Barlow, and Peter-Baden(29); in spite of this diagnosis procedure, only a sub-dislocated, or an early stage dislocated hip, is detected and may miss dysplasia.

In this study, an acoustic procedure in the audible frequency is presented in order to assess bones in neonates.

According to bone shape, this can be modeled as a solid piece. So the sound is transferred through it, according to material density and Young module. The sound velocity through the bone can be written as:

$$v_s = \sqrt{\frac{E}{\rho}}, \quad (52)$$

Where,  $E$  is the Young module, and  $\rho$  is the bone density.

For a first approximation, a bone is considered as a closed cylinder, so its resonance frequency can be modulated according to:

$$f_s = \frac{n v_s}{4L}, \quad (53)$$

Here,  $n = 1, 3, 5, 7, \dots$ , with fundamental frequency in  $n - 1$ ,  $v_s$  the sound velocity and  $L$  the cylinder length.

As long as an octave, under a closed cylinder, is written as:

$$f_s = \frac{n v_s}{4(L + 0.4d)}, \quad (54)$$

In this equation,  $d$  is the cylinder diameter.

Using these expressions, it is possible to record the natural or characteristic frequency of the bone and of the bone density according to:

$$\rho(f_s) = \frac{n^2 E}{16 f_s^2 (L + 0.4d)}, \quad (55)$$

With this expression, the bone density is estimated as a function of the frequency.

On the other hand, the sound propagation needs a material medium, so by using the above equation, it is also possible to have a direct diagnosis of hip dislocation in neonates in frequency changes. An alternative, or a complement measurement, is a power correlation between innings vs. outing signal intensity.

To perform the first pilot study a personal computer was firstly used and a software routine application was also implemented in a Matlab platform. So, by using the audio peripheral, a stimulating signal was generated, and using the same peripheral, the measured data from the stimulation was recorded and plotted in real time. After, a standalone system was designed to replace the computer and have a portable device based on a PIC16F877 microcontroller, with the same computational algorithm previously used, and loaded in its internal memory. An actuator is used in the system to promote the stimulation to the bone; this actuator comprises a coil and a magnet, when the coil produces a magnetic field, a mechanical vibration similar to a diapason (28) occurs, in this way the audio signal for stimulating the bone is generated. The registered signal of the sound travels through the bones, and a microphone at the opposite side of the bone recover this signal which is then amplified by an amplification stage. The signals are send to the analog inputs of the PIC16F877 microcontroller for processing.

To study the bone disease diagnosis (hipbone dislocation), a signal is transmitted to a focal area of the hipbone, selecting a point where the transmitter can make a good contact with the bone recommending the pubis region, this signal travels from the hipbone to the femur of the subject under study, the receiver is positioned in the femur bone to receive the sonic signal. This acoustic signal is amplified by an electronic amplifier stage and taken to the signal processing stage. To make a diagnosis the detected signal is analyzed. Note that the diagnosis depends on the sound transferred trough the bones union.



### 7.1.1.1 SOFTWARE DESCRIPTION

A developed multifunctional algorithm was stored in the memory of the microcontroller, implemented in order to generate a signal with different frequencies. An amplification stage was subjected to a stethoscope as the emitting signal on the femoral bone for dislocations of the hipbone diagnosis.

### 7.1.1.2 DEVICE CHARACTERIZATION

The operation of the device is based on the detection of irregularities of the skeletal system. It measures changes in the power of an audio signal that travels through the femur, from one edge to another, and it arrives at the hip pubis. The position of the transmitter and receiver can be changed if preferred. In order to know the signal behavior, an experiment and its theoretical basis was performed. For the experiment, wood cylinders (*Pinus sylvestris*) are submitted to sound transmission analysis, having a humidity factor of 12 %, a modulus of Young (E) of 9109 N/m<sup>2</sup> in the direction of the fibers, each with a length, 25 mm, 35 mm, 45 mm; respectively.

For one experiment, the pieces were submitted to a linear scanning of frequencies stimulation, from 200 Hz to 2000 Hz, then from 2000 Hz to 200 Hz; at the same time the signals were recorded by a sensor fixed on the middle of the bar, and a second one on the apposite edge of the bar, see figure 2.35.

For a second experiment, white noise stimulus generated in the Matlab platform was carried out on one end of the sample, then one measurement was recorded on middle and finally one more on the other end of the sample. The signal was analyzed by the use of the fast Fourier transform, to obtain the natural system response, see figure 2.37.

Table 7.1. A comparison between theoretical and measured frequencies shown.

Sample [MF]	Middle Point ( ) Hz	Dominant frequencies ( ) Hz	Theoretical estimation (Hz)	Recorded (Hz)	Percentage Difference (%)
25	4.064	2.75 & 5.5	1538.27	1420.30	7.67
35	4.626	1.79 & 7.4	784.83	742.64	5.37
45	4.104	1.21 & 6.74	664.15 & 474.77	721.91 & 486.63	8 & 2.44

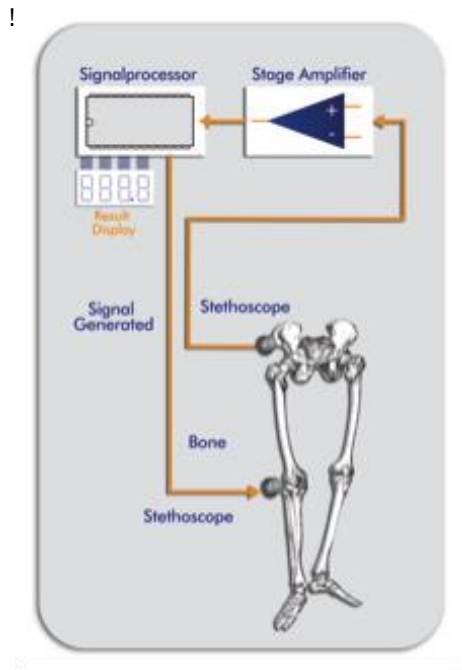


Figure 7.1. Instrumentation used for the measurements of acoustic resonance in the human bone.

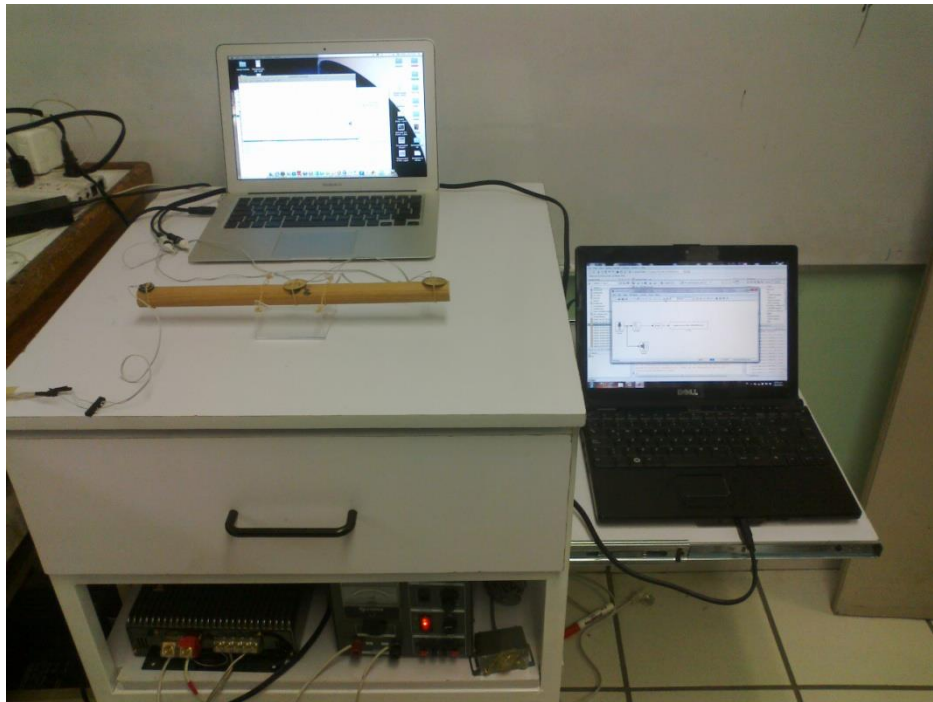


Figure 7.2. System used for the measurements of acoustic resonance in the human bone.

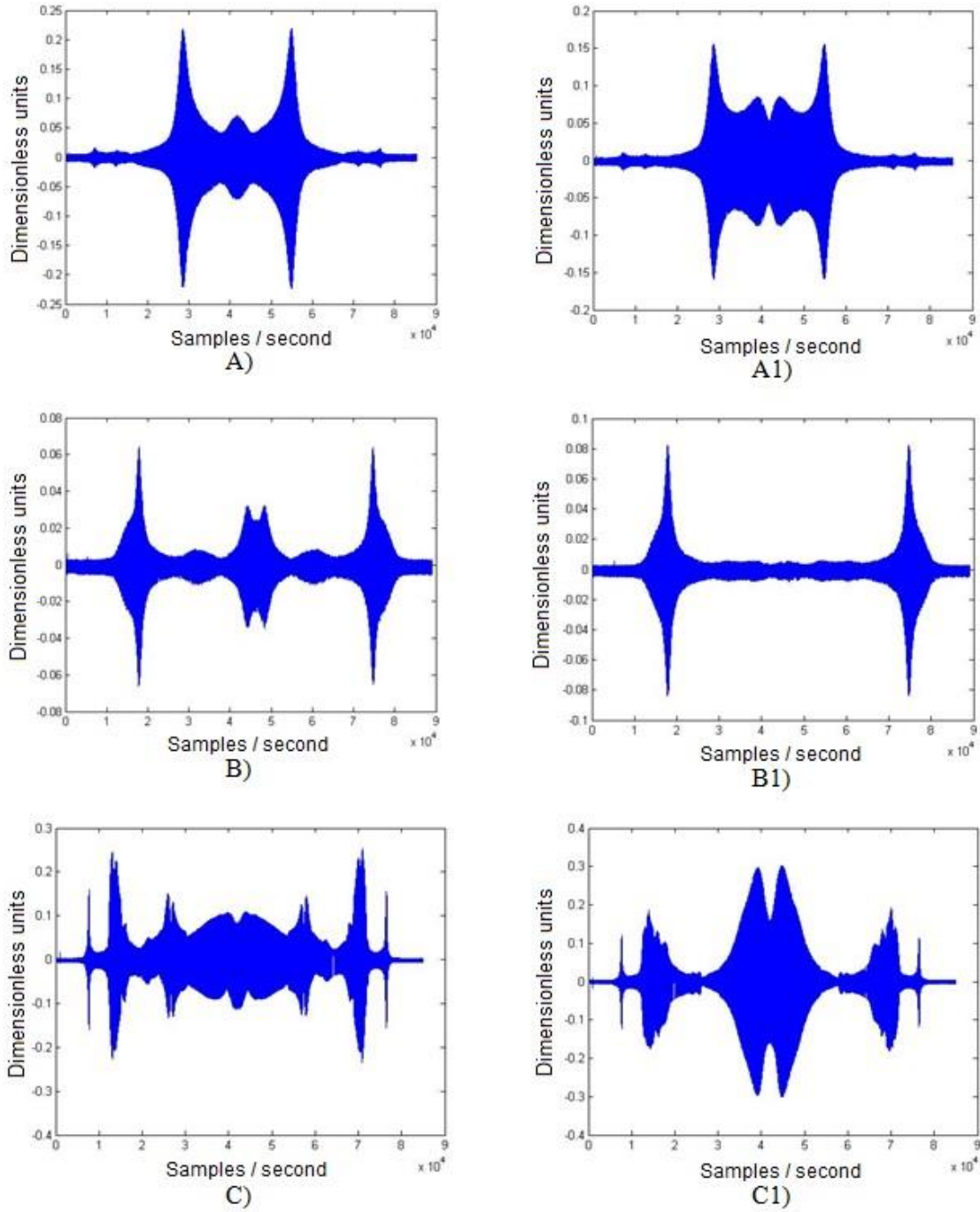


Figure 7.3. The measured signal from an evoked ascending – descending signal for linear vibration frequencies, from 200 Hz to 2000 Hz, then from 2000 Hz to 200 Hz, is shown. Recordings associated to: a) sensor fixed on the middle of the wood bar of 25 MF, a1) sensor put on the opposite edge of the stimulation for the same wood bar of 25 MF. b) Sensor fixed on the middle of the wood bar of 35 MF, b1) sensor placed on the opposite edge of the stimulation for the same wood bar of 35 MF. c) Sensor fixed on the middle of the wood bar of 45 MF, c1) sensor placed on the opposite edge of the stimulation for the same wood bar of 45 MF.

A frequency spectrum was obtained applying the fast Fourier transforms (FFT). In each one of the maximums points associated to the calculated resonant frequency, ranges of harmonics frequencies were obtained in relation to frequency estimations, see figure 2.37.

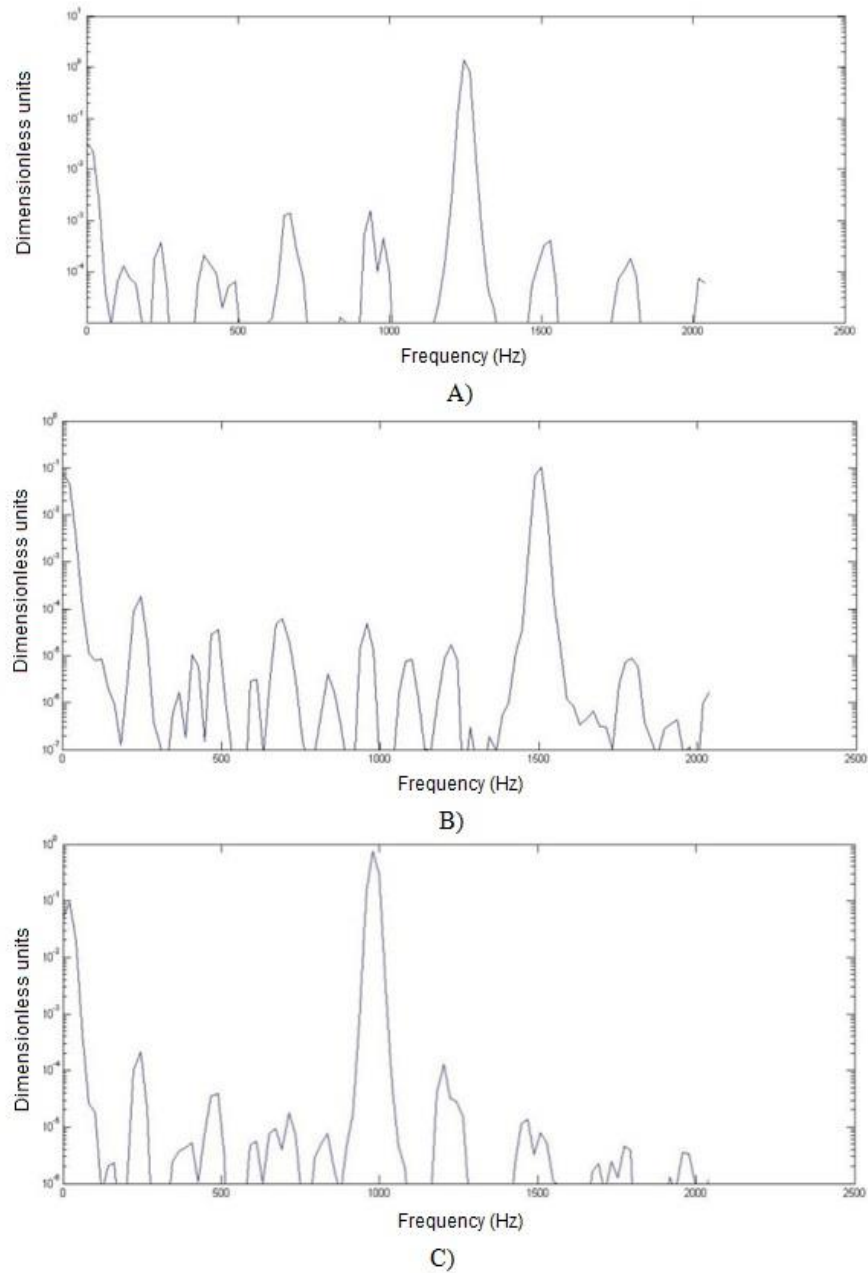


Figure 7.4. The frequency spectrums from the FFT in a) bar of 25 MF, b) bar of 35 MF, and c) Bar of 45 MF, are shown.

### 7.1.2 MEASURING GASTROESOPHAGEAL REGION FREQUENCIES: PRELIMINARY RESULTS

Shown here is a new measurement technique for the contractions and Gastro esophageal (GE) motility. Several studies have been performed with the purpose of measuring the contractions of the gastrointestinal tract, as well as studies of gastric emptying in the laboratory. In these studies, ferromagnetic particles have been used as magnetic tracers, showing a great utility to describe the gastric emptying and gastric contractions. Nevertheless, this is the only region where well motor function information can be obtained(30).

Some of the advantages of the use of magnetic techniques are the ability to measure the gastric activity (evacuating, transit, the influence of stress in the gastric evacuating, and the acceleration of the activity in the different stages from the menstrual cycle), as well as the gastric transit that can be evaluated with other techniques, like fluxgate and nuclear magnetic resonance. It is possible to monitor the esophageal activity placing two sensors in different positions from the esophagus.

This study presents a procedure in which a magnetic marker has fixed in through the esophagus and gastric segments, while the magnetic signal was recorded coming from out of the human body.

The contractions of gastric and esophageal regions of 6 healthy subjects were evaluated, under their consent. The measurement procedures begin with the positioning of two magnetic particles in the bottom of the stomach; to have a well-defined position point of the magnets the operation should be carried on by using an endoscope. The magnets were fixed to a graduated thread that allowed moving them in a proximal direction, so that the positions of magnets in the gastroesophageal (GE) tract were known. The distal displacement may permit freedom of action to the particles in such a way that the contractile activity of the gastrointestinal (GI) system can move the particles. The measurements were carried out in two conditions of gastric bloat. The first measurement was conducted after the magnets had been placed in the region of fundus in the basal state. The measurements were taken in two positions within the stomach, fundus and cavern. After the measurements in the basal state, the subject ingested food based on bread, chicken, vegetables and water. Then measurements were taken again in fundus and the cavern. Finally, the magnets were crossed until the section of the esophagus and measurements were taken in three sections crossing in a proximal direction. The measurements taken in each of the bloat states were made with temporary separations of around 10 measurements in the postprandial state, the stomach, and esophagus had a 20 minutes separation.

The magnetic markers were neodymium-iron-boron magnets (NdFeB), with a cylindrical shape ( $d = 3$  mm,  $h = 4$  mm, and magnetic moment  $m = 1.42 \times 10^{-2}$  J/T). The used magnets generate a magnetic field that is detectable by magnetic fluxgate model sensors 539 from Applied Physics Systems. Two fluxgate magnetic sensors were arranged to coincide with their y-axis and were separated a distance of 10 mm and were registering at a rate of 30 samples per second.

To cancel high frequencies, a band-pass filter was used, maintaining only the low frequencies (LF) contribution of 1-5 cpm; consequently, cardiac activity and the breathing noises were eliminated. By means of the routine of Fast Fourier Transform (FFT) implemented in Matlab, the frequencies of

contraction of the different sections from tract GI were used to analyze both states. The spectrum signals were analyzed to search for the peak corresponding to the main contraction frequencies of each one of the monitored sections. In many cases, there were obtained several signal characteristic frequencies (several peaks in the graph), but only the maximum peaks were only taken into account as they were considered the most representative frequencies.

### 7.1.3 BIOMAGNETIC VALIDATION TO SKIN LEVEL FOR BLOOD PRESSURE CURVES AND VENOUS PRESSURE

Measurements were carried out with a recently patented medical device, capable of recording the curves of arterial pressure and venous pressure.

The arterial and venous pressures are values attributed to blood flow through the human body. Miguel Servet made the first description of the pulmonary circulatory system. Later, William Harvey raised the principle of hemodynamics to verify that the heart muscle had phases of movement and rest. Poiseuille used a pressure gauge in animals to evaluate the pressure in units of mmHg, Faivre used the Poiseuille hemodinamometer on a human being to measure intra-arterial pressure (31).

Some non-invasive studies have shown that hemodynamic forces have a relationship with the related to aortic pressure increase. Currently there are two methods of clinical routine used for the measurement of blood pressure, cardiac catheterization and sphygmomanometer to arteries, and only one to record venous pressure. Cardiac catheterization is the main standard to record venous-inside pressure, despite it being widely invasive and demands high trained personnel and special patient areas for implementation(31). Nevertheless, it presents an objective record. The second one is widely used, however, it provides a subjective register due to its nature.

The validation of recordings was performed by the pulse pressure cardiac gauge (PPC) on blood pressure in healthy subjects and patients. This diagnostic and monitoring device is able making a distinction in the recordings of the curve shapes from the arterial and venous pressures as those recorded by catheterization. It offers an express evaluation, with the advantage of carrying out the evaluation on the skin level; the ionizing radiation is avoided and does not require a sterile room for evaluation.

Each one of the patients enrolled in this study gave a written consent previous to carrying out measurements, which were performed according to the treaty of Helsinki for studies in humans.

These assessments did not present any risk nor exposed the patient to any ionizing radiation. Each volunteer was asked to be placed in semi-fowler position with the head turned to the right, then the artery or vein was identified by palpation and auscultation, this is, the location of the internal jugular vein and common carotid artery, as shown in next figure:



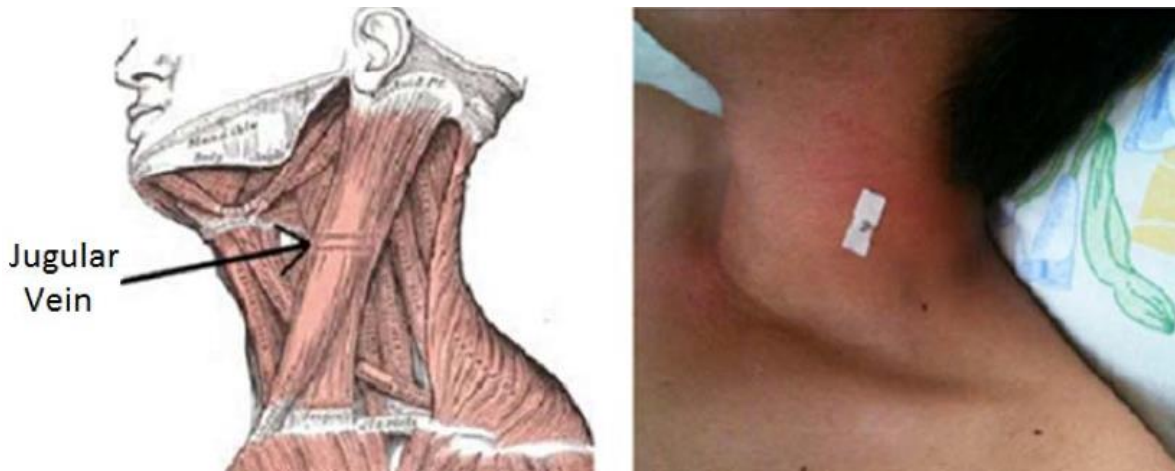


Figure 7.5. Schematization of the magnetic marker position on subject skin, it is right over the jugular artery.

When the right location under skin of the artery is found, a magnetic marker (a magnet of  $3 \times 4$  mm, diameter and height, respectively) is placed on the skin, then, the sensor base of the PPC in contact with the skin is fixed. Without exerting more pressure than the base and the magnetic sensor weight on the neck of the person, the magnetometer is always separated at a distance of 2.5mm from the magnetic marker on patient skin. This magnetic marker is light enough not to crush the vessel but has the sufficiently intensity of the magnetic moment to be detected,  $\mu = 0.13 \text{ Am}^2$ . The magnetic signal is registered with an excellent signal to noise ratio, then additional digital filtering is used to discriminate noises.

A mechanical action by the flow of blood in the vessel is transmitted to the magnetic marker. So, it generates a variable magnetic field, which increases as it approaches the sensor, recovering a signal to be analyzed.

In this validation study, 10 healthy subjects were measured, all with no history of heart disease and 5 patients who underwent cardiac catheterization for suspected coronary artery disease, while registered with the cardiac catheter. The experiment was done, placing the magnetic marker, and obtaining and registering the pressure curves for a period of 30 seconds according to the following order: 5 records for aspiratory inhalation and 5 records for aspiratory exhalation. An apnea was asked for around 30 s. These measurements were performed on the left side of the neck and suprasternal area, some of them also included alternate position: semi-fowler and supine.

The validation of the obtained signals was carried out by estimating the correlation coefficient of the reproduction of the signal (cross-correlation of a signal with itself), and using mathematical procedures for processing biological signals. First it was obtained for the same individual (auto-correlation) and then, by correlating measurements between healthy subjects and patients.

#### 7.1.4 EFFECT OF THE MICRO- MAGNETIC STIMULATION ELECTROENCEPHALOGRAPHIC PATTERNS

Depression is a mood disorder, either from the point of view of psychology and from the point of view of psychiatry, but within the realm of psychopathology (32). According to the medical model of psychiatry, it is described as a mood disorder and a common symptom is a state of gloom and unhappiness that can be transient or permanent. The medical term refers to it as a syndrome, or a set of symptoms, that primarily affect the affective sphere as: pathological sadness, decay, irritability, or mood disorder that can decrease performance at work, or limit the normal life activity, regardless that their cause is known or unknown. While this is the core of symptoms, depression can also be expressed through cognitive, volitional, or somatic conditions (33). In most cases, the clinical diagnosis differs from similar expression boxes, such as anxiety disorders.

Trying to combat this disorder, part of the hypothesis is that intervention with magnetic micro-stimulation decreases the symptoms related to major depression and increases alpha waves in the EEG measurement (34).

Currently there are no studies linking magnetic micro-stimulation influence and symptoms of Encephalopathic Electroencephalography (EEG) Patterns; so it is of interest to know if help is needed to reduce the symptoms and the characteristics associated with treatment-resistant depression using magnetic micro stimulation.

The necessary instrumentation is developed to investigate whether the use of magnetic micro-stimulation helps to reduce as far as symptoms and characteristics associated with treatment-resistant depression.

Unlike transcranial magnetic stimulation to stimulate with an intensity of about 1 Tesla, variable frequency magnetic micro-stimulation works at 20 micro Teslas. This in an attempt to try to reduce the side effects of this treatment, among which are the seizures, headache and local pain, decreased hearing, among others, but at the same time, continue with the same effectiveness in reducing stress symptoms, anxiety, and depression.

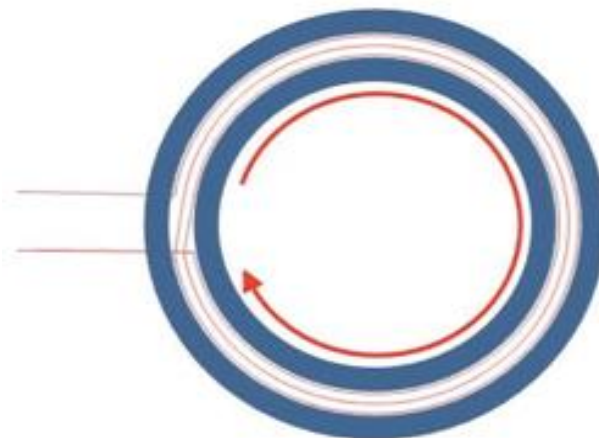


Figure 7.6. Magnetic coil for micro-magnetic stimulation



The designed device comprises a set of coils which are placed tangentially on the patient's scalp. Each set of coils is connected in series, letting the current flow in one direction. This can create several electromagnetic fields to extend through the brain in a specific direction. The coils are designed to maximize the effect of electromagnetic fields deep into the brain, integrating separate electromagnetic fields, which are projected into the skull from several points around its periphery.

The assumption suggests that the magnetic micro-stimulation is capable of stimulating the neuronal pathway of the brain's reward system, with a set of coils and a deeper level of five to six centimeters into the cerebral cortex. This way, it can treat depression. It is also capable of stimulating other brain areas associated with other mental illnesses.

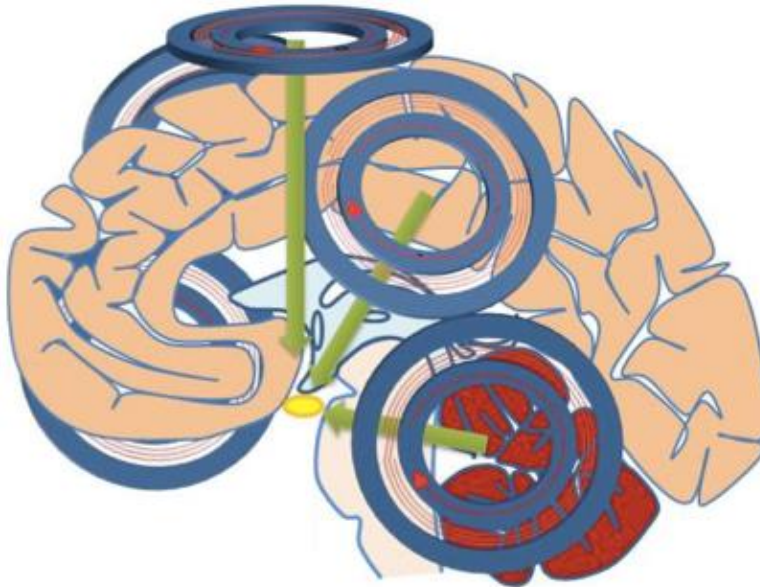


Figure 7.7: Magnetic coils diadem for the micro-magnetic stimulation device.

The study was applied in a population of adults with symptoms of major depression. The experiment was also applied to people over 18 years who are diagnosed with major depression.

To make a selection of the subjects to be studied and to avoid health risks on them, a first test was to be done. Those subjects who have had medication treatment and have not had significant improvements, must continue attending follow-up visits to the psychiatric hospital, at least a month after they have stopped taking drugs for depression, and agree to participate in research.

Those who meet the criteria to be assessed with the EEG technique, were submitted to more tests.

### 7.1.5 FARADAY EFFECT SENSOR

A Helmholtz coil has been chosen as actuators given its performance when used in magnetic induction.

This kind of coils is intended to work at frequencies between 80 and 400 KHz. So, the study of high frequency magnetic effects in culture would be ideal.

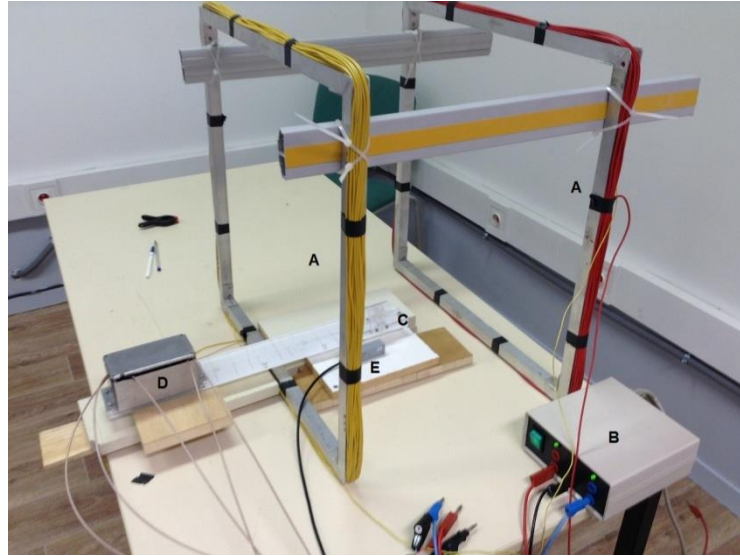


Figure 7.8. Instrumentation for generating and measuring magnetic fields, A) Helmholtz coil, B) Power Supply magnetic field sensor Faraday effect, C) electron Faraday effect magnetic sensor, D) flint glass.

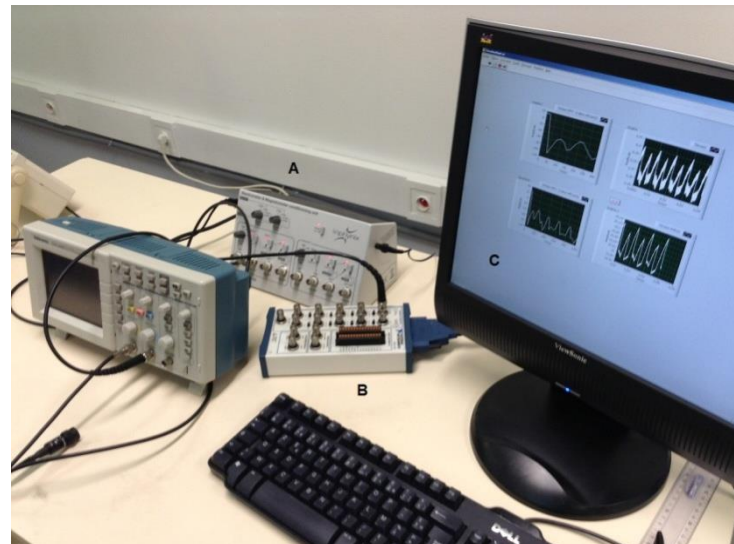


Figure 7.9. Magnetic field measurement and data acquisition system, A) amplifier for magnetic field sensor, B) data acquisition card from National Instruments, C) graphical interface developed in LabView, for filtering and viewing the captured information.

The information obtained by the Hall-effect magnetic sensors and the Faraday-effect sensor is captured on a personal computer, using a data acquisition National Instruments Card for importation. This information is filtered and is topic under analysis, using algorithms based on Fourier, transform to allude platform LabView.

In order to make measurements of low magnetic fields, a Faraday effect sensor has been developed. It has been constructed for a photodetector from a transimpedance amplifier series, which has made a different detection system with RC, a double filter for the purification of the feed, and a photodetector, which measures the difference in light intensity due to the polarization of a laser beam, which passes through a Faraday effect glass. The sensor has several filtering stages to eliminate any noise induced by magnetic fields. The Faraday effect sensor is designed to operate at a center frequency of 250 KHz.




Other types of amplifiers for measuring low and high frequency signals were also used to measure Redox systems effects in cell cultures subjected to magnetic field sources. These amplifiers can reach detected frequencies of 100 MHz, having an amplification factor of 10 and with the advantage that its amplification gain remains linear in frequency ranges from 100 Hz - 100 MHz, making them very stable for scientific experiments.

A variable gain amplifier, with a frequency range of 50 to 1000 MHz and ideal low noise signals in the order of micro-volts has also been designed. This amplifier has been conceived to improve the measurement instrumentation systems used in the study of magnetic fields on cell cultures. This type of amplifier may be cascaded with the high frequency amplifiers with cutoff frequency of 100MHz or above, to have a higher gain factor. The main application of these amplifiers' variables is to realize gain setting, so that the sensed signal can be set to the own ideal range level for storage and analysis.

The Helmholtz coil are intended to work at frequencies between 80 and 400 KHz, therefore ideal for the study of high-frequency magnetic effects on crops.

In addition, there have been drivers from current micro applicator that may have been high frequency coils for generating magnetic or electromagnetic fields, which may serve to further research study; these drivers can achieve current operating frequency of up to 100 MHz.

## 7.2 PATENTS AND PUBLICATIONS

			
<p><b>Instituto Mexicano de la Propiedad Industrial</b></p>		<p><b>INSTITUTO MEXICANO DE LA PROPIEDAD INDUSTRIAL</b>          Dirección Divisinal de Patentes          OFICINA REGIONAL DEL BAJO</p>	
<p><input checked="" type="checkbox"/> Solicitud de Patente  <input type="checkbox"/> Solicitud de Registro de Modelo de Utilidad</p> <p><input type="checkbox"/> Solicitud de Registro de Diseño Industrial, especifique cuál:  <input type="checkbox"/> Modelo Industrial <input type="checkbox"/> Dibujo Industrial</p>		<p>Uso exclusivo Delegaciones y Subdelegaciones de la Secretaría de Economía y Oficinas Regionales del IMPI</p> <p>Sello</p> <p>Folio de entrada</p> <p>Fecha y hora de recepción</p>	
<p>Antes de llenar la forma lea las consideraciones generales al reverso</p>		<p>Solicitud Expediente: MX/E/2011/011492          Fecha: 28/OCT/2011 Hora: 15:43          Folio: MX/E/2011/076501 86419</p> 	
<p><b>I DATOS DEL (DE LOS) SOLICITANTE(S)</b></p>			
<p>El solicitante es el inventor <input type="checkbox"/> El solicitante es el causahabiente <input checked="" type="checkbox"/></p>			
<p>1) Nombre (s): UNIVERSIDAD DE GUANAJUATO</p>			
<p>2) Nacionalidad (es): MEXICANA</p>			
<p>3) Domicilio; calle, número, colonia y código postal: LASCURAIN DE RETANA NO. 5, COLONIA CENTRO, CP.36000</p>			
<p>Población, Estado y País: GUANAJUATO, GUANAJUATO, MEXICO</p>			
<p>4) Teléfono (clave): 014737320006 EXT. 5012 Y 4501 5) Fax (clave): 01 473 73 29312</p>			
<p><b>II DATOS DEL (DE LOS) INVENTOR(ES)</b></p>			
<p>6) Nombre (s): TEODORO CORDOVA FRAGA, HUEZTZIN AARON PEREZ OLIVAS, MODESTO ANTONIO SOSA AQUINO</p>			
<p>7) Nacionalidad (es): MEXICANA, MEXICANA, MEXICANA</p>			
<p>8) Domicilio; calle, número, colonia y código postal: LASCURAIN DE RETANA NO. 5, COLONIA CENTRO, CP.36000</p>			
<p>Población, Estado y País: GUANAJUATO, GUANAJUATO, MEXICO</p>			
<p>9) Teléfono (clave): 014737320006 EXT. 5012 Y 4501 10) Fax (clave): 01 473 73 29312</p>			
<p><b>III DATOS DEL (DE LOS) APODERADO(S)</b></p>			
<p>11) Nombre (s): LUIS MANUEL OROZCO ARROYO 12) R.G.P.D.A.J. 10120</p>			
<p>13) Domicilio; calle, número, colonia y código postal: CALZADA DE GUADALUPE NO. 5, COLONIA CENTRO, CP.36000</p>			
<p>Población, Estado y País: GUANAJUATO, GUANAJUATO, MEXICO 14) Teléfono (clave): 014737320006 EXT. 4501</p>			
<p>15) Fax (clave): 01 473 73 29312</p>			
<p>16) Personas Autorizadas para oír y recibir notificaciones: DR. MIGUEL TORRES CISNEROS, ING. ROBERTO CARLOS SALAS SEGOVIANO</p>			
<p>17) Denominación o Título de la invención: <b>RADAR OSEO</b></p>			
<p>18) Fecha de divulgación previa</p> <p>Día Mes Año</p>		<p>19) Clasificación Internacional</p>	
<p>20) Divisinal de la solicitud</p> <p>Número</p>		<p>21) Fecha de presentación</p> <p>Día Mes Año</p>	
<p>22) Prioridad Reclamada:</p> <p>País</p>		<p>Figura jurídica</p> <p>Fecha de presentación</p> <p>Día Mes Año</p>	
<p>No. de serie</p>		<p>No. de serie</p>	
<p><b>Lista de verificación (uso interno)</b></p>			
<p>No. Hojas</p> <p>Comprobante de pago de la tarifa</p> <p>Descripción y reivindicación (es) de la invención</p> <p>Dibujo (s) en su caso</p> <p>Resumen de la descripción de la invención</p> <p>Documento que acredite la personalidad del apoderado</p>		<p>No. Hojas</p> <p>Documento de cesión de derechos</p> <p>Constancia de depósito de material biológico</p> <p>Documento (s) comprobatorio(s) de divulgación previa</p> <p>Documento (s) de prioridad</p> <p>Traducción</p> <p>TOTAL DE HOJAS</p>	
<p>Observaciones:</p>			
<p>Bajo protesta de decir verdad manifiesto que los datos asentados en esta solicitud son ciertos.</p>			
<p><u>LUIS MANUEL OROZCO ARROYO</u></p> <p>Nombre y firma del solicitante o su apoderado</p>		<p><u>GUANAJUATO, GTO. 27 DE OCTUBRE DE 2011</u></p> <p>Lugar y fecha</p>	
<p>Página 1 de 2</p>		<p>IMPI-00-009</p>	



<div style="border: 1px solid black; padding: 5px; margin-bottom: 5px;"> <input checked="" type="checkbox"/> Solicitud de Patente  <input type="checkbox"/> Solicitud de Registro de Modelo de Utilidad         </div> <div style="border: 1px solid black; padding: 5px;"> <input type="checkbox"/> Solicitud de Registro de Diseño Industrial, especifique cuál:  <div style="display: flex; justify-content: space-around;"> <input type="checkbox"/> Modelo Industrial           <input type="checkbox"/> Dibujo Industrial         </div> </div>	<div style="text-align: right;"> <b>INSTITUTO MEXICANO DE LA PROPIEDAD INDUSTRIAL</b>          Dirección Divisional de Patentes       </div> <div style="border: 1px solid black; padding: 5px; margin-top: 5px;">         Uso exclusivo Delegaciones y Subdelegaciones de la Secretaría de Economía y Oficinas Regionales de IMPI          Sello          Folio de entrada          Fecha y hora de recepción       </div> <div style="margin-top: 5px;">         OFICINA REGIONAL DEL BAJIO          Solicitud: MX/a/2012/013988          Expediente: 30/NOV/2012 Hora: 16:08          Folio: MX/E/2012/088628 159805       </div> <div style="text-align: center;"> </div>												
Antes de llenar la forma lea las consideraciones generales al reverso													
<b>I DATOS DEL (DE LOS) SOLICITANTE(S)</b> El solicitante es el inventor <input type="checkbox"/> El solicitante es el causahabiente <input checked="" type="checkbox"/> 1) Nombre (s): UNIVERSIDAD DE GUANAJUATO 2) Nacionalidad (es): MEXICANA 3) Domicilio; calle, número, colonia y código postal: LASCURAIN DE RETANA NO. 5, COLONIA CENTRO, CP.36000 Población, Estado y País: GUANAJUATO, GUANAJUATO, MEXICO 4) Teléfono (clave): 014737320006 EXT. 5059 Y 4501 5) Fax (clave): 014737320006 EXT.5059													
<b>II DATOS DEL (DE LOS) INVENTOR(ES)</b> 6) Nombre (s): TEODORO CORDOVA FRAGA, HUETZIN AARÓN PÉREZ OLIVAS, JOSÉ MARÍA DE LA ROCA CHIAPAS, JOSE EDUARDO HUERTA LEPEZ, MARTHA ALICIA HERNÁNDEZ GONZÁLEZ, SERGIO LÓPEZ BRIONES, GLORIA BARBOSA SABANERO, SERGIO EDUARDO SOLORIO MEZA 7) Nacionalidad (es): MEXICANA, MEXICANA, MEXICANA, MEXICANA, MEXICANA, MEXICANA, MEXICANA 8) Domicilio; calle, número, colonia y código postal: LASCURAIN DE RETANA NO. 5, COLONIA CENTRO, CP.36000 Población, Estado y País: GUANAJUATO, GUANAJUATO, MEXICO 9) Teléfono (clave): 014737320006 EXT. 5059 Y 4501 10) Fax (clave): 01 473 73 29312													
<b>III DATOS DEL (DE LOS) APODERADO (S)</b> 11) Nombre (s): LUIS MANUEL OROZCO ARROYO 12) R G P:DDAJ-20358 13) Domicilio; calle, número, colonia y código postal: LASCURAIN DE RETANA NO. 5, COLONIA CENTRO, CP.36000 Población, Estado y País: GUANAJUATO, GUANAJUATO, MEXICO 14) Teléfono (clave): 014737320006 EXT. 5059 15) Fax (clave): 014737320006 EXT. 5059 16) Personas Autorizadas para oír y recibir notificaciones: ING. ROBERTO CARLOS SALAS SEGOVIANO													
17) Denominación o Título de la Invención: <b>DISPOSITIVO MICRO ESTIMULADOR MAGNÉTICO</b>													
18) Fecha de divulgación previa Día Mes Año	19) Clasificación Internacional uso exclusivo del IMPI												
20) Divisional de la solicitud Número Figura jurídica País Día Mes Año	21) Fecha de presentación Día Mes Año												
22) Prioridad Reclamada: País Día Mes Año No. de serie													
<b>Lista de verificación (uso interno)</b>													
No. Hojas <table border="1" style="width: 100%; border-collapse: collapse;"> <tr> <td style="width: 50%;">Comprobante de pago de la tarifa</td> <td style="width: 50%;">Documento de cesión de derechos</td> </tr> <tr> <td>Descripción y reivindicación (es) de la invención</td> <td>Constancia de depósito de material biológico</td> </tr> <tr> <td>Dibujo (s) en su caso</td> <td>Documento (s) comprobatorio(s) de divulgación previa</td> </tr> <tr> <td>Resumen de la descripción de la invención</td> <td>Documento (s) de prioridad</td> </tr> <tr> <td>Documento que acredite la personalidad del apoderado</td> <td>Traducción</td> </tr> <tr> <td></td> <td><b>TOTAL DE HOJAS</b></td> </tr> </table>	Comprobante de pago de la tarifa	Documento de cesión de derechos	Descripción y reivindicación (es) de la invención	Constancia de depósito de material biológico	Dibujo (s) en su caso	Documento (s) comprobatorio(s) de divulgación previa	Resumen de la descripción de la invención	Documento (s) de prioridad	Documento que acredite la personalidad del apoderado	Traducción		<b>TOTAL DE HOJAS</b>	
Comprobante de pago de la tarifa	Documento de cesión de derechos												
Descripción y reivindicación (es) de la invención	Constancia de depósito de material biológico												
Dibujo (s) en su caso	Documento (s) comprobatorio(s) de divulgación previa												
Resumen de la descripción de la invención	Documento (s) de prioridad												
Documento que acredite la personalidad del apoderado	Traducción												
	<b>TOTAL DE HOJAS</b>												
Observaciones:													
Bajo protesta de decir verdad, manifiesto que los datos asentados en esta solicitud son ciertos. <div style="display: flex; justify-content: space-between;"> <div style="text-align: center;">   <b>LUIS MANUEL OROZCO ARROYO</b>          Nombre y firma del solicitante o su apoderado       </div> <div style="text-align: center;"> <b>GUANAJUATO, GTO. 12 DE NOVIEMBRE DE 2012</b>          Lugar y fecha       </div> </div>													





INSTITUTO MEXICANO DE  
LA PROPIEDAD INDUSTRIAL

Dirección Divisinal de Patentes

OFICINA REGIONAL DEL BAJIO

Solicitud  
Expediente: MX/a/2012/013844  
Fecha: 28/NOV/2012 Hora: 15:34  
Folio: MX/E/2012/087372

998015



MX/E/2012/087372

☒ Solicitud de Patente  
☐ Solicitud de Registro de Modelo de Utilidad

☐ Solicitud de Registro de Diseño Industrial,  
especifique cuál:

☐ Modelo Industrial ☐ Dibujo Industrial

Antes de llenar la forma lea las consideraciones generales al reverso

Uso exclusivo Delegaciones y  
Subdelegaciones de la Secretaría de  
Economía y Oficinas Regionales del  
IMPI

Sello

Folio de entrada

Fecha y hora de recepción

I DATOS DEL (DE LOS) SOLICITANTE(S)	
El solicitante es el inventor <input type="checkbox"/>	El solicitante es el causahabiente <input checked="" type="checkbox"/>
1) Nombre (s): UNIVERSIDAD DE GUANAJUATO	
2) Nacionalidad (es): MEXICANA	
3) Domicilio; calle, número, colonia y código postal: LASCURAIN DE RETANA NO. 5, COLONIA CENTRO, CP.36000	
Población, Estado y País: GUANAJUATO, GUANAJUATO, MEXICO	
4) Teléfono (clave): 014737320006 EXT. 5059 Y 4501	5) Fax (clave): 014737320006 EXT. 5059

II DATOS DEL (DE LOS) INVENTOR(ES)	
6) Nombre (s): TEODORO CORDOVA FRAGA, HUETZIN AARÓN PÉREZ OLIVAS, JULIO CESAR VILLAGOMEZ CASTRO, ORLANDO MARTINEZ CANTO, SERGIO LÓPEZ BRIONES, GLORIA BARBOSA SABANERO, SERGIO EDUARDO SOLORIO MEZA	
7) Nacionalidad (es): MEXICANA, MEXICANA, MEXICANA, MEXICANA, MEXICANA, MEXICANA, MEXICANA	
8) Domicilio; calle, número, colonia y código postal: LASCURAIN DE RETANA NO. 5, COLONIA CENTRO, CP.36000	
Población, Estado y País: GUANAJUATO, GUANAJUATO, MEXICO	
9) Teléfono (clave): 014737320006 EXT. 5059 Y 4501	10) Fax (clave): 01 473 73 29312

III DATOS DEL (DE LOS) APODERADO (S)	
11) Nombre (s): LUIS MANUEL OROZCO ARROYO	12) R G P: DDAJ-20358
13) Domicilio; calle, número, colonia y código postal: LASCURAIN DE RETANA NO. 5, COLONIA CENTRO, CP.36000	
Población, Estado y País: GUANAJUATO, GUANAJUATO, MEXICO	
14) Teléfono (clave): 014737320006 EXT. 5059	15) Fax (clave): 014737320006 EXT. 5059
16) Personas Autorizadas para oír y recibir notificaciones: ING. ROBERTO CARLOS SALAS SEGOVIANO	

17) Denominación o Título de la invención: ESTIMULADOR CELULAR MAGNÉTICO CON FERRO FLUIDO	
18) Fecha de divulgación previa Día Mes Año	19) Clasificación Internacional uso exclusivo del IMPI
20) Divisional de la solicitud Número	21) Fecha de presentación Día Mes Año
22) Prioridad Reclamada: País	Figura jurídica Fecha de presentación Día Mes Año
	No. de serie

Lista de verificación (uso interno)	
No. Hojas	No. Hojas
<input type="checkbox"/> Comprobante de pago de la tarifa	<input type="checkbox"/> Documento de cesión de derechos
<input type="checkbox"/> Descripción y reivindicación (es) de la invención	<input type="checkbox"/> Constancia de depósito de material biológico
<input type="checkbox"/> Dibujo (s) en su caso	<input type="checkbox"/> Documento (s) comprobatorio(s) de divulgación previa
<input type="checkbox"/> Resumen de la descripción de la invención	<input type="checkbox"/> Documento (s) de prioridad
<input type="checkbox"/> Documento que acredita la personalidad del apoderado	<input type="checkbox"/> Traducción
	TOTAL DE HOJAS

Observaciones:

Bajo protesta de decir verdad, manifiesto que los datos asentados en esta solicitud son ciertos.

LUIS MANUEL OROZCO ARROYO  
Nombre y firma del solicitante o su apoderado

GUANAJUATO, GTO. 12 DE NOVIEMBRE DE 2012  
Lugar y fecha

## Biomagnetic Validation to Skin Level for Blood Pressure Curves and Venous

T. Cordova-Fraga<sup>1\*</sup>, Francisco Gómez-Aguilar<sup>1</sup>, T. Bravo-Arellano<sup>1</sup>, M. A. Hernández-Gonzalez<sup>2</sup>,  
S. Solorio-Meza<sup>2</sup>, H. A. Perez-Olivas<sup>1</sup>, M. Sosa-Aquino<sup>1</sup>, J. J. Bernal-Alvarado<sup>1</sup>,  
C. R. Contreras-Gaytan<sup>3</sup>

<sup>1</sup>Departamento de Ingeniería Física—DCI, Universidad de Guanajuato Campus León Loma del Bosque, León, México

<sup>2</sup>Unidad de Investigaciones Médicas, Los Paraísos, León, México

<sup>3</sup>Facultad de Ingeniería en Computación y Electrónica, Universidad De La Salle Bajío Campus Campestre,  
Lomas del Campestre, León, México

Email: [theo@fisica.ugto.mx](mailto:theo@fisica.ugto.mx), [theocordova@yahoo.com](mailto:theocordova@yahoo.com)

Received May 31, 2012; revised June 28, 2012; accepted July 12, 2012

### ABSTRACT

An analysis of the reproducibility from signal record bioelectric heart activity is presented. The measurements were carried out with a recently patented medical device, which one is able to record the curves of pressure arterial and venous as those obtained using the gold standard technique in these evaluations, the cardiac catheterization technique. The measurements were carried out 15 health subjects and patients; each one was measured 5 times in order to have auto-correlations and correlations of these records. Analysis indicates correlations from 0.9 to 1 as long as  $p$  values were below 0.05. It is indicated an excellent reproducibility of evaluated patients.

**Keywords:** Bioelectric Heart Activity; Curves of Pressure Arterial and Venous; Correlation Coefficient; Statistical Analysis

### 1. Introduction

The arterial and venous pressures are values attributed to blood flow through human body [1,2]. As far as it is known, the first record about blood circulation existence was performed in China by Nei Ching, 2600 years a. C. [3] Although Miguel Servet made the first description of pulmonary circulatory system [4]. Later, William Harvey raised the principle of hemodynamics to verify that the heart muscle had phases of movement and rest [5]. Poiseuille used a pressure gauge in animals to evaluate the pressure in units of mmHg [6]. Faivre used the Poiseuille hemodinamometer on a human being to measure intra-arterial pressure [7].

Some non-invasive studies have shown that hemodynamic forces have a relationship with the pulse pressure [8]. It has also been noted that with age, it is increased cardiovascular risk, and it is directly related to aortic pressure increase [8-12]. Currently there are two methods of clinical routine use for measurement of blood pressure and only one to record venous pressure: cardiac catheterization and sphygmomanometer to arteries. The second one is widely used, however provides a register subjective due to its nature. As long as, the technique of

cardiac catheterization is able to record venous pressure in their inside, it is considered the gold standard in these assessments, despite it is widely invasive and it demands high trained personnel and special patients areas for implementation [9]. Nevertheless, it presents an objective record.

In this paper, it is presented the validation of records on blood pressure in healthy subjects and patients. It has been used a device recently patented, the pulse pressure cardiac gauge (PPC). This diagnostic and monitoring device is able to have a distinction of recording of the curves shape of pressure of arterial and venous as those recorded by catheterization, it offer an express evaluation with the advantage of carrying out the valuation on skin level; the ionizing radiation is avoided and does not require a sterile room for evaluation.

### 2. Methodology

Each one of the patients enrolled in this study gave a written consent previous to carrying out measurements, which were performed according to the treaty of Helsinki for studies in humans. These assessments did not present any risk or exposed the patient to any ionizing radiation. To each volunteer was asked to be placed in semi-fowler position with the head turned to the right, then the artery

\*Corresponding author.

or vein was identified by palpation and auscultation, this is, the location of the internal jugular vein and common carotid artery as shown in **Figure 1**; when the right location under skin of artery or vein is done, on skin is placed a magnetic marker (a magnet of  $3 \times 4$  mm, diameter and height, respectively), then, it is fixed the sensor base of the PPC in contact with the skin. Without exerting more pressure that the base and the magnetic sensor weight on the neck of the person, the magnetometer is always separated a distance of 2.5 cm from magnetic marker on patient skin. This magnetic marker is light enough not to crush the vessel but has the intensity of the magnetic moment sufficiently intense,  $\mu = 0.13 \text{ Am}^2$ . Magnetic signal is registered with an excellent signal/noise rate, such it is not required filtering digital additional so that the detected signal is read.

Mechanical action by the flow of blood in the vessel is transmitted to magnetic marker. So, it generates a variable magnetic field which increases as it approaches the sensor having variability in time and decreases away from this one.

In this validation study were measured 10 healthy subjects, all with no history of heart disease and 5 patients who underwent cardiac catheterization for suspected coronary artery disease, while they were registered with the cardiac catheter. So, after placing the magnetic marker, it was measured pressure curves repetitively every 30 seconds according to following order: 5 records for aspiratory inhalation and 5 records for aspiratory exhalation. It was asked an apnea around of 30 s. These measurements were performed on the left side of the neck and suprasternal area, some of them also included alternate position: semi-fowler and supine.

Validation of the obtained signals is carried out estimating the correlation coefficient of the reproducibility of the signal (cross-correlation of a signal with itself) using mathematical procedures for processing biological signals, first among the same individual (auto-correlation) and then correlate measurements between healthy subjects and patients.

### 3. Results

The first part of the measurements performed with the PPC device shows an excellent behavior of the pulse waves from arterial and venous, see **Figures 2 and 3**; it is a stage of apnea where it is shown the wave morphology of the artery and vein of the pulses according to the physiological theory of the cardiac cycle, this was done in healthy subjects.

A typical blood pressure waves recorded with the PPC in an apnea segment is shown in **Figure 4**.

The positive waves of pulse venous coincide with a delay or with the reverse of the flow, while each depression indicates an acceleration of venous return.

When contracting the right atrium (RA), the blood cannot enter the right ventricle (RV) flows back to the vena cava, resulting in venous pulse wave. The wave "a" is produced by the contraction of the RA in a presystolic period; the wave "c" occurs immediately after the wave "a" and at the beginning of "x", is produced by interference in the carotid arterial pulse, see **Figure 5**.

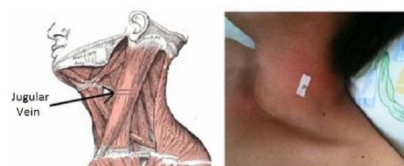


**Figure 1.** Schematization of magnetic marker position on subject skin, it is right over jugular artery.

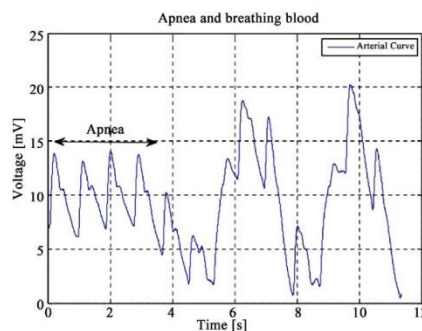


**Figure 2.** Arterial pressures register on suprasternal region for a healthy subject and stage of apnea in the supine position.

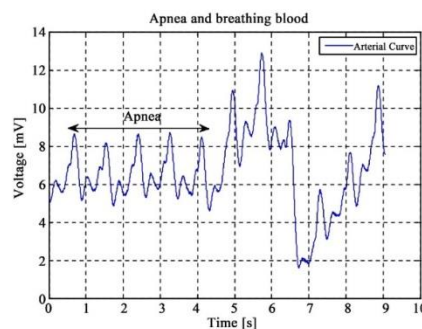


**Figure 3.** Pressure waveform in internal jugular artery, it was recorded with two stages: breathing and apnea. Similar pattern is repeated for a blood pressure pulse, at the stage of apnea the signal present pattern defined according to the morphology searched.



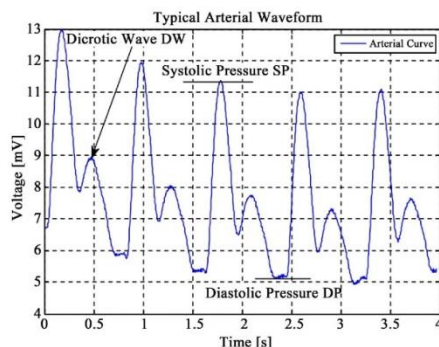


Figure 4. Typical pressure wave recorded, using the PPC device, on zone suprasternal in supine position with breathing noise. In the curve is reached to clearly distinguish three points of interest, dicrotic waves due to backflow of blood as well as maximal and minimal corresponding to the systolic pressure (SP) and diastolic pressure (DP) as the cardiac cycle.

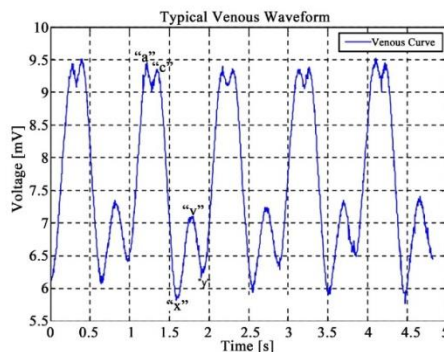


Figure 5. Waveform pressure recorded from the internal jugular vein, taken on the left side of the neck, in a healthy subject in inspiratory apnea phase and semi-fowler position. Note the characteristic morphology "a", "c", "v", and declines called "x" and "y".

The sine "x" is one of the predominant decreases, occurs during diastole atrial due to pressure drop in the atria, then follows the wave "v", due to increased atrial filling pressure right under the return of blood through the vena cava and finally the depression "y" is produced because the pressure in the RA descends to the open tricuspid valve in the relaxation phase in the filling period RV.

When the registration is made by reversing the polarity of the magnet there is an inversion of the curves and venous blood pressure in the temporary space, the Figure

6 shows the case of arterial register, there are the same waveforms with an inverted orientation only.

For the standardization phase, waveforms are obtained for healthy subjects, see Figures 7 and 8. The records have the following identification: ica (internal carotid in apnea aspiratory), ici (internal carotid in apnea inspiratory), ija (internal jugular in apnea aspiratory) and iji (internal jugular in apnea inspiratory). Measurements in the suprasternal area with two variants are: saa (suprasternal in apnea aspiratory) and sai (suprasternal in apnea inspiratory).

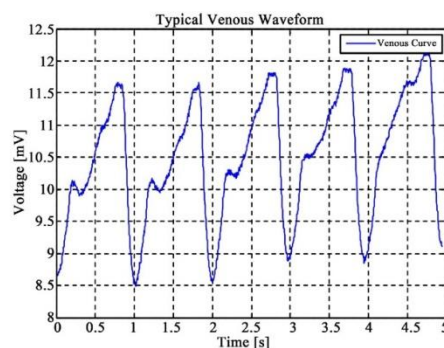


Figure 6. Waveform pressure from suprasternal area, in a healthy subject, at the stage of apnea aspiratory and supine position. It shows the morphology characteristic of the curve of blood pressure.

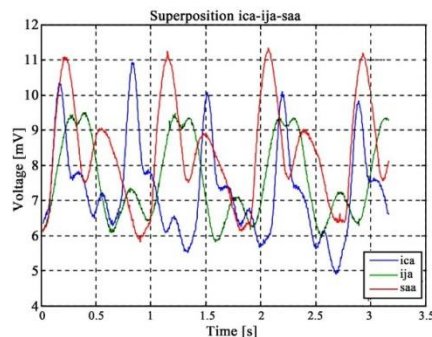


Figure 7. Pressure waves ica, ija and saa, superimposed on the phase of respiration in apnea aspiratory for the same subject. The pressure in ica and ija are in semi-fowler position, while the saa is supine. Note the difference in amplitude, and morphological consistency that emerges as the cardiac cycle, regardless of the different areas where each record was taken, this is mentioned for blood pressure supine and semi-fowler.

### 3.3. Hemodynamic Study and Calibration

In the cardiac catheterize lab of highly specialized medical unit (HSMU) No.1 at the Mexican Social Security Institute (IMSS), printed data were obtained from the pressure curves recorded by catheterization in 7 patients. The **Figure 12** shows one of the curves obtained simultaneously with the PPC and the polygraph in a cardiac catheter intervention, considering the gold standard.

### 4. Discussion

PPC is a device which measures variations in the intensity of a magnetic field generated by a magnetic marker at a fixed distance from a transducer that converts mechanical movement to analog signals and a source to amplify the signals recorded, filter, and stored in a computer as digital signal, becoming text file for further study and manipulation. Each of the elements constituting the complete device are easy to transport and install in any area where it is required to measure, only consists of a horseshoe that supports the sensor connected to a flexible tube attached to a microphone stand for easy positioning at the time of measurement and a computer with the software needed to acquire the data.

Because of the magnetic field measurements provide a good approximation to see the angular dependence exists around a coaxial cable or a cylindrical permanent magnet, it is the possibility to register the oscillations of a source for a determined distance. This measurement modalities relates the blood pressure carried by the conduits different called vessels and they are divided according to their morphology and function in arteries, veins and capillaries, which not being rigid conduits tend to contract and expand due to the strength that is against the walls to resist the flow of blood pumped by the heart, and this motion due to it is soft waves can be recorded by the PPC successfully locating the vessel to be measured.

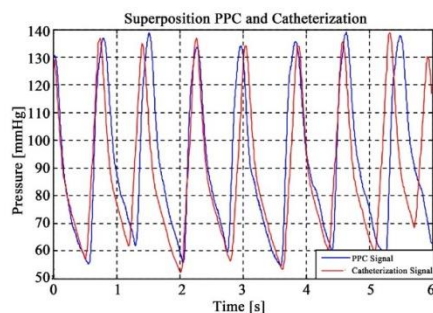


**Figure 12.** Superposition of signals obtained with the PPC and polygraph and made the switch from units of volts to millimeters of mercury in the PPC signal.

The PPC device provides information (voltage-time) about the compliance of the arteries or veins. The maximum value of each wave equals the pressure systolic and the minimums is equal to pressure diastolic, while the decrease or dicrotic wave is related to the backflow of blood, thus has a new way of measuring the patient's health status, graduating flexibility and arterial diameter with the pressure non-invasively and continuously.

The PPC has a good correlation " $r \approx 0.9$ " values of pressure vs. sphygmomanometer (anaerobic/digital), but unlike the sphygmomanometer no have operation on the whole sample. Excluded are subjects mainly in the suprasternal space not have a reflection of the rebound of the arteries confined and also in subjects in which their side zones to the neck is not palpable the location of the carotid arteries and the internal jugular vein, this group includes those individuals who have a body mass index (BMI) greater than  $25 \text{ kg/m}^2$  and elderly patients.

The waveforms obtained with the PPC correspond to the cardiac cycle and are similar to the curves obtained by cardiac catheterization. The PPC can help determine one of the many parameters of the catheterization, since it is easy to use and does not require specialized personnel for its use.

The waveforms obtained with the PPC are very sensitive to any movement of the test subject among which are: respiration, the fluid passes through the esophagus or involuntary displacement.

When is standardized the protocol to PPC shows that for venous pressure and arterial pressure the waveforms were very similar in terms of amplitude, frequency and period, being that biologically come to have a value deferred of at least 60 mmHG between blood pressure and venous, since the venous for transport higher amounts of blood is not pulsatile compared with the pressure in arteries reaching values of 120 mmHg, while the vein is 5 mm Hg, this is an important consideration when calibrating the PPC in the modalities of arterial and venous pressure.

During the measurements to the same test subject was observed that had a change in amplitude in curves when the variants were apnea in inspiration or aspiration, as, when there deep breath, the chest cavity and the lungs expand, the chest wall expands and diaphragm low. This causes the pressure intrapulmonary becomes more negative, which causes the lungs, heart and the thoracic vein cava is expand decreasing the pressure inside them. As the right atrial pressure decreases during inspiration, the pressure gradient between the inferior vein cava and right atrium increases, which impulse blood into the right atrium (there is an effect of "suction"), thereby increasing the volume of right ventricular ejection, to the pulmonary circulation. On the other hand, although the atrium and left ventricle also increases volume during inspiration,

- sticidad y Amortiguamiento Parietal de Arterias Sistémicas: Análisis Isopulsátil de la Relación Presión-Diámetro Arterial," *Revista Española De Cardiología*, Vol. 58, No. 2, 2005, pp. 844-847.
- [12] D. R. Armentano and Y. Zócalo, "Disipación Energética y Protección Vascular Durante La Hipertensión Arterial Sistémica: Rol Del Músculo Liso," *Revista Uruguaya de Cardiología*, Vol. 20, No. 3, 2005, pp. 125-135.
- [13] L. A. Romero, "Validación del Dispositivo Pulso Presiómetro Magnético para la Medición de la Presión Arterial Sistémica," Universidad de Guanajuato División de Ciencias de la Salud, 2011.
- [14] M. Maldonado, "Medición Biomagnética de las Curvas de Presión Arterial y Venosa," Universidad de Guanajuato, 2009.



## **Portable device for magnetic stimulation: Assessment survival and proliferation in human lymphocytes**

H. Pérez, T. Cordova-Fraga, S. López-Briones, J. C. Martínez-Espinosa, E. F. Rosas et al.

Citation: *Rev. Sci. Instrum.* **84**, 094701 (2013); doi: 10.1063/1.4819796

View online: <http://dx.doi.org/10.1063/1.4819796>

View Table of Contents: <http://rsi.aip.org/resource/1/RSINAK/v84/i9>

Published by the AIP Publishing LLC.

---

### **Additional information on Rev. Sci. Instrum.**

Journal Homepage: <http://rsi.aip.org>

Journal Information: [http://rsi.aip.org/about/about\\_the\\_journal](http://rsi.aip.org/about/about_the_journal)

Top downloads: [http://rsi.aip.org/features/most\\_downloaded](http://rsi.aip.org/features/most_downloaded)

Information for Authors: <http://rsi.aip.org/authors>





## Portable device for magnetic stimulation: Assessment survival and proliferation in human lymphocytes

H. Pérez,<sup>1,2,a)</sup> T. Cordova-Fraga,<sup>1,b)</sup> S. López-Briones,<sup>3,c)</sup> J. C. Martínez-Espinoza,<sup>4,d)</sup> E. F. Rosas,<sup>1,a)</sup> A. Espinoza,<sup>1,a)</sup> J. C. Villagómez-Castro,<sup>5,e)</sup> M. Sosa,<sup>1,a)</sup> S. Topsu,<sup>2,f)</sup> and J. J. Bernal-Alvarado<sup>1,a)</sup>

<sup>1</sup>Department of Physical Engineering - DCI, Universidad de Guanajuato campus León, Loma del Bosque 103, Lomas del Campestre, 37150 León, GTO, Mexico

<sup>2</sup>Université de Versailles, Saint-Quentin-en-Yvelines, 10-12 avenue de l'Europe, 78140 Vélizy-Villacoublay, France

<sup>3</sup>Department of Medical Sciences - DCS, Universidad de Guanajuato campus León, 20 de Enero No. 929, Col. Obregon, 37000 León, GTO, Mexico

<sup>4</sup>Academy of Mechatronics, Instituto Politécnico Nacional campus Guanajuato Av. Mineral de Valencia No. 200, Silao de la Victoria, 36275 Silao, GTO, Mexico

<sup>5</sup>Department of Biology - DCNE, Universidad de Guanajuato campus Guanajuato, Noria Alta s/n, 36050 Guanajuato, GTO, Mexico

(Received 9 June 2013; accepted 9 August 2013; published online 9 September 2013)

A device's instrumentation for magnetic stimulation on human lymphocytes is presented. This is a new procedure to stimulate growing cells with ferrofluid in vortices of magnetic field. The stimulation of magnetic vortices was provided at five different frequencies, from 100 to 2500 Hz and intensities from 1.13 to 4.13 mT. To improve the stimulation effects, a paramagnetic ferrofluid was added on the cell culture medium. The results suggest that the frequency changes and the magnetic field variation produce an important increase in the number of proliferating cells as well as in the cellular viability. This new magnetic stimulation modality could trigger an intracellular mechanism to induce cell proliferation and cellular survival only on mitogen stimulated cells. © 2013 AIP Publishing LLC. [<http://dx.doi.org/10.1063/1.4819796>]

### I. INTRODUCTION

The magnetic stimulation is a technique that has been used in different study areas, such as nuclear magnetic resonance and biomagnetic signals in magneto-encephalography, thus like the effect of magnetic field on living organisms for fermentation process and some biological self-organization studies.<sup>1–8</sup>

Biological side effects in systems exposed to a magnetic field have been studied in the last decades. Many studies were published about the magnetic stimulation on the algal growth and its nutrition composition, the ability of prokaryotic microorganisms to activate strategies in adapting themselves to the environmental stress induced by exposure to extremely low frequency electromagnetic fields, the growth of yeasts *Saccharomyces cerevisiae*, the magnetic field effect in children with acute lymphoblastic leukemia, among other.<sup>9–15</sup>

The implementation of a portable magnetic stimulator device for growing cells presented in this work was tested in a human lymphocytes pilot study from healthy volunteer donors. The effect of magnetic field exposition was analyzed

by flow cytometry (proliferation and cell survival), which one is an instrument largely used in biomedical applications to determine cell division, clinical pathology in immunology, analysis of bacteria, and mammalian sperm in the areas of reproductive toxicology, identification of neoplastic marker probes for DNA-diploid disease, and so many other areas where cellular systems are involved.<sup>16–20</sup>

### II. MATERIALS AND METHODS

The magnetic stimulator system assembled is a device that includes three parts: (i) hardware, (ii) software, and (iii) a magnetic field source.

#### A. Hardware description

There is a microprocessor plus it contains an electronic stage for sine wave generation, which consists of a limited counter; its design allows saving the parameters in an electronic memory, according to the frequency and the time intervals of the magnetic stimulation selected for the biological sample. Furthermore, the system permits setting different time intervals for each operating frequency previously designated. The switch exit is connected to a Fourier block diagram, this converts a constant frequency value to an astern signal, so in this block, other parameters can be established, such as the power, the central value for the signal, the RMS value, and the power of harmonics in sinusoidal signals. The out frequency generated is connected to an audio amplifier

<sup>a)</sup>Electronic addresses: huetzin@msn.com; weeks686@licifug.ugto.mx; bernal@fisica.ugto.mx; modesto@fisica.ugto.mx; and aag85@licifug.ugto.mx

<sup>b)</sup>Author to whom correspondence should be addressed. Electronic addresses: theo@dcf.ugto.mx; theo@fisica.ugto.mx; and theocordova@yahoo.com

<sup>c)</sup>lobris@yahoo.com

<sup>d)</sup>jcmartinez@ipn.mx

<sup>e)</sup>castroj@ugto.mx

<sup>f)</sup>suat.topsu@uvsq.fr

TABLE I. Theoretical and experimental data recorded in the Rodin coil characterization.

Frequency (Hz)	Z ( $\Omega$ )	Intensity current (A)	Magnetic field intensity (mT)		
			Theoretical	Experimental	fem (V)
100	6.86	1.60	3.80	4.13	0.20
800	8.78	1.25	2.97	3.05	0.85
1500	12.41	0.89	2.10	1.98	1.10
2450	18.26	0.60	1.42	1.16	1.14
2500	18.58	0.59	1.42	1.13	1.00

with power of 1000 W and 12 V of amplitude, this feeds a magnetic field source where the sample is deposited.

### B. Software

Instrumentation is monitored and controlled through an algorithm performed in assembly language and installed in a microprocessor. This algorithm was designed to generate sinusoidal oscillations at different frequencies, in particular, in this work it worked at frequencies of 100, 800, 1500, 2450, and 2500 Hz in segments of 360 s each one; this frequency cycle was repeated four times in a pilot work. So, the experimental sample group was stimulated for 2 h.

### C. Magnetic field resource

A Rodin system coil was assembled with two identical coils; they have an average diameter of 2.2 cm and winding of 21 turns; these two coils plugged in series, so this arrangement of coils has an electrical resistance of  $R = 6.83 \Omega$ . The geometry of this magnetic stimulator device is a 12-sided polygon; furthermore, a particularity of coil geometry and its wire winding is the magnetic vortices. Such an approximation of the magnetic field sample position was estimated by using the Biot-Savart Law:

$$\vec{B}_1 = \hat{e}_r N \left[ \frac{6\mu_0 I}{\pi r} \sin\left(\frac{\pi}{12}\right) \right],$$

where  $N$  is the number of coils,  $r$  is the distance from source to the sample center, and  $\mu_0$  is the magnetic permeability. But this magnetic source is an assembly of two coils, then, for the theoretical magnetic characterization was used this expression:

$$\vec{B} = \vec{B}_1 + \vec{B}_2.$$

### D. Device characterization

The sinusoidal signal generated for this device was amplified through the electronic stage, then the total impedance,  $|Z|$ , of the circuit was measured. These data were used for calculating the electric current and then to have a theoretical estimation of the resource magnetic field. The magnetic field was also measured in the sample position with a scientific gauss meter from Magnetic Instrumentation Inc, Model 210 and sensibility from  $\mu\text{T}$  to T. All this information is summarized in Table I.

The theoretical and experimental behavior of the coil magnetic field is shown in Figure 1. A Pearson correlations coefficient for these registers is  $r = 0.9999$ , as long as, the experimental data were fitting to a first-order exponential function using Origin software. The obtained parameters, with  $R^2 = 0.99$ , are shown in Eq. (1):

$$MF = -0.97 + 5.32 \exp(-3.75 \times 10^{-4} f). \quad (1)$$

On the other hand, the magnetic field and electromotive force variation are affected by frequency and impedance of the coil, these behaviors are shown in Figures 2(a) and 2(b), respectively.

In order to have an evaluation of the working of this magnetic exposure, the device was tested in a biological sample of cell culture (human lymphocytes) according the next procedure.

### E. Protocol

The local bioethics committee approved this study protocol; furthermore, a written informed consent was obtained from each volunteer. In basal conditions, 20 ml of blood was donated for each volunteer.

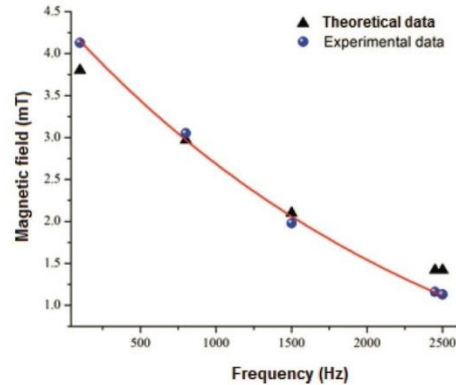


FIG. 1. Frequency responses of the magnetic field in the Rodin coil according excitation frequency.

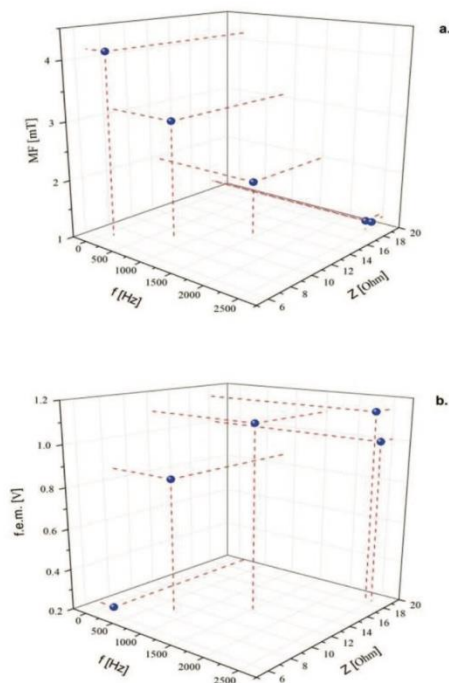


FIG. 2. This is the behavior of the magnetic field (a) and the fem (b). (a) Magnetic field vs. electrical impedance, depending on the frequency of the sinusoidal signal supplied. (b) Electromotive force vs. electrical impedance, depending on the frequency of the sinusoidal signal supplied.

### 1. Ferrofluid substance

A paramagnetic suspension as ferrofluid was used in order to increase the effect of magnetic field excitation in growing cells.<sup>21–23</sup> So, the paramagnetic Gadolinium suspension of commercial use in MRI studies was added into the cell culture of these experiments.

### 2. Peripheral blood mononuclear cells purification and Carboxyfluorescein Succinimidyl Ester (CFSE) labeling

Blood samples were collected from 12 subjects of 24 to 35 years old. All individuals included in this study were healthy, non-smokers, and they had no history of alcohol abuse or drug consumption. PBMCs were isolated from 20 ml of blood by conventional centrifugation in a density gradient of Ficoll-Hypaque.

After centrifugation, PBMCs were collected from the Ficoll-histopaque interface. Then, cells were washed twice with phosphate saline buffer. They were counted and the cell viability was detected by exclusion of trypan blue staining.

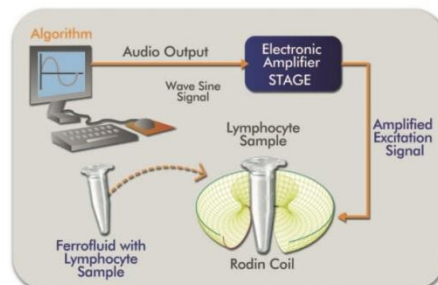


FIG. 3. Schematic setup of the magnetic excitation system applied on the prepared white blood cells.

After that, PBMCs were loaded with cell tracker dye CFSE ( $0.5 \mu\text{M}$ ; Molecular Probes) to monitor proliferation. Next CFSE staining,  $5.71 \mu\text{L}$  of Gadolinium was added to the lymphocyte samples. Each sample was placed in a 2 ml Eppendorf tube containing the lymphocytes in RPMI-1640 medium, see Figure 3.

### 3. In vitro stimulation with concanavalin A and exposition to magnetic field

Two groups of samples from same donor, control, and experimental groups were prepared.

The tubes containing the PBMC plus Gadolinium were exposed to magnetic field at frequencies of 100, 800, 1500, 2450, and 2500 Hz. Each frequency was remained for 6 min, then, it changes to other of the four frequencies; this frequency cycle was repeated four times, so that the whole magnetic stimulation on the sample took 2 h. The magnetic field intensity was also changing from 1.13 to 4.13 mT, this was according to each frequency applied. Then, cells were adjusted at a concentration of  $1 \times 10^6/\text{ml}$  in RPMI-1640 tissue culture medium (GIBCO, Eugene, OR) supplemented with 10% fetal bovine serum, 2 mM L-glutamine, 50 U/ml penicillin, and 50 g/ml streptomycin and cultured with or without  $2.5 \mu\text{g}/\text{ml}$  of concanavalin A (Con A, Sigma Aldrich) for 72 h or 7 days at  $37^\circ\text{C}$ , 100% humidity, and 5%  $\text{CO}_2$  (in survival experiments, the cells were cultured for 20 days, as will be indicated in brk Sec. III). The proliferation and cell survival were analyzed with a FACSCanto II flow cytometer by using the Diva software (Becton Dickinson, San Jose, CA).

### III. RESULTS

A non-invasive device for stimulation with magnetic vortices in growing cells was presented. The vortices of magnetic field were programmed to work in random segments at frequencies of 100, 800, 1500, 2450, and 2500 Hz. As far as it is known, this is the first time that magnetic vortices and suspension of Gadolinium were added to the PBMC samples to improve the effect of magnetic field.



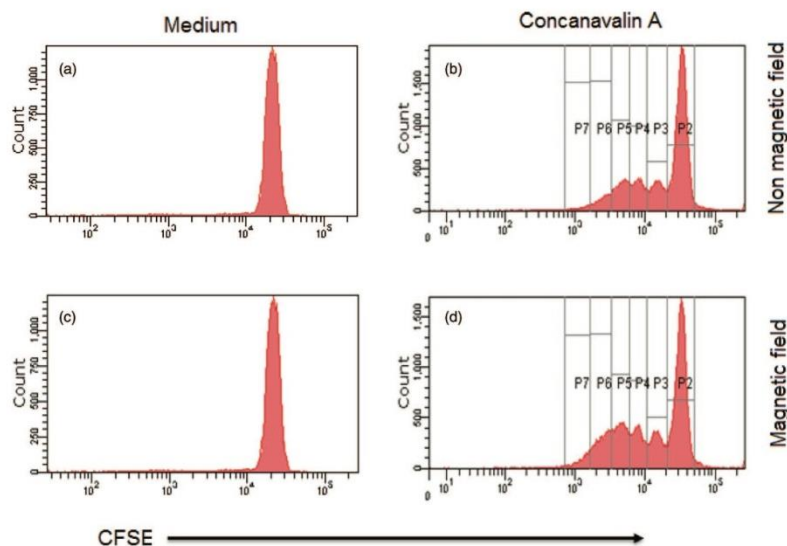


FIG. 4. Proliferation of human T cells stimulated with concanavalin A and magnetic field. (a) PBMC cultured in RPMI without concanavalin A neither magnetic field. (b) PBMC stimulated with concanavalin A but not magnetic field. (c) Concanavalin A stimulated cells without magnetic field and (d) cells stimulated with both concanavalin A and magnetic field. Percentages of cells reaching 2 (P4), 3 (P5), 4 (P6), and 5 (P7) cell divisions were significantly higher in cells stimulated with concanavalin A plus magnetic field, than those stimulated with concanavalin A alone.

In order to determine the effect of the magnetic field stimulation, a primary culture of human lymphocytes isolated from healthy donors was used. After 72 h there were no changes in cell proliferation or cell survival when the PBMCs were co-stimulated with magnetic field and concanavalin A, in comparison with those PBMCs treated only with concanavalin A (data not shown). However, after 7 days of culture, it was found that magnetic field stimulation did not induce any change on human lymphocytes without mitogenic treatment (Figure 4(c)). When human lymphocytes were co-stimulated with magnetic field and concanavalin A, an important increase in proliferating cells was detected (Figure 4(d)), thus when lymphocytes were treated with concanavalin A, but not stimulated with a magnetic field, the proliferation was observed in a lesser extent (Figure 4(c)). In Figure 4 representative plots are shown for the CFSE dilution. *In vitro* concanavalin A induced T cell proliferation, evaluated in healthy donor. The CFSE-labeled PBMCs were stimulated or not stimulated under a magnetic field, and then cultured with or without concanavalin A for 7 days and the percentage of divided cells was determined by flow cytometry.

On the other hand, when 20 days cultures of human lymphocytes were analyzed, an important increase in the number of surviving cells was detected on lymphocytes co-stimulated with magnetic field and concanavalin A (Figure 5(d)), while only few lymphocytes treated with concanavalin A but not stimulated with a magnetic field were viable after 20 days on culture (Figure 5(b)). It must be remarked that cells stimulated under a magnetic field but not treated with concanavalin

A survived more than those stimulated with concanavalin A alone (Figure 5(c)).

#### IV. CONCLUSIONS AND DISCUSSION

It has described a new noninvasive instrumentation; this is a magnetic stimulator device, in which vortices of magnetic field are generated by a magnetic source assembly with an arrange of Rodin coil, through a sinusoidal signal and it was programmed to work at frequencies of 100, 800, 1500, 2450, and 2500 Hz. It is important to put out that these frequencies were selected after doing a pilot study and find that the effects of proliferation were evident. The effect of sinusoidal varying magnetic fields was tested on fresh human mononuclear cells stimulated *in vitro* for 7 and 20 days with a mitogen. The PBMCs were collected from healthy donors to avoid any possible alteration on cells as consequence of diseases or infections, because it is well known that different diseases and infections could alter the proliferation capacity of human cells.

These data had shown that after 72 h of culture the magnetic stimulation had not any effect in both cell proliferation and survival. However, it has been reported that exposition to electromagnetic field decreases the proliferation after mitogenic stimulation,<sup>24</sup> nevertheless, the very low frequency (3 Hz) and time of exposition used in other experiments were different than those used here. Controversially, others have reported an important increase of cell proliferation after electromagnetic stimulation.<sup>25,26</sup> Therefore, it is clear that the effect of exposition to electromagnetic field could be influenced



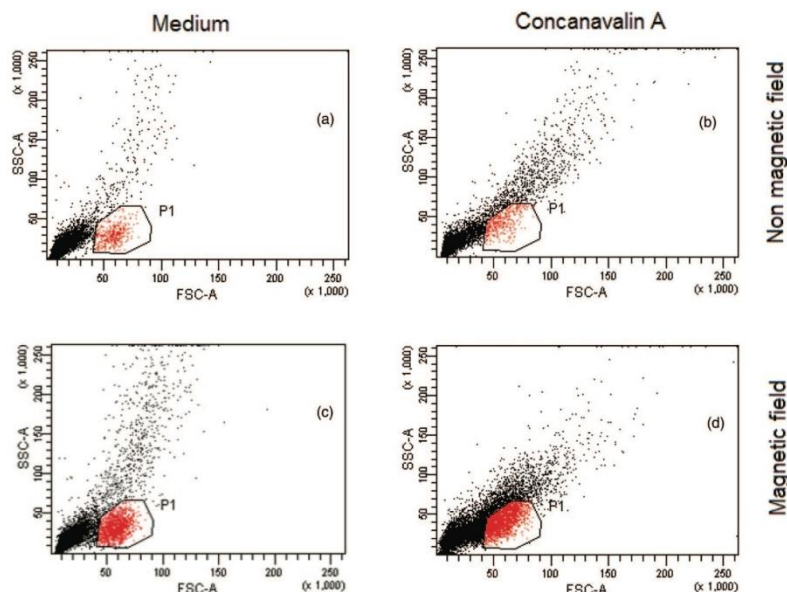


FIG. 5. Cell population and histogram obtained from flow cytometric analysis of a magnetic field excited samples from volunteer patients. P1 represents proliferating cells and P5 represents dead cells. (a) Cell divisions unstimulated with concanavalin A, (b) stimulated cells division with concanavalin A, (c) cell population unstimulated with concanavalin, and (d) cell divisions with concanavalin and magnetic stimulation.

by several experimental conditions such as, biological model, exposure system, exposure length, intensity, frequency, and pulse width.

On the other hand, it has been reported that a minimum of 6 h of exposure to electromagnetic field is necessary to induce any affect but, in most cases, a single frequency of exposure was used;<sup>24,27</sup> also, effects of electromagnetic fields have been observed as soon as 24 h.<sup>26</sup> Here, PBMC was stimulated for 2 h, in intervals of 6 min with five different frequencies and after 5 days of culture an important increase in cell proliferation on cells co-stimulated with mitogen and electromagnetic field was observed, but not on those PBMCs stimulated with mitogen alone. Moreover, the effect of electromagnetic field and mitogen also increased the survival after 20 days of cell culture. Thus, some mechanisms of cell survival have been reported to be activated by exposure to electromagnetic field such as increase in the synthesis of RNA<sup>28</sup> and  $\text{Ca}^{+2}$  influx and efflux have been observed.<sup>29,30</sup> In the same way, previously, it has been reported that cell exposition to magnetic fields increases cell survival by inhibiting apoptosis via modulation of  $\text{Ca}^{2+}$ /influx.<sup>14</sup>

Finally, this is an instrumentation description of the implemented device, where segments of five frequencies, in periods of 6 min were supplied in a biological sample. Despite this work and multiple studies performed around side effects of electromagnetic field on biological model, to date there are still not enough conclusive results that indicate whether a ma-

lignant or beneficial effect is induced through electromagnetic field. Therefore, additional experiments are being carried out in our laboratories and other labs in the world in order to elucidate the intracellular mechanisms induced after electromagnetic field stimulation.

#### ACKNOWLEDGMENTS

The authors thank the Universidad de Guanajuato campus León, Transversal Project 2012, and DAIP Institutional Projects 2012 for the financial support.

- <sup>1</sup>R. König, C. Sieluzky, and P. Durka, *J. Low Temp. Phys.* **146**(5-6), 697-718 (2007).
- <sup>2</sup>P. C. Lauterbur, *Nature (London)* **242**, 190-191 (1973).
- <sup>3</sup>J. Virtanen, L. Parkkonen, R. J. Ilmoniemi, E. Pekkonen, and R. Näätänen, *Med. Biol. Eng. Comput.* **35**(4), 402-408 (1977).
- <sup>4</sup>O. Rodríguez-Justo, V. Haber-Pérez, D. Chacon-Alvarez, and R. Monte-Alegre, *Appl. Biochem. Biotechnol.* **134**, 155-163 (2006).
- <sup>5</sup>F. Popp and Z. Jinzhu, *Sci. China, Ser. C* **43**(5), 507-518 (2000).
- <sup>6</sup>R. Goodman, Y. Chizmadzhev, and A. Shirley, *J. Cell. Biochem.* **51**, 436-441 (1993).
- <sup>7</sup>B. Holmberg, *Environ. Health Perspect.* March **103**(Suppl 2), 63-67 (1995).
- <sup>8</sup>R. Hunt, A. Zavalin, A. Bhatnagar, S. Chinnasamy, and K. Das, *Int. J. Mol. Sci.* **10**, 4515-4558 (2009).
- <sup>9</sup>L. Zhi-Yong, G. Si-Yuan, L. Lin, and C. Miao-Yan, *Bioresour. Technol.* **98**, 700-705 (2007).
- <sup>10</sup>L. Cellini, R. Grande, E. Di Campli, S. Di Bartolomeo, M. Di Giulio, I. Robuffo, O. Trubiani, and M. A. Mariggio, *Bioelectromagnetics* **29**, 302-311 (2008).

- <sup>11</sup>J. Novák, L. Strašák, L. Fojt, I. Slaninová, and V. Vetter, *Bioelectrochemistry* **70**(1), 115–121 (2007).
- <sup>12</sup>M. Linet, E. Hatch, R. Kleiner, L. Robison, W. Kaune, D. Friedman, R. Severson, C. Haines, C. Hartsock, S. Niwa, S. Wacholder, and R. Tarone, *N. Engl. J. Med.* **337**, 1–8 (1997).
- <sup>13</sup>M. R. Scarfi, M. B. Lioi, M. Della Noce, O. Zeni, C. Franceschi, D. Monti, G. Castellani, and F. Bersani, *Bioelectrochem. Bioenerg.* **43**, 77–81 (1997).
- <sup>14</sup>C. Fanelli, S. Coppola, R. Barone, C. Colussi, G. Gualandi, P. Volpe, and L. Ghibelli, *FASEB J.* **13**(1), 95–102 (1999).
- <sup>15</sup>J. C. Hernández-Pavón, M. Sosa, T. Córdova, G. Sabanero, S. Solorio, and M. Sabanero, *Acta Universitaria* **19**, 65–70 (2009).
- <sup>16</sup>A. B. Lyons and C. R. Parish, *J. Immunol. Methods* **171**(1), 131–137 (1994).
- <sup>17</sup>P. F. Virgo and G. J. Gibbs, *Ann. Clin. Biochem.* **49**, 17–28 (2012).
- <sup>18</sup>B. Herald, B. Erik, S. Kirsten, B. Bloon, G. Tore, and M. Salim, *Cytometry* **2**(4), 249–257 (1982).
- <sup>19</sup>E. Cordelli, P. Eleuteri, G. Leter, M. Rescia, and M. Spanò, *Contraception* **72**(4), 273–279 (2005).
- <sup>20</sup>B. Barlogie, M. Raber, J. Schumann, T. Johnson, B. Drewinko, D. Swartzendruber, W. Göhde, M. Andreeff, and E. Freireich, *J. Cancer Res.* **43**, 3982–3997 (1983).
- <sup>21</sup>O. O. Ahsen, U. Yilmaz, M. D. Aksoy, G. Ertas, and E. Atalar, *J. Magn. Magn. Mater.* **322**(20), 3053–3059 (2010).
- <sup>22</sup>P. Cantillon, L. Wald, E. Adalsteinsson, M. Zahn, and E. Atalar, *J. Magn. Magn. Mater.* **322**, 727–733 (2010).
- <sup>23</sup>R. Rosensweig, *Ferrohydrodynamics* (Cambridge University Press, 1985), p. 344.
- <sup>24</sup>P. Conti, G. E. Gigante, M. G. Cifone, E. Alesse, G. Ianni, M. Reale, and P. U. Angeletti, *FEBS Lett.* **162**(1), 156–160 (1983).
- <sup>25</sup>A. Cossarizza, D. Monti, F. Bersani, M. Cantini, R. Cadossi, A. Sacchi, and C. Franceschi, *Biochem. Biophys. Res. Commun.* **160**(2), 692–698 (1989).
- <sup>26</sup>G. Emilia, G. Torelli, G. Ceccherelli, A. Donelli, S. Ferrari, P. Zucchini, and R. Cadossi, *Electromagn. Biol. Med.* **4**(1), 145–162 (1985).
- <sup>27</sup>R. Cadossi, F. Bersani, A. Cossarizza, P. Zucchini, G. Emilia, G. Torelli, and C. Franceschi, *FASEB J.* **6**(9), 2667–2674 (1992).
- <sup>28</sup>R. Goodman, C. A. Bassett, and A. S. Henderson, *Science* **220**, 1283–1285 (1983).
- <sup>29</sup>J. Walczek and R. P. Liburdy, *FEBS Lett.* **271**(1–2), 157–160 (1990).
- <sup>30</sup>P. Conti, G. E. Gigante, E. Alesse, M. G. Cifone, C. Fieschi, M. Reale, and P. U. Angeletti, *FEBS Lett.* **181**(1), 28–32 (1985).

## Measuring Gastroesophageal Region Frequencies for Long time: Preliminary Results

E Hernández-Torres<sup>a</sup>, T Cordova<sup>a</sup>, Huetzin Pérez<sup>a</sup>,  
M Sosa<sup>a</sup>, O Reynoso-Orozco<sup>c</sup>, ME Cano<sup>c</sup> and A Mendosa<sup>c</sup>

<sup>a</sup>Dept. Physics & Engineering, University of Guanajuato campus León, GTO, MEXICO.

<sup>b</sup>Centro Universitario de la Ciénega, Universidad de Guadalajara, México.

<sup>c</sup>UMAE, Clínica TI-León, Instituto Mexicano del Seguro Social, GTO, México.

E-mail: [theo@fisica.ugto.mx](mailto:theo@fisica.ugto.mx), phone 52 (477) 788-5100, ext: office 8475, fax 8410, Lab 8475

**Abstract** Measurements registered in the gastro-esophageal section with a implemented biomagnetic modality is presented, this procedure is based on magnetic markers and magnetometers system. It is shown that with this biomagnetic modality of evaluation, the gastric-esophageal activity can be monitored per prolonged times and in well defined regions. Registered frequencies in specific zones agree with the values traditionally reported in literature and it is also shown that with this biomagnetic modality it is possible to measure the speed of transit of the alimentary bolus in the esophagus.

**Keywords:** *gastroesophagica motility, esofágical activity, magnetic markers, magnetometers.*

### 1. Introduction

The main aim in this work is to show a new biomagnetic modality in order to measure gastro-esophageal motility. Several studies have been performed with this purpose, evaluating the contractions through the gastrointestinal (GI), as well as studies of gastric emptying carried out in our Lab [Cordova *et al.*, 2004, Cordova-Fraga *et al.*, 2005, De la Roca *et al.*, 2007, and Cordova-Fraga *et al.*, 2008]. In these studies were used ferromagnetic particles as magnetic tracers, they have shown a great utility to describe the gastric emptying and gastric contractions. Unfortunately, this is the only segment of the GI tract where motor function information is measured, this can be because of magnetic particles are not concentrated in a small space, so the magnetic intensity signal is not enough to be recorded by a magnetometer who works at room temperature. Nevertheless, some advantages in using magnetic techniques are ability to assess gastric activity as gastric peristalsis, half time of gastric emptying, influence of stress in the gastric emptying and colon transit time in different stages of the menstrual cycle, as well as the gastric transit that can be evaluated with other techniques like MRI technique. (NMR). [Di Pace *et al.*, 2011]. Although is possible to monitor the esophageal activity taking place, in the same way that in manometry, placing two sensors, in different positions from the esophagus.

In this study is presented an implementation of a magnetic marker and a fluxgate sensor, the first one was fixed through esophagus and gastric segments while the magnetic signal was recorded outside of the human body.

### 2. Material and Methods

In this study 6 healthy subjects without GI diseases were evaluated, they gave their written consent prior to participation in this study, which was performed according to the Treaty of Helsinki. The measurement procedures begin with the positioning of two magnetic particles in bottom of the stomach helped with an endoscope, so the starting point of magnets was well defined. Magnets were united to a

graduated thread that allowed moving them in a proximal direction, then magnet positions through GI tract were known in each time. Distal displacement was made giving freedom to the particles of such form that the contractile activity of the GI system moved the particles.

Peristalsis measurements were carried out in two gastric states of distension. First measurement was after that magnets have been placed in the region of fundus in basal state. Then, measurements were taken in two positions within the stomach, fundus and antrum. After those measurements in basal state were done, subject ingested a test meal that included bread, chicken, vegetables and water. Then measurements were taken again in fundus and the antrum. Finally the magnets were moved esophagus section, and measurements were taken in three sections crossing in a proximal direction.

Evaluations taken in each of distension states were made with temporal separations of 10 min. As long as in measurements in gastric section had a separation of around 2 hours. Measurements in postprandial state, in stomach and in esophagus had a 20 minutes separation.

The magnetic marker were identical, they include neodymium-iron-boron (NdFeB) and they had a cylindrical shape ( $d = 3$  mm,  $h = 4$  mm, diameter and height and magnetic moment  $m = 1.42 \times 10^{-2}$  J/T). These magnet markers generate a magnetic field that is detectable by fluxgate sensors Model 539 (Applied Physics Systems). Two fluxgate sensors were arranged to coincide with their "y" axis and were separated a distance of 10 cm and they were registering a rate frequency of 30 samples per second.

### 3. Analysis

To eliminate high frequencies, a routine of Fast Fourier Transform was implemented in Matlab, it was used a band-pass filter, leaving only the contributions of low frequencies, from 1 to 5 cpm (cycles/minute), consequently cardiac activity and the breathing noises were eliminated. Frequencies of contraction in different sections of the GI tract were used to analyze each one of the two states. The spectra of the signals were analyzed to search for the peak corresponding to the main contraction frequencies of each one of the monitored sections. In many cases there were several frequencies characteristics of the signal (several peaks in the graph) but the maximum peaks were only considered, which were considered as the most representative frequency.

### 4. Results

The registered signals showed, in the majority of the registries the contractile activity of the subjects in the different sections from the gastro esophageal tract (See Figure 2).

#### 4.1. Basal activity

The contractile activity for this relaxed state of distension was between the 1,5 and 3 cpm.

#### 4.2. Postprandial activity

The contractions are better defined by less noisy signals, with the frequencies that went from the 1,5 to 3 cpm, being more recurrent frequencies of 2,5 cpm or grader. Unlike the shown activity in the basal state, in the after-lunch state are fewer harmonics for the main frequency of contractions in the different sections from the stomach.

#### 4.3. Esophageal activity

The predominant activity of this region was around the 1,5 cpm, although in some subjects were shown harmonic frequencies of around 3 cpm. In figure 2 the behavior of the main frequencies of contraction for a subject can be observed in each one of the gastric states of distension (basal and postprandial) and for each of the regions (stomach and gullet). In figure 2 the variation of the main



contraction frequencies can be appreciated, and how they change depending of the GI section, and the distention states in which it is.

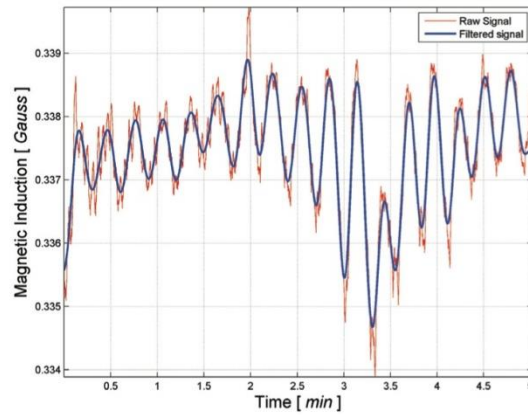


**Figure 1.** Contractil activity of the stomach after the food ingestion. It is possible to appreciate that the contractions in the stomach are around three contractions per minute.

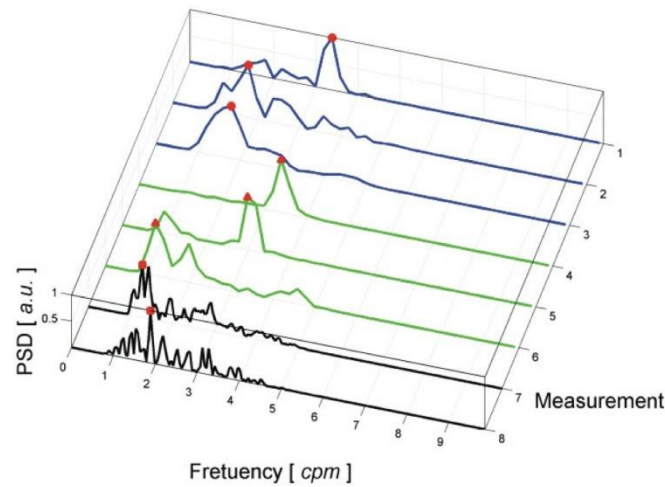


**Figure 2.** Graphic of the spectral densidades indicating the main frequencies in the different regions from the GE tract, from the antrum region (measurement 1) to the middle esophagus (last measurement). This graphic contains all the measurements realised in a subject. The blue lines show the measurements in basal state. It is observed in these measurements how the contractions frequency were slowing while the stomach went away relaxing. In the green lines were shown the frequencies after the subject ingested food. It is easily perceivable that as the stomach has more luminar containing the gastric activity returns smoother and as the empty stomach the activity becomes much noisy.

## 5. Discussion

The frequencies of contraction for the different distention states presented a wide range of frequencies, in particular the stretched state. This is clearly because while the particles move throughout tract GI in proximal direction the frequencies are mixed, which is a high influence in the esophageal activity. Besides this phenomenon, other factors can be considered to have influence in results. Some of them are that we are considering the characteristic frequencies to be the frequencies that correspond to the maximum tips in our spectral densities of power, and since the stomach behaves in different forms for different subjects, in particular in the state to base, the characteristic tips in this state of distension are not always is the same.

Different modalities to measure gastro esophageal activity have been used, among them emphasize the manometry, Radionuclide Imaging, magnetic resonance (to secure references of these techniques) with which have obtained registries. On the other hand measurements were made during the food ingestion; hopefully the sharp variation alteration of the magnetic moments direction of the markers originates a great change in the amplitude of the magnetic induction. This shows the potential to register gastro esophageal regions frequencies.

## Acknowledgements

Authors want to thank DAIP under grant number 000017/10, FESE 2010 and UDLSBajio 2010, for their partial support in this study.

## References

- Cordova T, Gutierrez J G, Sosa A M, Vargas L F, Bernal A J J, *Gastric activity studies using a magnetic tracer*. Institute of Physics Publishing, 25, 2004,1261-70.
- Cordova-Fraga T, Carneiro AA, de Araujo DB, Oliveira RB, Sosa M, Baffa O. Spatiotemporal evaluation of human colon motility using three-axis fluxgates and magnetic markers. *Med Biol Eng Comput.* 43(6):712-5 (2005).
- De la Roca J M, Hernández S E, Solís M S, Sosa A M, Córdova F T. *Magnetogastrography (MGG) reproducibility assessments of gastric emptying on healthy subjects*. *Physiol Meas.* 28(2) 175-183 (2007).
- Cordova-Fraga T, Sosa T, Wiechers C, De la Roca-Chiapas JM, Maldonado Moreles M, Bernal-Alvarado J, Huerta-Franco R. *Effects of anatomical position on esophageal transit time: A biomagnetic diagnostic technique*. *World J Gastroenterol* 14(37): 5707-5711 (2008).
- Di Pace MR, Caruso AM, Catalano P, Casuccio A, De Grazia E. *Evaluation of esophageal motility using multichannel intraluminal impedance in healthy children and children with gastroesophageal reflux*. *J Pediatr Gastroenterol Nutr.* 52(1): 26-30 (2011).

**Magnetic exposure system to stimulate human lymphocytes proliferation**

H. Perez-Olivas, T. Cordova-Fraga, F. Gómez-Aguilar, E. Rosas-Padilla, S. Lopez-Briones et al.

Citation: *AIP Conf. Proc.* **1494**, 146 (2012); doi: 10.1063/1.4764626

View online: <http://dx.doi.org/10.1063/1.4764626>

View Table of Contents: <http://proceedings.aip.org/dbt/dbt.jsp?KEY=APCPCS&Volume=1494&Issue=1>

Published by the AIP Publishing LLC.

---

**Additional information on AIP Conf. Proc.**

Journal Homepage: <http://proceedings.aip.org/>

Journal Information: [http://proceedings.aip.org/about/about\\_the\\_proceedings](http://proceedings.aip.org/about/about_the_proceedings)

Top downloads: [http://proceedings.aip.org/dbt/most\\_downloaded.jsp?KEY=APCPCS](http://proceedings.aip.org/dbt/most_downloaded.jsp?KEY=APCPCS)

Information for Authors: [http://proceedings.aip.org/authors/information\\_for\\_authors](http://proceedings.aip.org/authors/information_for_authors)

# Magnetic Exposure System To Stimulate Human Lymphocytes Proliferation

H Perez-Olivas<sup>a</sup>, T Cordova-Fraga<sup>a</sup>, F Gómez-Aguilar<sup>a</sup>, E Rosas-Padilla<sup>a</sup>,  
S Lopez-Briones<sup>b</sup>, AA Espinoza-García<sup>a</sup>, JC Villagómez-Castro<sup>c</sup>,  
JJ Bernal-Alvarado<sup>a</sup> and M Sosa-Aquino<sup>a</sup>

<sup>a</sup>*Departamento de Ingeniería Física – DCI, Universidad de Guanajuato, campus León.  
Loma del Bosque No. 103 Col. Lomas del Campestre, 37150. León, GTO. México*

<sup>b</sup>*División de Ciencias de la Salud, Universidad de Guanajuato, campus León  
37150, León, GTO, México.*

<sup>c</sup>*Departamento de Biología – DCNE, Universidad de Guanajuato, campus Guanajuato  
Apartado Postal 187, Guanajuato, GTO 36000, México.*

**Abstract** Magnetic stimulation (MS), a non-invasive technique to stimulate different kind of cells by a sinusoidal magnetic signal through a coil put on the scalp have been widely used in studies in clinical treatments on human. A modality of this MS technique to stimulate cell viability, proliferation and longevity, of human lymphocytes by using magnetic field is presented. AC magnetic stimulation was applied in a human range of audible frequency. A computer algorithm was implemented, which is combined with a power system to generate a cell magnetic stimulus via a coil variation. To generate and increase the stimulation, a ferromagnetic fluid is added on the cell culture medium, demonstrating, in this pilot study, that a sinusoidal magnetic signal applied on cell culture can increase cell longevity and produce proliferation without changes in cell viability.

**Keywords:** Magnetic therapy, electromagnetic fields, paramagnetic fluid, human Lymphocytes.

**PACS:** 41.20.Gz, 87.50.C-

## INTRODUCTION

Magnetic stimulation (MS) is a non-invasive technique used to stimulate different kind of cell grows by a constant or sinusoidal magnetic field. Biophysical mechanism underlying its effect is however largely unknown. Magnetic fields can generate a potential action in the cell structure [1]. Such as effects including a long inhibitory period. In this work, it is implemented a study in order to test a new procedure for magnetic stimulation of human Lymphocytes [2].

## METHODOLOGY

Lymphocytes samples were obtained from specimen blood of clinically healthy donors and some diabetic's patients from 24 to 35 years. Using a gradient density method, it was separated the lymphocytes from the peripheral blood [3]. Then they were magnetically stimulated with a system that consists of a computer algorithm (FIGURE 1), which one was combined with a power system to generate a cell magnetic stimulus via a magnetic coil. Around 2.0 mT peak to peak of sinusoidal varying magnetic fields



[4] was applied at 100, 800, 1500, 2450, and 2500 Hz; these frequencies segments of six minutes each one were random in order to induce changes in the dynamics of the plasma membrane and enhancing cell proliferation [5]. A ferromagnetic fluid was also added on the cell culture medium in order to generate and increase the stimulation.

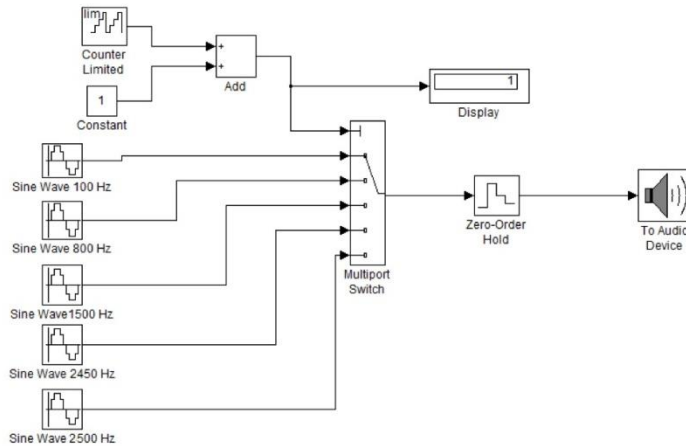


**FIGURE 1:** Diagram for the signal generating system, which was implemented in Matlab platform.

## RESULTS AND DISCUSSION

Applying the Flow Cytometry Analysis to the studied leveled cells with CellTrace, human peripheral blood lymphocytes were harvested and stained [6] on day 0. As can be seen in FIGURE 2 all generations are present, not only the parent generation. Allowing proliferation for a 7 day period, FIGURE 2 presents the parent generation peak P2, and successive generations peaks P3-P5. Where cells exposed to magnetic stimulation, applying stimulation frequencies from 100-2500 Hz MFs, were not cells damaged or considerably affected, observing an increment of the lymphocytes proliferation in the P3 to P4 generations.

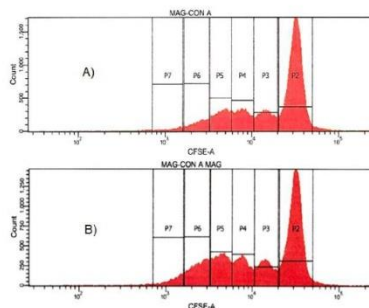


**FIGURE 2.** Flux Cytometer cell counting, A) control cells count, B) magnetic stimulated cells count.

## CONCLUSIONS

In this work it was shown that a sinusoidal magnetic signal applied to cell culture can increase the cell longevity and produce proliferation without changes in cell viability.

## ACKNOWLEDGMENTS

This work was partially supported by DAIP 017/2010

## REFERENCES

1. M.R. Scarfi, M.B. Lioi, M. Della Noce, O. Zeni, C. Franceschi, D. Monti, G. Castellani, F. Bersani, *Exposure to 100 Hz pulsed magnetic fields increases micronucleus frequency and cell proliferation in human lymphocytes*, Bioelectrochem. Bioenerg. 43. Pags. 77 – 81. (1997).
2. Julio César Hernández-Pavón, Modesto Sosa, Teodoro Córdova, *Study of Electromagnetic Fields on Cellular Systems*. Acta Universitaria 19. Pags. 65-70. (2009).
3. William E. Biddison. *Preparation and Culture of Human Lymphocytes*. Current Protocols in Cell Biology. (1998)
4. J. Antonio Heredia Rojas, Abraham O. Rodríguez-De la Fuente. *Cytological Effects of 60 Hz Magnetic Fields on Human Lymphocytes InVtro: Sister-Chromatid Exchanges, Cell Kinetics and Mitotic Rate*. Bioelectromagnetics 22. Pags. 145-149. (2001)
5. R. Cadossi, F. Bersani, A. Cossarizza, P. Zucchini. *Lymphocytes and low-frequency electromagnetic fields*. FASEB J. 6. Pags. 2667-2674. (1992).
6. S. Lopez-Briones, D.P. Portales-Perez, L. Baranda, H. de la Fuente, Y. Rosenstein, R. Gonzalez-Amaro. *Stimulation through CD50 preferentially induces apoptosis of TCR1+ human peripheral blood lymphocytes*. Cell Adhes. Commun. 6. Pags. 465-79. (1998).

# Cell Behavior Undergoing Random Segments of Oscillating Magnetic Field

H.A. Perez<sup>1</sup>, J.C. Villagomez<sup>2</sup>, T. Cordova<sup>1</sup>, M. Sosa<sup>1</sup>, and J.J. Bernal<sup>1</sup>

<sup>1</sup> Physics & Engineer Department - DCI, Universidad de Guanajuato, Leon, GTO, Mexico

<sup>2</sup> Departamento de Biología - DCNE, Universidad de Guanajuato, Guanajuato, GTO, Mexico

**Abstract** – This *Entamoeba* cells, the amoebic dysentery is highly motile, but this motility is an essential feature of the pathogenesis and morbidity of amoebiasis. A description of the motility in cell grown of the *Entamoeba* Invadens is presented. These cells were undergone to random segments in several frequencies of magnetic field; pictures of this cell grown were recorded and processed in order to have a correlation of the applied frequencies with natural movements. The natural cell behavior was observed, this is, controlled agglutination, cell movement velocity, and membrane structural form. A correlation between applied frequencies and cells movement is discussed.

**Keywords** – *Entamoeba* Invadens, magnetic stimulation, cell dynamics, densitometry, image processing.

## I. INTRODUCTION

Amoeboid motility requires spatiotemporal coordination of biochemical pathways regulating force generation and consists of the quasi-periodic repetition of a motility cycle driven by actin polymerization and actomyosin contraction [1].

*Entamoeba* motility and chemotaxis have been studied by using relatively few methods, including in haemocytometers, tube migration, and Boyden chamber assays. Under the first two conditions, cells have almost no resistance to their movement except substrate adhesion. During the invasive disease, however, amoebae move in more restrictive conditions, similar to metastasis and extravasation. Under-agarose (under-agar) assays provide such an environment and have been used to study the motility and chemotaxis of a variety of cells, including neutrophils, macrophages, and the free-living amoeba *Dictyostelium*, an evolutionary relative of *Entamoeba*. Under-agar assays have the added advantage of allowing moving cells to be visualized and parameters such as cell shape to be studied in detail [2].

In the last years, biomedical effects of low frequency's electromagnetic fields (ELF) on signal transduction have gained considerable interest as results obtained from various species point to a possible interaction between ELF with ion transport mechanisms in the cell membrane [3,4].

The aim of this work used the above technique. It was applied in order to study cell movement. The cells were undergone to random segments in several frequencies of

magnetic field, then; the effects of this magnetic-field stimulation were observed and considered the results obtained to understand more off the cell behavior, specifically in their dynamics and cellular cycle.

## II. MATERIALS AND METHODS

*E. invadens*, strain IP-1, are maintained and propagated under axenic conditions in TYI-S-33 medium at 26°C. Entamoebas were Ice-chilled at 4° C for 15 minutes to detach them from the vial, then counted in a Neubauer chamber and resuspended in TYI-S-33 to density of 50,000 cells/ml. One milliliter of previously prepared cells was placed in a 3 milliliter crystal vial, plus 2 ml of TYI-S-33 [5-7]. Each vial is then sealed by a sterilized transparent tape on the upper side to let the microscope light go through. All experiments are performed in the original culture media.

A cylindrical observation chamber was made of Plexiglas (diameter 300 mm, depth 350 mm) with a Plexiglas plate on the lower side [3]. For adaptation, cell is left undisturbed inside the crystal vial for 10 minutes, and then put inside the chamber to starting the measurements.

The observation chamber is placed in the center of a coil, with effective flux densities around 2.0 mT. The temperature is controlled by a liquid flux control system; Furthermore, a PID was used to hold temperature at 26° C. No significant temperature changes within the observation area at flux densities were registered.

An ELF signal is generated by a Simulink subsystem implemented in Matlab platform, which generate a sinusoidal signal in a specific frequency. Random lapses of six minutes were sent trough the audio card output of the computer during four hours from 15 Hz to 750 Hz.

A coil on an inverted microscope with a CCD cam was coupled and connected to a computer that shows the real time cell's image, and performs the cell movement analysis by image processing, see Fig. 1.

The 5,000 cell grown control is put over the inverted microscope, and the movement and cell form is analyzed. Furthermore, 5,000 cells grown in another vial was situated

at the microscope in the coil, and exposed to an oscillating magnetic field.

A picture was taken each 0.72 seconds, then; a comparison between actual and previous pictures was done; this is, difference pixel to pixel is made and recorded, see Fig. 2B. This movement area is stored with stimulation frequency and time value in the experiment.

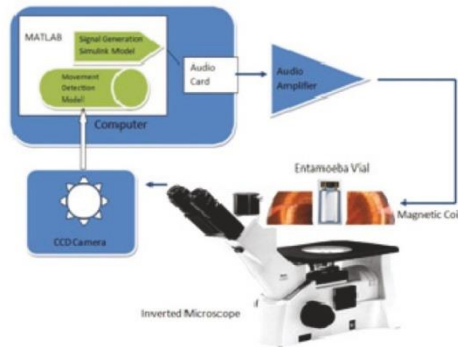


Fig. 1 Set-up of the stimulation system.

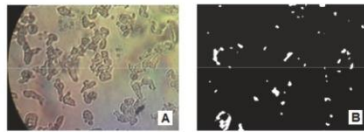


Fig. 2 A) Raw image recorded with the CCD cam, B) Pixels marked when there is a difference between an actual and one instant before the image frame.

### III. RESULTS

*Paper Size:* It was found that an image taken two minutes before of the change at 100 Hz, cells are growing in a natural state according to pseudopodia elongation and exterior morphology, see Fig. 3A. This pattern was repeated at frequencies from 15 Hz to 150 Hz. While, agglutinations were made at frequencies from 400 Hz to 750 Hz, this is shown in Fig. 3B.

A control cell grown movement was observed and analyzed during four hours, movement's values were from 0.18 to 0.28 a.u.

An experiment cell grown movement in similar to above conditions, but undergoing magnetic field at frequencies from 15 Hz to 750 Hz, was from 0.13 - 0.335 a.u.

Several segments for four hours of applied frequencies for six minutes are shown in Fig. 4. Furthermore, the answer of the cells grown to above stimulation is shown for each one of the periods.

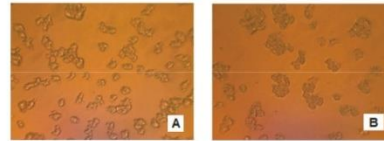


Fig. 3: Images of a stimulated cell grown at frequency of: A) 100 Hz and B) 700 Hz.

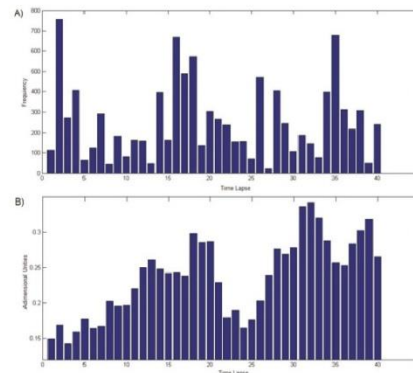


Fig. 4: A) Magnetic field applied in different frequencies on cell grown. B) Cellular movement average undergo magnetic field of A).

### IV. DISCUSSION

When frequencies lower than 400 Hz are applied, a maximum movement of stimulated cells is observed. If the cells are exposed in a long time period in frequencies from Hz 400 to 750 Hz, their movement is reduced at the length of period of time because of the stress given by the ELF.

Furthermore, it is observed that the frequency change rate affects the speed response of the cell movement, this is, cells have a faster movement response when they are exposed to low frequencies, while a response of lower movement is obtained at frequency from 400 Hz to 750 Hz. So it

was shown that *E. Invadens* in cell grown medium and undergo to ELF at several segments of frequencies are

affected in their motility. The response to conditioned medium includes an increase in both speed and negative chemotaxis [1]. This study also shows a direct effect of ELF's inducing change phenomena in the Ameba behavior; the swimming velocity and structure changes of the cell culture [8]. And a possible effect on of (F-actin) and (MyoII), and because of the observed mechanical variations, they can be considered capping protein's modulation changes.

#### ACKNOWLEDGMENT

Authors want to thanks DAIP project 017/2010.

#### REFERENCES

1. Ruedi Meili (2010) Myosin II Is Essential for the Spatiotemporal Organization of Traction Forces during Cell Motility. *Molecular Biology of the Cell* 21: 405–417.
2. Nagasaki A, Uyeda TQ (2008) Chemotaxis-mediated scission contributes to efficient cytokinesis in *Dictyostelium*. *Cell Motil Cytoskeleton* 65: 896–903.
3. Ruth Hemmersbach 1997. Influence of Extremely Low Frequency Electromagnetic Fields on the Swimming Behavior of Ciliates. *Bioelectromagnetics* 18: 491–498
4. Julio César Hernández-Pavón, Modesto Sosa, Teodoro Córdova, (2009), Study of Electromagnetic Fields on Cellular Systems. *Acta Universitaria* 19: 65-70.
5. E. López-Romero and J.C. Villagómez-Castro (1993) "Encystation in *Entamoeba invadens*". *Parasitology Today*. 9(6):225-227.
6. Anuradha Lohia (2003). The cell cycle of *Entamoeba histolytica* *Molecular and Cellular Biochemistry* 253: 217–222.
7. Mehreen Zaki (2006) *Entamoeba histolytica* cell movement: A central role for self generated chemokines and chemorepellents. *PNAS Microbiology* 18751–18756.
8. Junji Miyakoshi 2005. Effects of static magnetic fields at the cellular level. *Progress in Biophysics and Molecular Biology* 87:213–223.

Corresponding author:

Author: Teodoro Cordova-Fraga  
 Institute: Universidad de Guanajuato  
 Street: Loma del Bosque No. 103, Lomas del Campestre  
 City: Leon, GTO  
 Country: Mexico  
 Email: theo@fisica.ugto.mx



# Device to Evoke the Bone System in Hip Dislocation Diagnosis

H A Perez<sup>1</sup>, T. Cordova<sup>1,\*</sup>, N. Padilla<sup>2</sup>, and M. Sosa<sup>1</sup>

<sup>1</sup> Physics & Engineer Department - DCI, Universidad de Guanajuato, Leon, GTO, Mexico

<sup>2</sup> Nursing & Midwifery Department - DCSI, Universidad de Guanajuato, Celaya, GTO, Mexico

**Abstract** – Device and procedure for detecting irregularities in the bone system is presented; it can assess fractures, lesions, osteoporosis or irregularities *in vivo*. The resonance system is found or a system characteristic frequency is transmitted in order to determinate density bone or its sound propagation. This patented procedure bases its operation through a transmitter and a receiver in surface contact, just over the bone evaluated, which one is simultaneously observed on a screen, and it is also possible to storage measurements for subsequent assessments. Preliminary measurements determined that the dominant frequency for evaluated femoral bones in several subject is around 160 Hz, this suggests that this procedure is power for the proposed assessments in neonates.

**Keywords** – sound transmission, acoustic bone resonance, osteoporosis, densitometry.

## I. INTRODUCTION

Around one hundred thousand new patients of osteoporosis and bone metastases o diseases related to bones are added to the list each year only in the United States of North America [1]. It is known that among the malformations most common in orthopedics, it is reported the congenital hip dislocation, which is replaced by the current of dysplasia disease of development of hip. Its overall incidence is controversial, from 0.65 to 4 per 1000 live new-born [2]. So, early diagnosis of this pathology is suggested for new born in order to have opportune medical attention on time. In congenital hip dislocation, clinical diagnosis is made with traditional maneuver's Ortolani, Barlow, Peter-Baden [3], spite this diagnosis procedure; it is only detected sub-dislocated or dislocated hip early stage and may miss dysplasia [4-7].

As far as it is known, only a 17 % of affected children with this problem are diagnosed by the medical doctor, while the other, 83 % of them, is found by family members, when they present problems to start to walk [8].

In this study is presented an acoustic procedure in the audible frequency in order to assess bones in neonates.

## II. MATERIALS AND METHODS

According to bone shape, this can be modeled as a solid piece, so the sound is transferred through it according to

material density and Young module, so, the sound velocity is through the bone can be written as

$$v_s = \sqrt{\frac{E}{\rho}},$$

where,  $E$  is the Young module and  $\rho$  is the bone density.

In first approximation, a bone is a closed cylinder, so, its resonance frequency can be modulated according to

$$f_s = \frac{nv_s}{4L},$$

here,  $n=1, 3, 5, 7, \dots$ , with fundamental frequency in  $n-1$ ,  $v_s$  is the sound velocity and  $L$  the cylinder length.

As long as, an octave under a closed cylinder is written as

$$f_s = \frac{nv_s}{4(L+0.4d)},$$

in this equation  $d$ , is the cylinder diameter.

Using these expressions, it is possible to record natural or characteristic frequency of the bone and the bone density according to

$$\rho(f_s) = \frac{n^2 E}{16 f_s^2 (L+0.4d)^2}.$$

With this expression, it is estimated the bone density in function of the frequency.

On the other hand, the sound propagation needs a material medium, so, using the above equation is also possible to have a direct diagnosis of hip dislocation in neonates in frequency changes. An alternative or complement measurements is a power correlation between innings *vs.* outting signal intensity.

Measurement procedure includes a computer in order to have a white noise using random Source in a Matlab application; this is connected to a zero order hold digitization of the signal, so the audio card of the computer can optimally use it. It also adds a Chirp block to produce a frequency sweep to verify the correct operation by the spectrum analyzer. Also added is a stage that can be sent at a fixed

frequency to verify the results obtained by the analysis stage, or for a fixed frequency, in order to make the study of sound transmission used in study cases of dislocations or fractures. This audio is amplified previous to arrive in an actuator speaker, which one produces an ac magnetic field affecting a magnet fixed on a membrane, see Fig 1. So, a vibration in same frequency is created and transmitted to the bone segment under study. Noise white evokes the natural bone resonance that is registered with an electronic stethoscope and stored in order to assess density bone problems by using signal processing in platform Matlab.

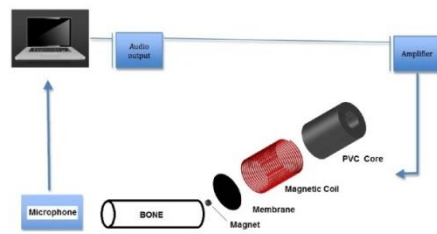


Fig. 1 Setup of the implemented device.

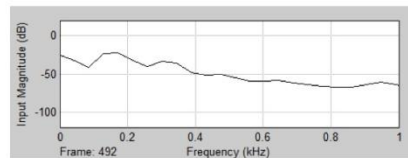


Fig. 2 Power spectral recorded and plotted in real time.

### III. RESULTS

Power spectral density performed in platform Matlab of this signal is shown in Fig. 2. This is the sound transmitted through the bone; the maximum curve indicates the fundamental harmonic for this bone. Furthermore, for stored signal, a routine performed in platform Matlab was done in order to get additional information or have a verification of the data acquisition in space-time. In Fig 3 is shown a signal in time space, in Fig 4 is shown a table of data after a power spectral was performed, there are PWR value, index point data and dominant frequency; as long as, in Fig. 5 a power spectral density is shown in order to identify the dominant frequency or resonant frequency.

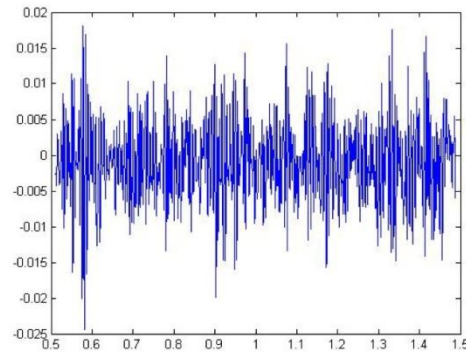


Fig. 3 Data recorded in time space.

PWR =
4.6552e-004
I =
161
Frec =
164.5349

Fig. 4 Table of main data.

### IV. DISCUSSION

It is important to point out that this is diagnosis technique proposal for evaluation of bone density and mainly, for hip dislocation in neonates, babies in the first 3 week of life. Traditional techniques for performing this evaluations use ionization radiation, in this case, sound in audible range is used, as far as it is known, side effects will be unexpected in these studies, so the babies will have a better quality of life.

In order to avoid the use of the PC, a portable device is developed and the registration of a patent of this procedure and instrumentation has been acquired.

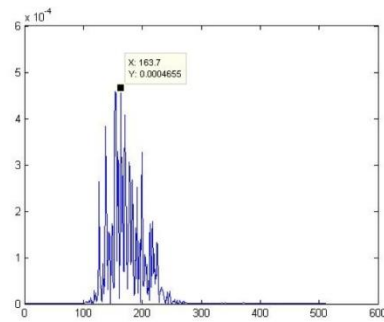


Fig. 5 Power spectral density

## ACKNOWLEDGMENT

Authors want thankful to patients and CONCYT grant number GTO-2011-C04-164448 for the partial support.

## REFERENCES

1. Wagramer Strasse (2008) Criterios para el tratamiento paliativo de la metástasis ósea – Aplicaciones clínicas, Sección de Medicina Nuclear, Organismo Internacional de Energía Atómica: Viena, Austria.
2. Murillo-Quiroga M, Zegarra-Mita H, Castellón-Tamez JL (2008) Desplacia de cadera en desarrollo. *Rev Pacea Med Fam* 5(8): 88-91.
3. Stone M, Richardson J, Bennet G (1987) Another clinical test for congenital dislocation of the hip. *Lancet* 1:954-955
4. Figueroa Ferrari RC y Padilla-Raygoza N (1994) La luxación congénita de cadera en el recién nacido macrosómico. Aspectos ultrasonográficos. *Rev. Med. IMSS* 32(3): 277-279
5. Padilla N, Figueroa RC (1992) Diagnóstico de la luxación congénita de cadera, mediante la transmisión comparada del sonido. *Rev Mex de Pediatr*; 59(5):149-151
6. Padilla N (2008) Enfermedad displásica del desarrollo de la cadera. En: Martínez R, ed. *La Salud del niño y del adolescente*, México, 6ª ed. El Manual Moderno.
7. Padilla N, Figueroa RC (1996) Pruebas de transmisión del sonido en el diagnóstico de la luxación congénita de cadera en el neonato. *Rev Mex de Pediatr* 63(6):265-268.
8. Fernandez E. 1989. Luxación congénita de cadera: reducción con tirantes de Pavlik modificados en niños de un año de edad. *Rev Mex Ortop Traumatol*;3:30-34

Author: Teodoro Cordova, Ph D  
 Institute: Universidad de Guanajuato campus Leon.  
 Street: 103, Loma del Bosque, Lomas del Campestre  
 City: Leon, GTO  
 Country: MEXICO  
 Email: theo@fisica.ugto.mx



**Memoria de Resúmenes**  
**13° Seminario de Investigación**  
Del 16 al 18 de mayo de 2012  
Aguascalientes, Ags. México

**D.R. © UNIVERSIDAD AUTÓNOMA DE AGUASCALIENTES**  
**DIRECCIÓN GENERAL DE INVESTIGACIÓN Y POSGRADO**

Departamento de Apoyo a la Investigación  
Av. Universidad no. 940, Ciudad Universitaria  
C.P. 20131 Aguascalientes, Ags.  
Tel. (449) 910-74-42 [www.uaa.mx/investigacion](http://www.uaa.mx/investigacion)

*Memoria de Resúmenes* es una publicación periódica anual, editada y distribuida por el Departamento de Apoyo a la Investigación de la Universidad Autónoma de Aguascalientes. Edición: Rosa del Carmen Zapata. Corrección de texto: Mónica Ávalos Valladares. Impresa por el Departamento de Procesos Gráficos de la Universidad Autónoma de Aguascalientes. Este número se terminó de imprimir en abril de 2013 con un tiraje de 500 ejemplares.

Los artículos firmados son responsabilidad de su autor y no reflejan necesariamente el criterio de la institución, a menos que se especifique lo contrario.

Queda estrictamente prohibida la reproducción parcial o total de los contenidos e imágenes de la publicación sin previa autorización del Instituto Nacional del Derecho del Autor.

- **ISSN 1870-4921** del Instituto Nacional del Derecho de Autor.
- Reserva de Derechos al Uso Exclusivo no. 04-2008-102319113900-102 del Instituto Nacional del Derecho de Autor.
- Licitud de título no. 13450 otorgada por la Comisión Calificadora de Publicaciones y Revistas Ilustradas de la Secretaría de Gobernación.
- Licitud de contenido no. 11023 otorgada por la Comisión Calificadora de Publicaciones y Revistas Ilustradas de la Secretaría de Gobernación.

Impreso en México/Printed in Mexico

## LIST OF MAIN CONTRIBUTIONS

### Publications

Pérez H, Cordova-Fraga T, López-Briones S, Espinoza A, et al. "Portable Device for Magnetic Stimulation: Assessment Survival and Proliferation in Human Lymphocytes," Rev. Sci. Instrum., 84(9), 094701 (2013).

Cordova-Fraga, Francisco Gomez-Aguilar, T. Bravo-Arellano, M.A. Hernandez-Gonzalez, S. Solorio-Meza,

H.A. Perez-Olivas, et al, "Biomagnetic Validation Skin Level for Blood Pressure Curves and Venous," O. J. of Appl. Sciences, 2, 128-134 (2012).

Hernandez E, Córdoba T, Perez Huetzin, Sosa M, Reynoso O, Cano M, Mendosa A, "Measuring Gastroe-sophageal Region Frequencies for Long time : Preliminary Results," Int. J. Bioelectromagnetism, 13(4), 245–8, (2011).

### Filed Patents

T. Córdoba, H. Perez, J. C. Villagomez, O. Martínez, S. López, G. Barbosa, S. Solorio. Estimulador Celular Magnético con Ferro Fluido, folio MXE202087372 IMPI (2012).

T. Córdoba, H. Perez, J. M. de la Roca, J. Huerta, M. Hernández, S. López, G. Barbosa, S. Solorio. Dispositivo Micro Estimulador Magnético, folio MXE2012088628 IMPI (2012).

T. Córdoba, H. Perez, M. Sosa. Radar Óseo, folio MXE2011076501 IMPI (2011).

### Conference Proceedings

H. Perez-Olivas, T. Córdoba-Fraga, F. Gómez-Aguilar, A. Espinoza-García, et al. "Magnetic exposure system to stimulate human lymphocytes proliferation," AIP Conf. Proc. 1494, 146-148 (2012).

Perez HA, Córdoba T, Padilla N, Sosa M., "Device to Evoke the Bone System in Hip Dislocation Diagnosis," IFMBE Proc., 39,1386–8. (2013).

H.A. Perez, J.C. Villagómez, T. Cordova, et al, "Cell Behavior Undergoing Random Segments of Oscillating Magnetic Field," World Congress on Medical Physics and Biomedical Engineering, IFMBE Proceedings 39, 654-656, (2013). Springerlink.